BUDOWNICTWO
I ARCHITEKTURA

BUDOWNICTWO
I ARCHITEKTURA

Vol. 19(2) 2020

SPIS TREŚCI
CONTENTS

The innovation of accounting and certification of historic architectural monuments using BIM technology

Olga Kysil¹, Raddamila Kosarevska², Oleksii Levchenko³

¹ Department of Information Technology in Architecture;
Kyiv National University of Construction and Architecture; Povitroflotskyi Av. 31, 03037 Kyiv, Ukraine;
solomyab@gmail.com (iD) *0000-0003-2873-6901*
² Department of Drawings and Paintings; Kyiv National University of Construction and Architecture;
Povitroflotskyi Av. 31, 03037 Kyiv, Ukraine;
e-mail:kosarevska.ro@knuba.edu.ua (iD) *0000-0003-1076-0364*
³ Department of Information Technology in Architecture Kyiv National University of Construction and Architecture; Povitroflotskyi Av. 31 03037 Kyiv Ukraine;
levchenko.ov@knuba.edu.ua (iD) *0000-0002-5254-2114*

Abstract: Presented research shows Building Information Modeling (BIM) technology as a highly promising tool for architectural heritage conservation. Analyses of contemporary publications by BIM topic and HBIM (Historic Building Information Modeling), its specific division, are conducted. The usage of modern technology analysis for digitizing monuments along with the outdated 'manual' of accounting and passportization methods are executed, and a lack of automation of the above processes is observed. Additionally, the research reveals that during the operational period of historical objects, there was no method of fixing their architectural transformations. The necessity of automation of the abovementioned processes by the capabilities of the BIM technology is emphasized. Automation methods developed utilizing the BIM model properties as a relational database, are described. An example of the method implementation in architectural and construction software applications is given. The case uses the rules of filling in the state accounting card of Ukraine. Nonetheless, the automatic formation of a document like this by the standards of any country is underscored.

Keywords: *BIM, HBIM, BIM* 4D, the life cycle of a building, information modeling of historical buildings, cultural heritage objects, Allplan software

1. Introduction

In the current context of urbanization and rapid urban development, problems related to the protection of urban and architectural heritage, as well as their historical environment, are of great importance. The use of Building Information Modeling (BIM) technologies, and in particular Historic Building Information Modeling (HBIM), while monitoring the state of architectural heritage

sites is a very effective tool for their comprehensive and complete preservation. However, it is not yet used for certification and for displaying changes (transformation or modification) of the architectural forms and elements of these objects that have occurred during the history of their operation.

Before the advent of the BIM technology, architects also redesigned at the level of urban infrastructure and individual clusters, including geometry, spatial relationships, and geographic information. Examples of such changes can be found in Bruno Fortier's work, in which the stages of the historical and urban development of Paris were visualized against the backdrop of its three-dimensional structure in the 1980s. [1] The work that combines the historical periods of operation of the Saint Sofia Cathedral in the 11th and 17th centuries presenst a similar concept [9]. Considerable works on the construction of the ensemble were carried out at the end of the 18th century and continued until the middle of the next century. At that time, most of the current structures were built. The cathedral was renovated in the 19th century. (Fig.2)
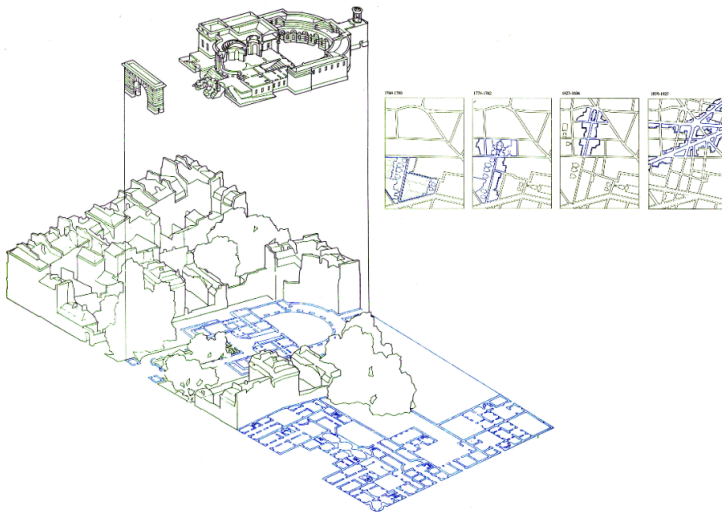

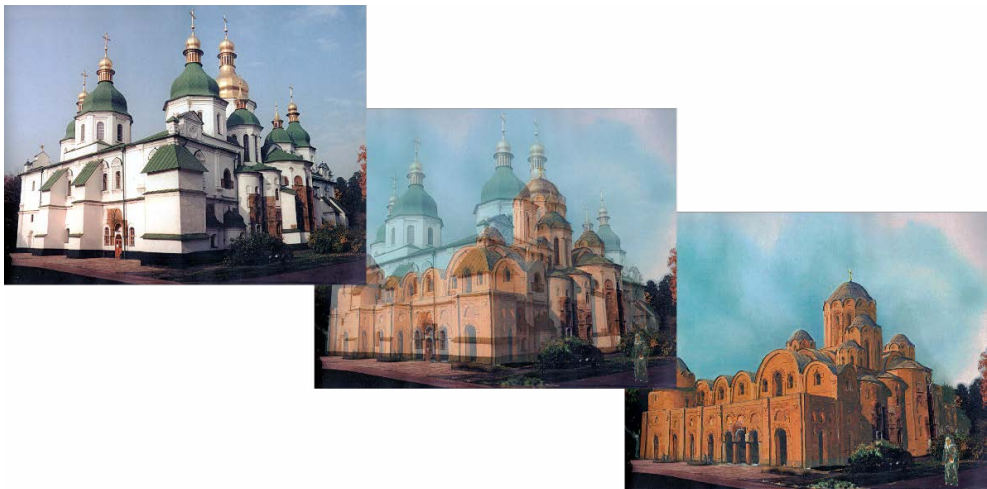Fig. 1.   The work of Bruno Fortier, L'atlasdeParis, source: [1]

Fig. 2.   Saint Sophia Cathedral, 11th c. Transformations of architectural ensemble in time, source: [9]

2. The analysis of contemporary publications

'Although BIM technology was created for the design and construction industry, nowadays its modeling tools and software tools open up new opportunities in the field of architectural heritage. At the same time, developments such as BIM can be applied to existing architectural monuments as well as to so-called "aggregate" information relating to selected historical periods, geographical areas, or architectural styles. "Technological bridge" between the past and the present created by this technology is, first of all, libraries of elements – make technologically straightforward ideas of "old" architecture in the new design and construction' [13].

The abovementioned libraries or "intellectual containers" will allow us not only to present a volumetric model of an architectural heritage object at all stages of its operational existence, but also to compare models of its original or present appearance with models of other periods of exploitation to "go" to the level of integration with the "digital" historical environment to discover the dynamics of their development or decline [13]. Studying the works of scientists on the use of BIM technologies in the protection, preservation, and management of objects of architectural heritage, we have found the following.

In their article dedicated to the concept and history of BIM, A. Bilyk, and M. Belyaev confirmed that its development was marked by the emergence of a fundamentally new approach in architectural and construction design (consisting of the creation of a computer model of a new building that covers all information about the future object) [8]. BIM is used both to refer to the building information model and the information modeling process. Graphisoft has even introduced the term 'VB' (Virtual Building), a virtual building. BIM is the process of generating and managing data from a single infrastructure over its life cycle using unique 3D and real-time dynamic building simulation software to reduce time and resource wasting in design and construction. This process is carried out in the information model of infrastructure (also designated BIM), which includes the geometry, spatial relationships, geographical information of the building, the number and properties of infrastructure components, etc. In collaboration with E. McGovern and S.Pavia, Maurice Murphy presented Historic BIM developed by the Historic BIM tool in quality of the new system of modeling historical buildings. The article provides a detailed description of the process of creating a three-dimensional parametric model of an architectural heritage object (remote data acquisition using a terrestrial laser scanner and digital cameras, combining image data and scanning, and converting the cloud point into a 3D model) and a library of architectural elements based on historical data, from Vitruvius to the architectural specimens of the eighteenth century [4].

The article by Oreni D., Bruman R., Georgopuslos A., and Cook B. illustrates the feasibility of using the HBIM tool in the field of protection and conservation of architectural monuments as an example of data collection implementation of element libraries (parametric, geometric, stylistic, historical, architectural) [6].

V. Talapov conducted an analysis of the value of information technologies for the monuments of history and architecture. He determined that BIM is a new way of fixing monuments, conducting their monitoring and study as a whole and parts, and the "electronic passport" of the monument, which can be used at all stages of its construction work. Talapov examined the relationship between the components of the information model of the architectural monument and the features of its creation through BIM technologies, as well as the importance of developing libraries of typical elements for historical buildings. The author states that typical elements should be the 'results' of historical eras, architectural styles, geographical zones,

and buildings' contractural technologies. The article discusses the cultural connection between modern architecture and the periods of the past with the help of BIM [13].

Additionally, this study was based on a publication on a theoretical approach to the HBIM for conservation and management of architectural heritage objects, namely an overview of concepts and methods for storing architectural monuments in AEC. The foundation of HBIM technology is a database that can be used to collect and exchange information for monument registration and management [2]. According to Stefano Della Torre, bringing BIM technologies to the area of architectural monuments is a perspective area, although it raises some doubts about the effectiveness of its practical implementation – the process of preserving the architectural heritage is cardinally different from the process of construction of new structures. Any historical building is, first and foremost, a collection of architectural elements that emphasize its authenticity and architectural value. The reproduction of these elements in the BIM model can be done directly in its file model, as well as with the involvement of electronic libraries of typical aspects of historical architecture (in particular, Gothic-BIM, Renaissance-BIM, and Regens-BIM). Using these standard elements of libraries certainly make historical 3D models more realistic and attractive. Furthermore, such models should help to improve data sharing, not just be scripted videos. In his words, "the transition from drawings to BIM equals the transition from restoration, as an event, to protection, as a process." [7]. According to modern authors, the use of BIM technologies in restoration design requires the development of new methods and techniques for modeling the geometric shape of the architectural monument, namely:

1) a step-by-step model creation;
2) the 'parametricity' of typical architectural elements of libraries should be not only by design features (windows, columns, doors,profiles, etc.), but also by style and timing (classicism, modernity, or constructivism) and must contain elements or their compositions;
3) the modeling of various decorative elements (complex or small detail, which gives the building peculiarity), it is advisable to reproduce together with complex, that is, large and recurrent elements;
4) have a wider range of basic tools for BIM programs(the window tool is also suitable for modeling brick masonry niches and theprojecting profile for creating inter-floor curtain belts) [12].

The British article about BIM for Heritage, which is a guide for professionals working in heritage and construction, shows the potential benefits of BIM approach to its implementation in projects of heritage and efficiency of the building lifecycle management [5]. Moreover, research into digitization methods of existing building objects, that has been studied in the course of this work, indicates that the ground-based laser scanning technology can be beneficial for developing an inventory of an architectural object using BIM technology. It is essential to adhere to the proper methodology for collecting data, taking into account the principles of correct measurements and their subsequent analysis, as well as the processing of logged data using external software [14].

3. Scientific novelty, goal and practical benefit of research

The use of the BIM method in modeling an architectural monument is widely described in current research. Not only does it store spatial information and metadata, but it also provides the means of documenting changes such structures undergo. The scope varies

from a simple documentation repository, through storage planning tools, to modeling and reconstruction tools [15].

However, existing research does not describe the method of automatically retrieving information for the registration and certification of historic sites and the automation of recording their changes over time in the accounting card.

This study improves the method of adding attributes to model tables of property of model elements [15], and also offers automation of receiving a card for accounting of architectural monuments. It is proposed to develop the HBIM model up to a 4D level (this level is used exclusively for new construction). BIM Model 4D chart data can also be displayed on the accounting card. Thus, the composition of the account card becomes complete and more detailed.

The scientific novelty of the research is to develop a method of automated formation of a card of accounting of historical objects by the standard of any state using the example of the Ukrainian card of accounting [16, 17]. Also, filling the model with information to automatically generate the card develops the model to the BIM 4D level. This allows capturing an object's early transformations on time, as well as managing the life cycle of the object in the present and future state.

The described improvement in the HBIM method has both economic and social effects. This approach optimizes the operation of the facility, planning the necessary repairs, and changing the use of the upgrade function. The process of registration and accounting of architectural monuments is simplified against the background of significant improvement in accounting documents' quality and completeness.

The research benefits the field of professional work practically with historic building objects and the field of presentation and tourism. The 4D BIM level model software has tools for animated visualization of geometric transformations over time, which can be an exciting addition to the exhibits of architectural heritage museums.

4. A method of using the BIM tool to create an architecture monument accounting card. Fixation of geometric transformations of an architectural monument in its life cycle by the BIM 4D method

Currently, there are many software products in the field of BIM technology that can be used to accomplish complex tasks of protecting, preserving, and managing architectural heritage. The theoretical basis and relevance of using BIM for certification, restoration, and sometimes reconstruction of historical sites raises questions about methodological and functional tools that can be used to solve most of the tasks in the process.

The analytical method of comparing building model tools to BIM technology emits a fairly large number of software products. Still, it is possible to immediately identify the most common and versatile by rejecting specialized applications that perform a specific design or engineering function in the process of creating a BIM model.

Having a specific tool or toolkit in the app will help to identify the following branded products from software developers quickly: Autodesk with Revit, Nemetschek Group with Allplan, Graphisoft with Archicad, etc.

Investigating algorithmic features of the BIM design using the above products, an expert opinion can be expressed about the qualitative difference in model formation using 'stages',

which is inherent in Revit and tools called 'reconstruction' in Allplan and Archicad applications. Using a systematic approach to the requirements of adapting additional information blocks to three-dimensional information, which is created to describe elements and characteristics of an object that cannot be modeled, the authors preferred the coverage of Allplan as the most adaptive tool for HBIM (Fig. 3).
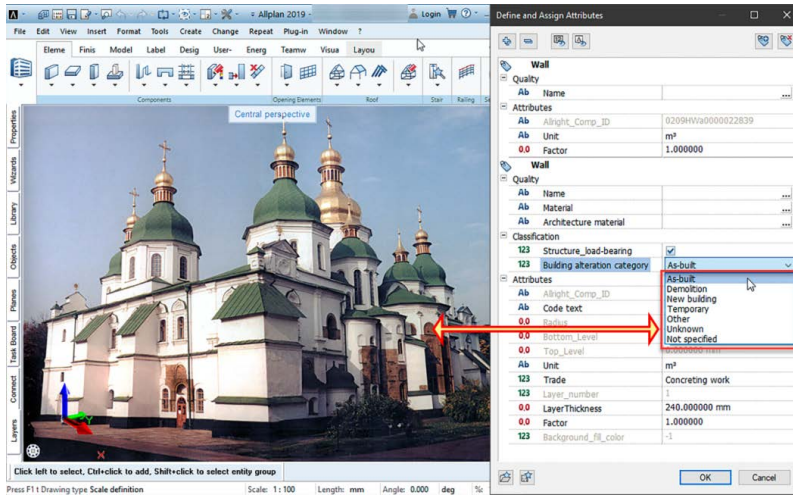
Fig. 3.   BIM Model Properties by Reconstruction Attribute Setting. Made in Allplan 2019 software with Partnership license (own elaboration)

Due to the structure of attribution – a database that connects to all elements of the model allows to set layer properties (Fig. 4) to building structures during their studies. In this way, the database of building materials and mortars used in the construction of the architectural heritage monument will help to catalog other findings in archaeological and restoration studies.

The individual database elements in the BIM model are used not only to describe the construction volume. Their adjustment is supported in the 'Reconstruction' mode by processing linear objects, surfaces, objects of landscape nature, and separate premises with an indication of the area (separate area) of filling the openings (doors, windows, etc.) (Fig. 5).
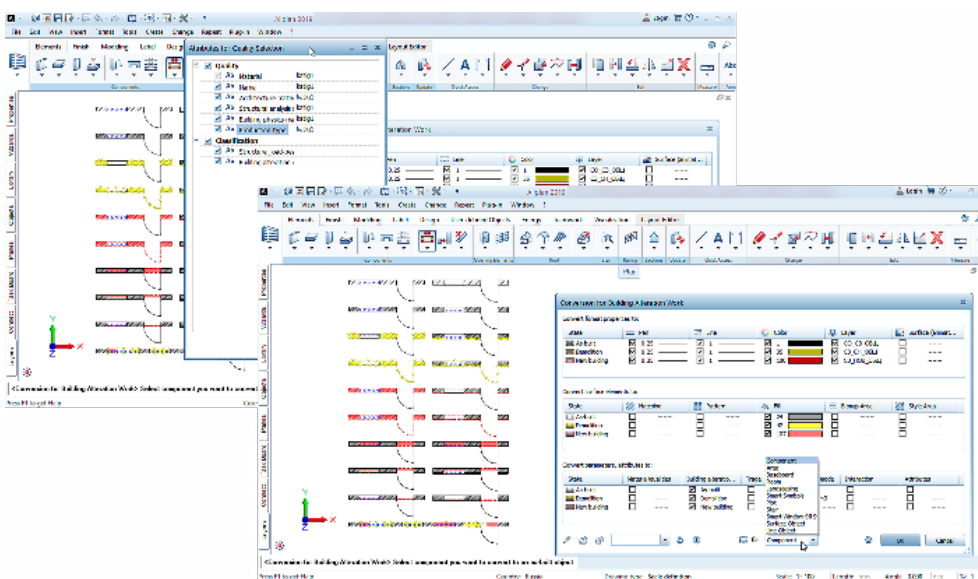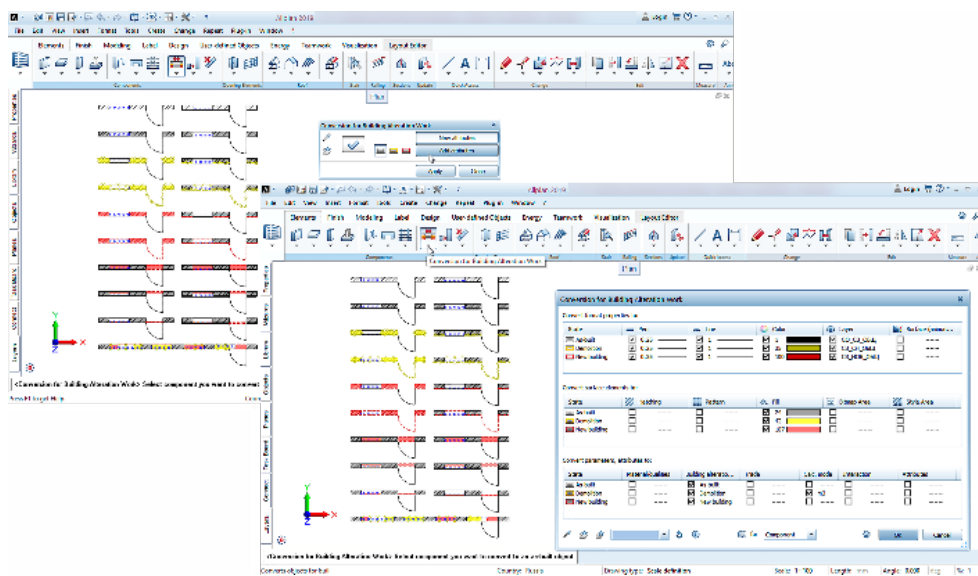
Fig. 4.   "Reconstruction" of the installation of properties for individual BIM components (Made in Allplan 2019 software with Partnership license) (own elaboration)

Fig. 5.   "Reconstruction" of components and databases of properties of building materials (Made in Allplan 2019 software with Partnership license) (own elaboration)

It is also necessary to note the peculiarities of the interaction of 3D elements with different parameters of the tool 'Reconstruction' (Fig. 6), which corresponds to the real situation of restoration and reconstruction work on the object of architectural heritage.
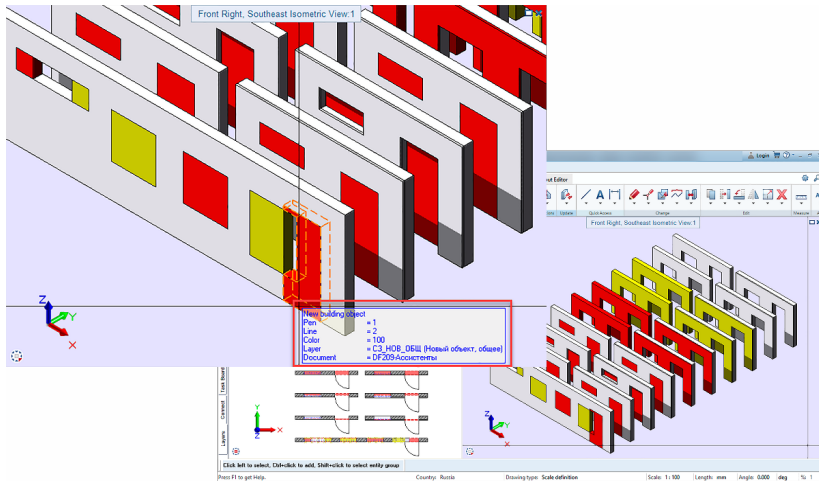
Fig. 6.   "Reconstruction" of the installation of properties for individual BIM component (Made in Allplan
            2019 software with Partnership license) (own elaboration)

The peculiarity of the life cycle of a historical building object in the HBIM model of
the 4D level (Fig. 8) in comparison with the common life cycle of the modern building object
(Fig. 7) should be emphasized.
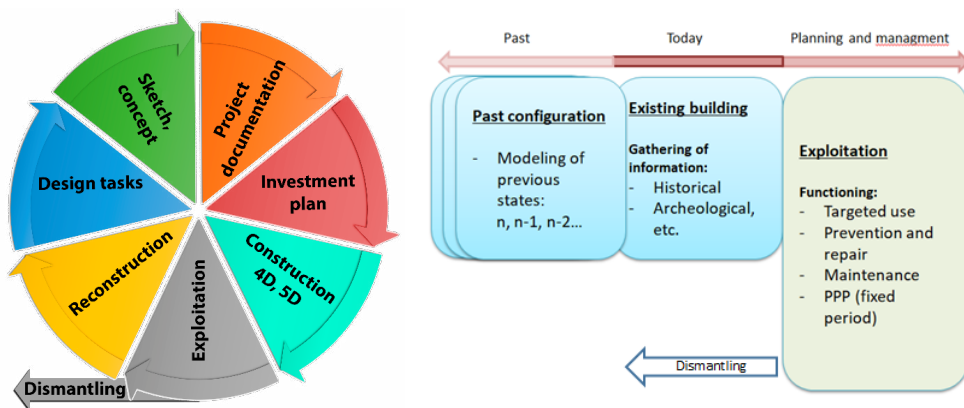
Fig. 7.   Life cycle on the BIM concept (own elaboration)
Fig. 8.   Life cycle on the HBIM concept (own elaboration)

Scientific research and innovation supplement the traditional HBIM-step approach,
followed in the 4D form (Fig.9). Speaking about the new BIM model, 4D becomes a logical
development of the model. This level is due to the availability of a certain amount of infor-
mation, making it possible to create a construction schedule. That is, determining the order
of gradual erection of building elements in reality.
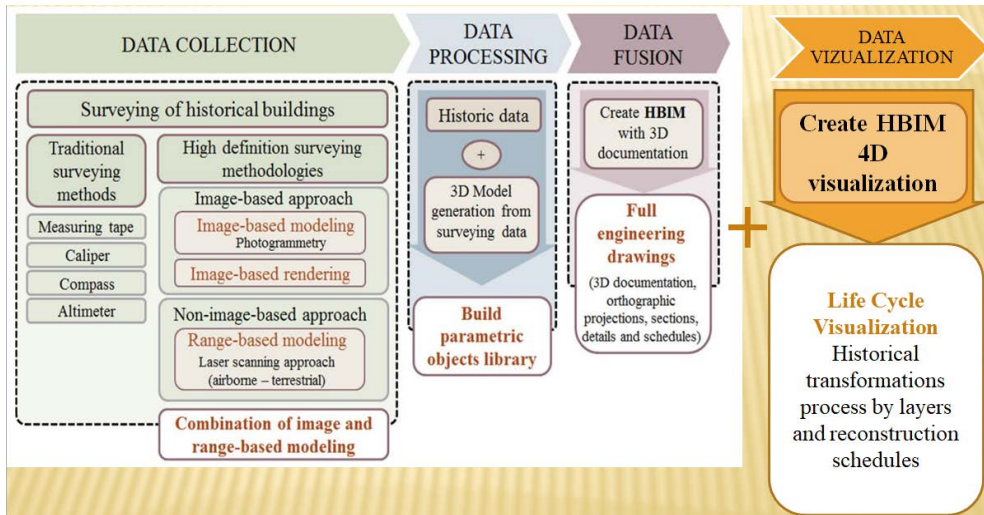
Fig. 9.   Theoretical framework for HBIM approach (source:[2]), supplemented according to the results of this study (own elaboration)

The authors of the research made the reasonable assumption that in the case of an existing historical object and the existence of data on its peculiarities over the years, the algorithm for constructing a graph of the building of new elements can be considered as a graph of the disappearance of old elements, or their change. Thus, with a historical BIM model, the concept of a life cycle describes an often non-existent configuration and several iterations of restructuring. The addition of HBIM technology also provides an opportunity to keep track of the dynamics of the restoration and repair stages to maintain the architectural monument in proper condition (Fig. 9).

It is necessary to check on the database of individual fragments descriptions of the model to preserve their authentic condition and restore the lost parts using modern building materials. The security passport must indicate which fragments are of historical value and which are less valuable, or fragments not of history but new buildings.

The certification of inherited monuments that have changed their architectural forms or elements during their lifetime is a different issue. Thus, as shown in the example of Saint Sophia's Cathedral in Kyiv (Fig. 2), the multi-layered historical content of the 3D model will reflect an animation of historical epochs and material culture – it will allow to study the composition of building materials by layers of structural elements in one object. The archaeological value of such a monument is increased because, in its example, modern methods of research were used (ultrasound, magnetic resonance, etc.). They show that it is possible to obtain standard characteristics of building materials and solutions for more accurate dating of other archeological objects of cultural heritage that have not survived until our time.

The proposed development of the BIM model of the monument to the level of 4D introduced in the study is possible not only in the presence of documented information and research on the past states of the object, but also under the condition of construction and hypothetical variants of the past configurations of the monument of a particular historical and architectural period. By adding to the altered elements information about the conditions in which this transformation took place (materials, construction technologies), the complete picture emerges for

further research and the change of the hypothesis to axiom. For example, by comparing this information with other BIM models of certain period monuments and placements for which historical documents are confirmed.

HBIM 4D technology provides the ability to fill the timeline both in the 'past' time and 'as it is now,' as well as 'as it will be.' The last section is related to the management of the operation of conservation of the building and the reconstruction, restoration, or repair plan. Particularly important for the preservation of the monument is the ability to schedule repair work, pre-entered in the schedule information about the duration and durability of the construction materials used, and preliminary results of expert surveys. The schedule automatically highlights the expiration date for the use of a particular material or element.
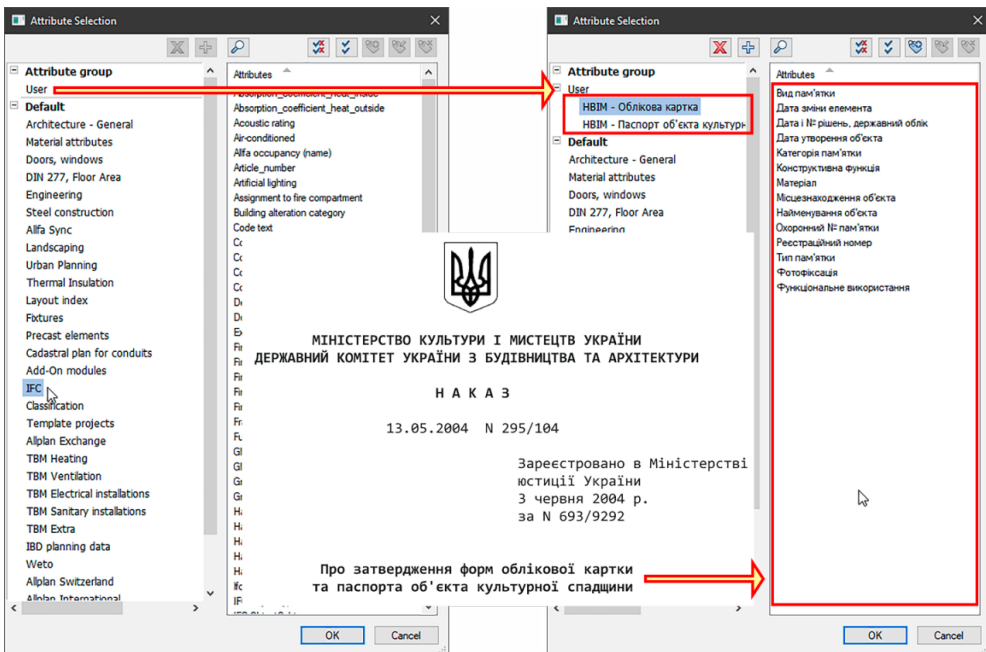
Fig. 10.   Adaptive ability to assign attributes in Allplan to the attribute database of BIM element (Made in Allplan 2019 software with Partnership license) (own elaboration)

Modern technologies allow high-precision laser scanning to build a point cloud. The electronic version of the card has links to 3D types of BIM models, where specialists check the condition of the building, including minimal geometric deviations from previous inspection. For this purpose, the corresponding coordinates of the points cloud of the previous inspection date and the current one are compared.

When the global experience in cultural heritage monuments is generalized, it is possible to build an information database to describe the object and attach these characteristics to a specific volume of the BIM model. The study proves that the flexible attribute structure in Allplan is well-suited to creating such a base – a registration card and passport of a cultural heritage object (Fig. 10).

One of the technical features of using a BIM design program, such as Allplan, is to create model layers for architects (architects, BIM specialists, etc.) and research specialists

(art critics, archaeologists, restorers, etc.). The general algorithm for creating a 3D model begins with the use of a scan of a building or structure; the second step is to build the architectural volume in the volume of the scanned shell. At this stage, BIM uses architectural and building elements embedded in the software in the design environment: wall, ceiling, column, beam, etc. From the name of each element at once, it is possible to derive certain information about the functional and spatial features of individual structures. That is, the first level of model information saturation is performed by indicating which elements make up the building.

LoI (Level of Object Information) as part of the general LOD (Level of Detail) concept should be spelled out in the EIR (Employer's Information Requirements) by the relevant specialists involved in the study, documentation, storage, or reconstruction of the architectural monument [10]. Thus, the object's electronic accounting card will have certain layers of specific non-graphic information corresponding to the LOD of the model itself.

Later in the restoration project, the research materials are aligned and combined with the 3D model. Technologically, this is solved by importing custom data from the cultural heritage description into the model in the BIM application environment. Imports can be performed sequentially – to each of the model elements, e.g., to each wall or column, or all model elements at once. It is clear that the second option requires a lot more support work to set up the links between the 3D data and the data from the security registry documents, which will be converted into a new model exchange format.

To establish such a connection, it is necessary to perform a manual task of certain properties and to check the export of attribute data of a 3D element through standard Allplan tools. This approach shows that it is possible to set up distributed data processing and creation of a standardized new card format (electronic data to BIM), objects of the virtual environment for research, restoration or reconstruction project, operational monitoring of cultural heritage objects (Figs. 11, 12, 13).
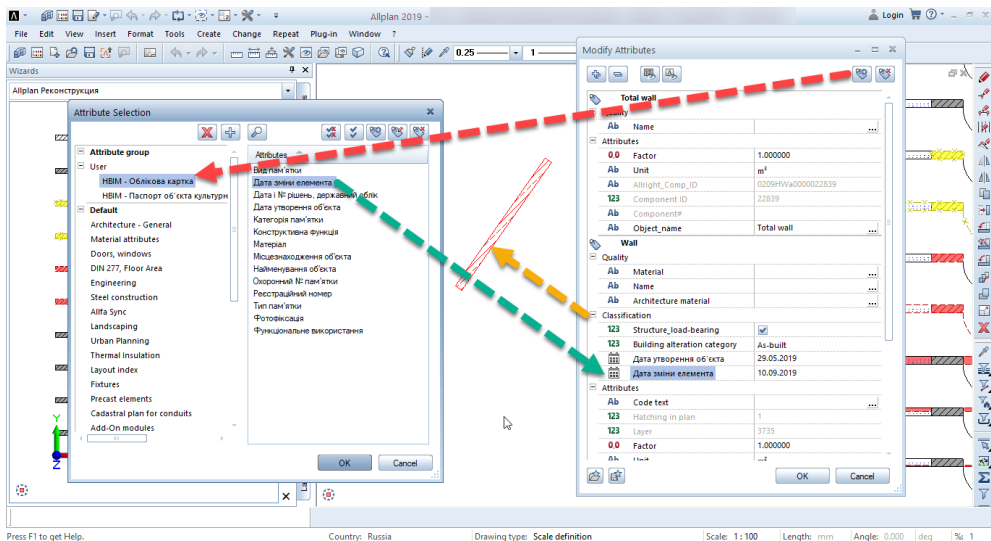
Fig. 11.   HBIM – attributes to model elements added by the properties of the "registration form"(Made in Allplan 2019 software with Partnership license) (own elaboration)

The sequence of operations can be changed with the number of layering components, automation of routine production operations and integration of the 'cloud' services.
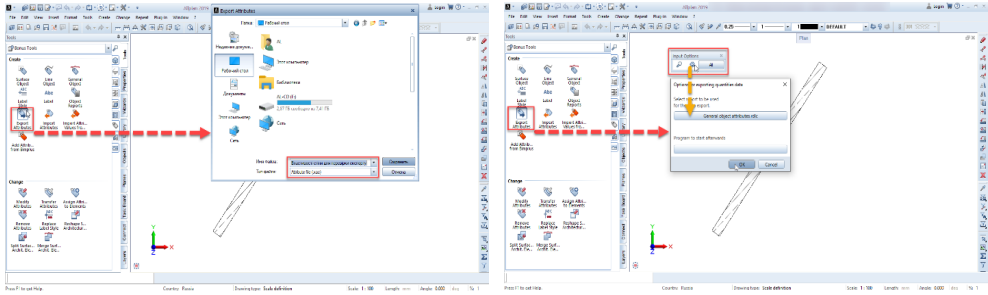
Fig. 12.   HBIM data for each model element (Made in Allplan 2019 with Partnership license) (own elabo-
            ration)
Fig. 13.   Attribute export settings to create a new sample account card (Made in Allplan 2019 software with
            Partnership license) (own elaboration)

In the future, it is possible to edit the data in tabular form (Fig. 14) by specialists in archeology, art, restoration, etc., since the saved attributes of elements (accounting card in the new format) of the model can be permanently replaced by the 'export-import' function in the interface of the BIM application Allplan (Fig. 11-14).

Fig. 14.   HBIM – A new sample of registration card to describe architectural monuments (Made in MS Office
            2019 software by for EDU) (own elaboration)

5. Conclusion

Presently, the use of information technologies (BIM) in the field of monitoring archi-tectural objects of cultural heritage is a highly effective tool for their preservation. It presents a 3D model of the current state of the monument, preserves historical information about the object and its environment, develops documentation for restoration design, and so on. However, BIM-developments, such as simulation tools and software tools, are not used for filling the accounting cards and fixation changes of architectural monuments that took place during their operational period.

The use of these technologies to capture the architectural transformations of cultural herit-age objects will allow the virtual display of their volumetric models at all stages of operational existence. It will also compare models of their original or current appearance with models of other periods of exploitation, to "go" to the level of integration with a "digital" historical environment to find out the dynamics of their development or decline.

During this research, the authors concluded that it is possible to create documentation for storage and security activities in the form of a new type of accounting cards, such that they can transfer the data in the property of three-dimensional elements using BIM technology. The use of these technologies to capture the architectural transformations of cultural heritage objects will allow them to virtually display their volumetric models at all stages of the change of historical objects that occurred during their operational period.

This development direction provides prospects for deepening research in urban studies, architecture, sociology, and sustainable urban development. With big data processing capabilities, there will be correlated links between heterogeneous factors that contribute to varying accounting for human settlements. In addition, it looks possible for each historical site to be easier to control by applying a repair schedule. In this way, information on materials and structures used in a building can be processed both in a protective and scientific context.

Further research has two major goals: to deepen cooperation with institutes and departments, where archaeological, restoration, and art historians are trained to prepare general proposals for changes to the practice of monumental protection and use of the technology of BIM-documentation of cultural heritage monuments and to generalize the experience of documenting and using information technologies of foreign partners in the field of cultural heritage protection.

6. Acknowledgements

References

[1]   Fortier, B., "L'atlas de Paris", *L'Architecture D'Aujourd'hui,* vol. 265, (1989)*,* pp.172–183.

[2]   Megahed N.A., "Towards a theoretical framework for HBIM approach in historic preservation and management," *Archnet-IJAR*, vol. 9, no. 3, (2015), pp. 130–147. https://doi.org/10.26687/archnet-ijar.v9i3.737

[3]   Murphy C., *Integration of Historic Building Information Modeling (HBIM) and 3D GIS for Recording and Managing Cultural Heritage Sites*. 2012. Available: https://arrow.tudublin.ie/beschreccon [Access: 10 Jan 2020]

[4]   Murphy M. et al., "Historic Building Information Modelling – Adding intelligence to laser and image based surveys of European classical architecture," *ISPRS Journal of Photogrammetry and Remote Sensing*, vol. 76, (2013), pp. 89–102. https://doi.org/10.1016/j.isprsjprs.2012.11.006

[5]   "BIM for Heritage | Historic England", Available: https://historicengland.org.uk/images-books/publications/bim-for-heritage/ [Accessed: 28 Apr 2020]

[6]   Oreni D. et al., "Hbim for conservation and management of built heritage: Towards a library of vaults and wooden bean floors," in ISPRS Annals of the Photogrammetry, Remote Sensing and Spatial Information Sciences, (2013), vol. 2, no. 5/W1, pp. 215–221. https://doi.org/10.5194/isprsannals-II-5-W1-215-2013

[7]   Della Torre S., "Perspectives on Historic BIM Developments in Italy", *AECbytes Viewpoint*, 2016. Available: http://www.aecbytes.com/viewpoint/2016/issue_82.html [Accessed: 28 Apr 2020]

[8]   Bilyk A.S., Belyaev M.A., "BIM modeling. Opportunities and Prospects in Ukraine", *Industrial Construction and Engineering*, vol. 2, (2015), pp.9-15.

[9] Dotsenko T., Lyabakh M. and Paramonov O., *KIEV: A Journey through Ancient City*, Kiev House, Kyiv. (1998).

[10] "Levels of definition – Technical Support – NBS BIM Toolkit". Available: https://toolkit.thenbs. com/articles/levels-of-definition [Accessed: 04 May 2020]

[11] Kozlova T., Talapov V., "Experience of information modeling of architectural monuments", *AMIT*, vol.3(8), (2009). Available: https://docplayer.ru/51557731-Opyt-informacionnogo-modelirovani-ya-pamyatnikov-arhitektury-t-i-kozlova-v-v-talapov.html [Accessed: 20 Aug 19]

[12] Kozlova T., Talapov V., "On the technique of BIM application in modeling of architectural monu-ments", *AMIT*, vol. 3 (12), (2010), Available: https://docplayer.ru/45661621-O-metodike-prime-neniya-bim-v-modelirovanii-pamyatnikov-arhitektury-about-methods-of-using-bim-in-mode-ling-of-architectural-monuments.html [Accessed: 25 Aug 2019]

[13] Talapov V.V., "BIM technology and its connecting role for different architecture epochs", *Balan-dinsky readings*, vol. 10(2), (2015), pp.325-328.

[14] Uchański Ł. and Karsznia K., "The use of Terrestrial Laser Scanning for the purposes of preparing technical documentation in BIM technology," *Budownictwo i Architektura*, vol. 17, no. 3, (2018), pp. 189–199. https://doi.org/10.24358/Bud-Arch_18_173_14

[15] Sztwiertnia D. et al., "HBIM (heritage Building Information Modell) of the Wang Stave Church in Karpacz–Case Study," *International Journal of Architectural Heritage*, (2019). https://doi.org/10.1080/15583058.2019.1645238

[16] Kysil O., and Levchenko O., Mikhalchenko S., "Theoretical and methodological principles for the creation of a state database of building objects certified by the BIM technology", *Web of Scholar*, vol. 6(24), (2018). https://doi.org/10.31435/rsglobal_wos/12062018/5761

[17] Kysil O. and Naichuk N., "Digital registration cards of HBIM-based architectural heritage as a new stage of historic preservation of Krakow (Poland)." *Modern Problems of Architecture and Urban Planning,* vol. 0, no. 56, (2020), pp. 66–72. https://doi.org/10.32347/2077-3455.2020.56.66-72

Crossref
Similarity Check
Powered by iThenticate

Orginal Article

Evaluation of the contact angle and wettability of hydrophobised lightweight concrete with sawdust

Małgorzata Szafraniec[1], Danuta Barnat-Hunek[2]

[1] Department of Construction; Faculty of Civil Engineering and Architecture;
Lublin University of Technology; Nadbystrzycka 40, 20-618 Lublin, Poland;
m.szafraniec@pollub.pl 0000-0002-5862-9456
[2] Department of Construction; Faculty of Civil Engineering and Architecture;
Lublin University of Technology; Nadbystrzycka 40, 20-618 Lublin, Poland;
d.barnat-hunek@pollub.pl 0000-0001-8409-3299

Abstract: The aim of the research presented in the paper was to evaluate the feasibility of using hydrophobic preparations based on organosilicon compounds for protection treatment on the lightweight concrete modified with sawdust. The experimental part of the work concerns the physical and mechanical properties of lightweight concrete and the influence of two hydrophobic agents on the contact angle of the material. Lightweight concrete contact angle (θ_w) was determined as a time function using one measuring liquid. Water repellent coatings in lightweight concrete structure with the coarse aggregate sawdust (CASD) using electron microscopy were presented. The effectiveness of hydrophobisation of porous lightweight concretes was determined on the basis of the research. For the hydrophobic surface, the contact angle decreased and it depended on the used agents. The lowest contact angle of 40.2° (t=0) was obtained for reference concrete before hydrophobisation and 112.2° after hydrophobisation with a methyl-silicone resin based on organic solvent. The results of scientific research confirm the possibility to produce lightweight concretes modified with CASD with adequate surface protection against external moisture.

Keywords: sawdust, lightweight aggregate-concrete, organosilicon compounds, hydrophobisation, contact angle

1. Introduction

A key global concern for societies, governments and industry, especially in the wood processing and production sector, is the sustainability of production systems. This sector is well placed to provide products that enhance long-term environmental sustainability through

products based on renewable natural resources from forests such as sawdust. Following the eco-trend in the nineteenth-century sawdust concrete was created. Due to its cost-effectiveness and lightweight, it has been well recognized [1–6]. To reduce the environmental impact, developed countries have now created opportunities for using wood waste in concrete structures. Besides sawdust in the production of building materials, the following waste materials from the wood industry is also used – wood shavings [7], wood fibre [8], wood ash [9–11], chips [12–14], cork [15], sawdust ash [16, 17].

Energy-saving blocks made from lightweight concrete are characterized by higher absorbability and they have much more pores compared to its trading equivalent, resulting from the porous structure of lightweight aggregate such as waste from the wood industry [18]. This is an essential problem when lightweight concrete mixes are designed. This causes the water transport, which is pulled up capillary (in the final product) [19], which significantly affects the heat flow process, increasing the thermal conductivity of materials several times [20, 21].

Damage caused by moisture is a major factor in the degradation of building materials [22–24]. Water repellent treatment is one of the methods of protecting the surface of lightweight aggregate-concrete [25, 26]. As a result of hydrophobisation, the absorption of capillary water decreases, which allows for proper water vapour permeability. In the case of impregnation, the so-called polymer cement concretes (PCC), obtained by adding polymer, oligomer or monomer to the concrete mix, gained popularity. This results in concrete with better workability of the mix and increased tensile strength compared to normal concrete [27]. In the case of existing facilities, polymer impregnated concrete (PIC) obtained by impregnating hardened concrete with a monomer or prepolymer is popular. For the hydrophobisation of concrete, organosilicon compounds such as methyl-silicone resins or siloxanes are mainly applied [28, 29].

The applications of silanes for surface modification of materials [30–32] or in the mass of concretes [33] and mortars [34–36] are known from the literature. These compounds make the concrete surface non-wetting by water and corrosive compounds, such as water-soluble salts [37]. The ability of building materials to be wetted by liquids is of particular importance, e.g. during their hydrophobisation, in the effectiveness of anti graffiti agents, during surface cleaning.

Materials' contact angle is an indicator of their wettability [38]. Higher wettability occurs at low contact angle (CA) <90° and water repellency at high contact angle > 90°. For determining the surface tension [39], the surface free energy (SFE) [40] and the adhesive action [41, 42] the contact angle can be used. CA is influenced by many factors. For example, CA is affected by the type of measuring liquid or droplet sizes of measuring liquids. The surface homogeneity, contamination and surface roughness, longitudinal elasticity coefficient of material which is being tested, ambient temperature or humidity also have an influence on CA [43, 44].

The most commonly used CA measurement methods include bubble method, geometric method, direct measurement and capillary liquid growth on a sample of the tested material [38]. A very popular method of contact angle determination is direct measurement. For example, a goniometer is used to test CA in this method but also a contact angle analyzer can be used [45, 46].

Based on the properties of waterproofing agents, there is a possibility to increase or reduce the CA and thus the material surface tension, resulting in their non-wetting properties, which is connected, inter alia, to frost resistance and chemical corrosion resistance.

Examining the structure of the topcoat of waterproofed lightweight concrete with CASD regarding wettability, among other things, it will allow evaluating the material's behaviour under the presence of corrosive compounds and water. In situations where significant resist-

ance of the surface layer of lightweight concretes to the corrosive environment is required, it is advisable to use preparations causing the highest contact angle.

2. Materials and methods

2.1. Concrete mixtures

The concrete mix consisted of CASD – lightweight with grain sizes from 8 mm to 16 mm, Portland cement CEM II 32.5 R, sand with grain sizes from 0 mm to 2 mm and water from the city's water distribution system. On the basis of standards EN 206-1:2003 [47] and PN-B-06265:2004 [48], an experimental formula was developed, which was used to produce specimens.

The following components must be used to make 1 m^3 of lightweight concrete: CASD – 157 kg, sand – 1350 kg, cement – 350 kg, water 280 kg, superplasticizer 5.25 kg.

Once the components were thoroughly mixed and the concrete was placed in the moulds, the concrete was compacted on a vibrating table. Immediately upon mixing of concrete components specimens with the following dimensions 150×150×150 mm were made. Concrete in the moulds was laid in two layers, each of which was vibrated until the appearance of the cement grout. For 24 hours, all specimens were prevented from losing moisture and kept at a temperature of approximately 23 °C till they were removed from the moulds. The samples were then inserted into the water tank for 14 days. By the time of the test (28 days after the samples are made), the specimens had ripened under constant laboratory conditions.

In accordance with standard EN 197-1 [49], Portland cement CEM II 32.5 R has been tested. The parameters of the cement CEM II 32.5 R are shown in Tab. 1.

Table 1.   Technical data of CEM II 32.5 R Portland cement. *Source: own study*

Parameters	Unit	
Specific surface	(cm^2/g)	3985
Initial setting time	(min)	248
Compressive strength after		
2 days	(MPa)	17.9
28 days		43.0
Density	(g/cm^3)	3.02
Loss on ignition by mass cement	(%)	5.0
Volume stability	(mm)	< 10

Polycarboxylate ethers were used as a superplasticizer in the amount of 1.5% by weight of cement. Its density at 20° C was 1.065 g/cm^3.

The sawdust was collected from a local sawmill. They have been dried by drying in a laboratory dryer to remove any moisture that might affect the final cement-water ratio (w/c) of the concrete. They were then sieved through sieves to obtain the 8-16 mm fraction for the production of coarse aggregate sawdust (CASD) with a specific gravity of 0.36 (g/cm^3), a water absorption capacity of 89% and a grinding module of 3.79.

2.2. Methods

The physico-mechanical properties of concrete with CASD have been established in accordance with the following standards: EN 1936:2010 [50], PN-EN 1389:2005 [51], EN 12390-7:2019 [52], EN 12390-3:2019 [53], PN-B-06250:1988 [54].

2.3. Applied water repellents

For laboratory testing, two commonly used hydrophobic agents on the market have been chosen, differing in solvent type, concentration and viscosity:

HA1 – water-based methyl-silicone resin in the potassium hydroxide,

HA2 – methyl-silicone resin based on organic solvent.

In Tab. 2, the primary characteristics of preparations that were used in the study are presented.

Table 2.   Properties of hydrophobic agents. *Source: own study*

Type of formulation	Surface tension σ (N/m$\cdot 10^{-3}$)	Viscosity η (Pa$\cdot$s$\cdot 10^{-3}$)	Density at 20°C (g/cm^3)	The quotient of the surface tension and viscosity σ/η
HA1	67.92	1.10	1.20	61.73
HA2	24.30	2.85	0.85	8.54

The lowest viscosity coefficient η has a formulation with the lowest concentration of the active substance and it is an aqueous solution of HA1 formulation. Methyl-silicone resin in petrol HA2 is characterized by higher viscosity by almost 250% compared to that of preparation HA1. The highest value of the ratio of surface tension to the viscosity of solutions is shown by the water-based preparation HA1.

The study did not analyse the concentration of the preparation and the number of layers applied. It should be assumed that these factors influence the penetration capacity of the preparations and at the same time the contact angle and effectiveness of hydrophobisation.

The agents were applied twice by brush, one layer after another, so as not to interrupt the capillary action ('wet on wet' method).

2.4. Evaluation of the contact angle

The contact angle of the measuring liquid droplet was determined on a test stand which consists of a goniometer. The goniometer was integrated with the camera in order to take pictures of the droplets placed on the samples surface. Fig. 1 shows the measurement of the CA of reference samples and samples protected by hydrophobisation at the beginning of the test ($t_1 = 0$ s).

(a) $t_1 = 0s$, $\theta_w = 40°$ (b) $t_1 = 0s$, $\theta_w = 102°$ (c) $t_1 = 0s$, $\theta_w = 112°$
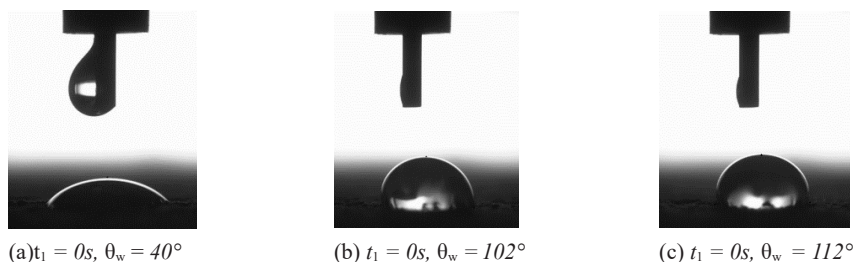
Fig. 1.   Lightweight concrete surfaces during CA test: (a) reference sample S, (b) sample protected with agent HA1, (c) sample protected with agent HA2. *Source: own study*.

For testing the CA, distilled water has been selected as the measuring liquid. The drops of liquid with a volume of 1.8 mm³ were applied with a micropipette [38, 55]. Due to the heterogeneity of the material, 6 drops were applied to each sample. Measurements were taken 3 times: at the time of application of the drops and after 5 and 45 minutes.

2.5. Scanning electron microscopy (SEM)

The morphology and microtopography of water-repellent concrete with CASD were analysed using FEI Quanta 250 FEG scanning electron microscopy. The device was equipped with a chemical composition analysis system which was based on energy dispersion spectroscopy (EDS). The specimens have been formed in thin-layer tiles. They were subjected to X-ray microanalysis under field conditions and the composition of the elements for concrete were assessed.

3. Results and analysis

3.1. Characteristics of lightweight concrete with CASD

Mechanical and physical characteristics of the studied concrete are shown in Tab. 3.

Table 3.   Properties of lightweight concrete with CASD. *Source: own study*

Density ρ_d (kg/m³)	Apparent density ρ_a (kg/m³)	Tightness (%)	Porosity (%)	Compressive strength (MPa)	Flexural strength (MPa)
2550	1504	59.0	41.0	26.6	5.9

The absorbability values after 1, 3, 7 and 14 days of concrete are shown in Fig. 2.

Type of sample	t (days)			
	1	3	7	14
S	8.25	8.99	10.43	13.75
HA1	1.0	2.13	5.14	7.84
HA2	0.55	1.03	1.70	2.27
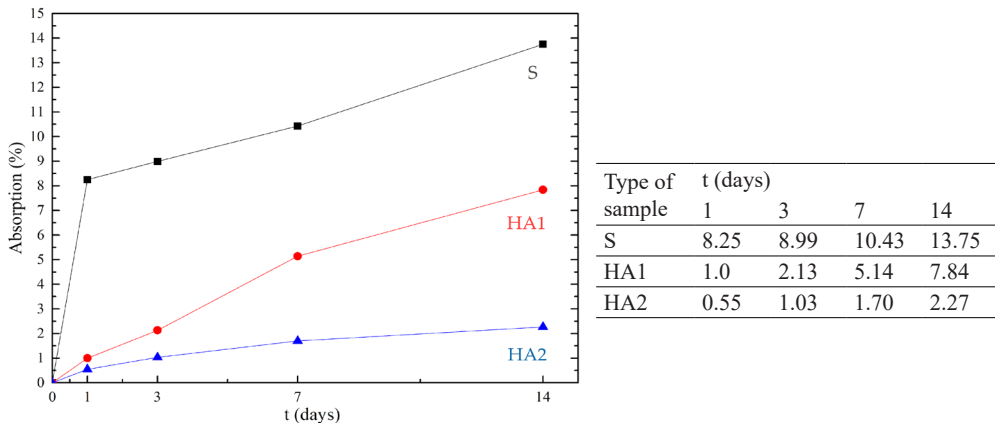
Fig. 2.   Absorption of concrete after 1, 3, 7 and 14 days. *Source: own study*

Analysing the above data, it can be seen that after 14 days of the water absorption test the reference concrete increased its mass by 67%. This is due to the porosity of the concrete with CASD, which was as much as 41%. This shows the need for concrete modifications to reduce

water absorption. Thus the surface water repellent treatment was applied. The best results were obtained for concrete protected with HA2. After the first day, it reduced the water absorption of concrete by 93% and after 14 days by 83%. On the last day of the test, absorbed water by concrete samples with CASD was 3.5 times lower for HA2 than for HA1.

Thalmaier G. et al. [56] made five different types of clay brick samples. The content of sawdust in the specimens was 15% for all, but they differed in the size of the sawdust fraction used to make them. They found a significant increase in water absorption from 23% to 25% depending on the sawdust fraction used. While the water absorption of the reference samples was 18%. It shows a significant influence of porosity, which was 25% and up to 40% for reference samples and those with sawdust, respectively. In their research, Md Noor et al. [57] examined water absorption of concrete with palm oil kernel shells (PKS). After the research, they found that water absorption values range from 4.1% to 4.7% for the reference concrete, but increased from 4.5% to 12.1% when 25% to 75% of the coarse aggregate was replaced by PKS. This is due to the porous structure of PKS. Oba and Amadi [16] in their work created a mathematical model for water absorption of Sawdust Ash (SDA) – Sand Concrete. They replaced the fine aggregate with 5% SDA in concrete and thus achieved a concrete water absorption rate of 3.734% to 9.568%. In the paper, Castro et al. [58] showed that water absorption by concrete may also depend on the way of sample conditioning and of the volume of paste in the samples. They have shown that specimens conditioned at 50% relative humidity can exhibit almost six times higher total water absorption than similar specimens at 80% relative humidity.

The porosity of the material is the main factor on which the effectiveness of hydrophobisation depends. Water repellency is more effective as the porosity of the material increases. This is because it reaches deeper parts of the material. Szafraniec et al. in [59] showed the effectiveness of surface hydrophilisation of porous mortars with perlite. Samples surface-treated with aqueous emulsion based on organofunctional silanes diluted in demineralised water in the ratio of 1:4 proved to be the most resistant to water absorption. Absorption of water was 7.5 times lower after 1 day and 2.9 times lower after 14 days in comparison with the reference mortars. Research conducted by Suchorab et al. [60] shows that lightweight aggregate concrete with sewage sludge, thanks to its porosity and absorbency, has absorbed more water repellent. This reduced the water absorption of this concrete by about 57 %. Zhu et al. [31] concluded that surface hydrophilisation of concrete with recycled aggregate reduces capillary water absorption by up to 96% and improves resistance to chloride penetration and carbonation.

3.2. Contact angles of water

Average wetting angles CA of water from six measurements are shown graphically in Fig. 3. Analysing the test results presented in Fig. 3, it can be seen that the values of contact angles depend on the type of hydrophobic agents.

The results of contact angle measurements showed that in all cases the contact angle (θ_w) decreases with time. The smallest contact angle $\theta_w=40.2°$ was obtained for standard samples at $t_1=0$ and the largest $\theta_w=112.2$ at $t_1=0$ for HA2, which indicates very good surface water repellency obtained by this preparation. The highest decrease by 57.2% of wetting angle value equal to $\theta_w=23°$ was observed after 45 minutes from applying water droplets on the reference specimens. Regarding hydrophobic concrete treated with HA2, the contact angle was reduced slightly by 7.75%. The CA for HA1 decreased after 45 minutes of testing by 19.65%.
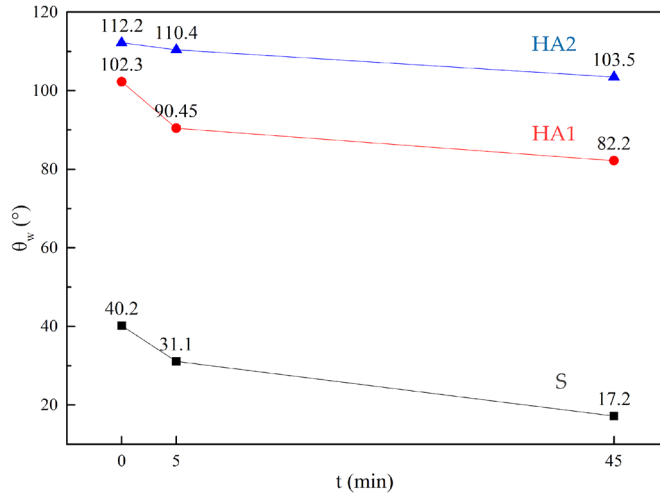
Fig. 3.   CAs for lightweight concrete containing CASD. *Source: own study*

The use by Barnat-Hunek et al. [61] of alkyl-alkoxy-siloxanes for surface hydrophobisation of porous mortar with expanded cork resulted in 2-3 times higher contact angle compared to unprotected samples. Qu and Yu [62] added ground granulated blast furnace slag as a waterproof admixture to lightweight concrete. This resulted in a contact angle of 92°. Barnat-Hunek et al. [63] in their work showed that surface waterproofing of lightweight concrete with sewage sludge with organic solvent-based methyl silicone resin increased 60-75-fold the contact angle values (compared to reference samples). A superhydrophobic concrete (S-concrete) was created in the work of Lei et al. [64]. By using copper mesh and stearic acid they achieved a contact angle of 159°. Contact angle at this level has been achieved because the micro-nano-structure of S-concrete has created a stable air bubble which is trapped between the droplet and the micro-nano-composite structure. It stops the droplet and prevents the specimen surface from wetting. Fic and Szewczak [65] have tested the effectiveness of hydrophobisation of building ceramics protected by polymers which have been disintegrated by ultrasound. Moreover, to the polymers, a filler in the form of microsilica was added. In their research, they determined the contact angles for two liquids (w - water and d – diiodomethane). For samples hydrophobised in pure (non-disintegrated) silicone solution, the average θ_d value was 92° and the θ_w value was about 125°. In the case of samples hydrophobised in the aqueous polymer solution, which has been disintegrated by ultrasound for 15 minutes, the θ_d value increased to 95°, with a θ_w of about 129°. For this reason, the developed coating is more effective as it prevents the absorption of both polar liquids (water) and organic solvents (apolar). For samples immersed in a disintegrated aqueous silicone solution with the addition of microsilica, there was a significant decrease in the θ_d value, while the θ_w value remained above 100°. This indicates the preservation of the hydrophobic character of the obtained coating.

3.3. SEM microstructural analysis

In order to determine the effectiveness and distribution of waterproof surfaces HA1, HA2, microscopic SEM analyses were performed. Fig. 4 shows the microstructure of the concrete.

The hardened mortar made of Portland cement consists mainly of about 67% of hydrated calcium silicates, the so-called C-S-H phases, about 22% of calcium hydroxide and products of hydration of aluminium and calcium aluminate ferroaluminium. Microscopic examination at the interface between cement mortar and CASD demonstrated good adhesion. No cracks or cavities in the joint between the two materials. Minor amounts of needle-shaped ettringite crystals are found (Fig. 4). CASD influenced the increased porosity of concrete compared with ordinary concrete.

(a)   (b)
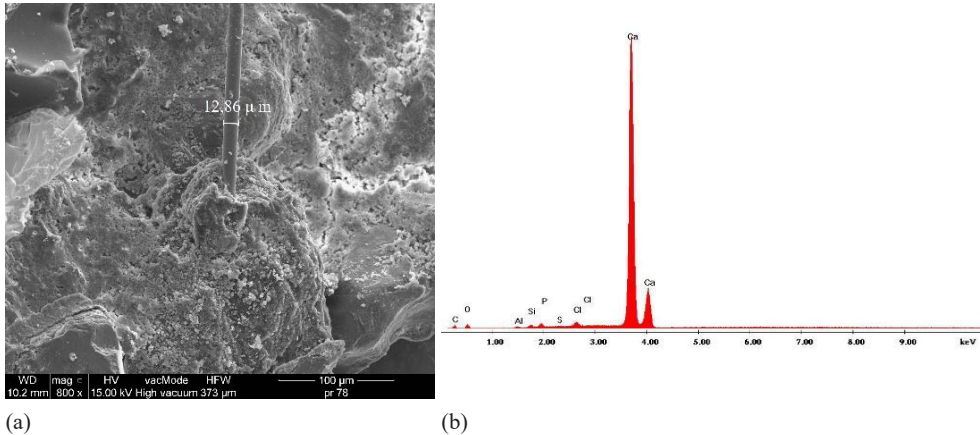
Fig. 4.   The scanning microscope structure of lightweight concrete with CASD (a) and results of elemental analysis in EDS micro-area (b) – compact clusters of C-S-H phase particles can be shown. *Source: own study*.

The distribution of polysiloxane gel in the structure of lightweight concrete with CASD is shown in Fig. 5.

(a)   (b)
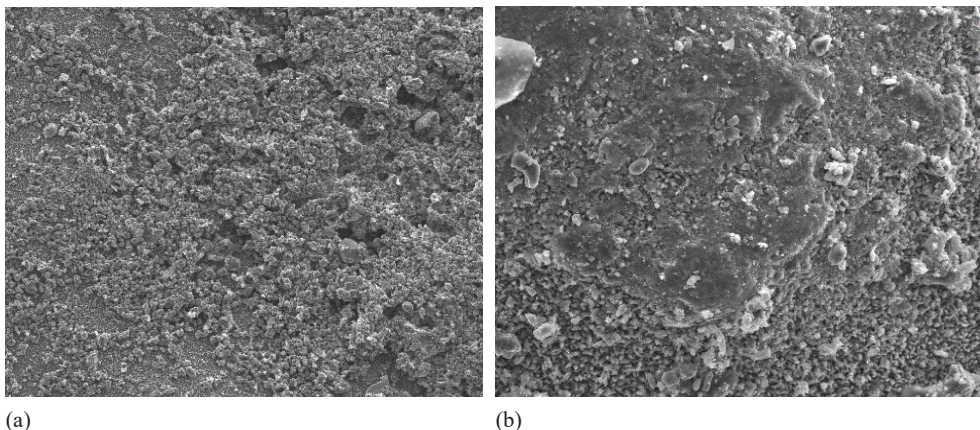
Fig. 5.   The structure of hydrophobised concrete with CASD: (a) water-soluble preparation HA1, (b) methyl-silicone resin HA2. *Source: own study*

On the structure of the reference samples, the products used produced an evenly distributed coating without visible cracks or scratches. Agent HA2 created a silicone coating which

covers the concrete structure most accurately (Fig. 5b). It has sealed the surface pores in this way, which may cause the porosity of the mortar to decrease slightly. In the case of CASD, their porosity remains unchanged. The preparation HA1 with an aqueous solvent has created a continuous and very thin film (Fig. 5a). HA1 has lessened the structure of lightweight concrete, which was also shown by CA measurements of a drop of water, which fell by 20º after 45 minutes, while in the case of HA2 only by 8.7º. The decomposition of both preparations does not cause too much sealing of the pores, so they should not interfere with steam permeability and diffusion.

In the paper by Qu and Yu [62], SEM images showed that samples containing 5% and 10% of GGBS have a denser structure. As the amount of GGBS increases, more pores appear in the concrete structure. With 20% addition of GGBS pores larger than 20 µm occurred in lightweight concrete. The SEM images shown in the work by Yoon et al. [66] pointed out the presence of calcium hydroxide and calcium silicate gels in conventional foam concrete. However, in the specimens of foam-concrete embedded in the aerogel, a large distribution of spherical nanoparticles was observed on the surface of pores and products of hydration. The structure of S-concrete shown in the study Lei et al. [64] presents a hierarchical micro-nano-structure and irregular fibres at the nanoscale. This structure contributes to the roughness of the sample surface. Furthermore, it was proved that stearic acid contributed to reducing the surface energy of the concrete and preventing the penetration of water into the concrete. Meso and micromorphology of concrete surface treated with control and superhydrophobic (SC) emulsion are presented in the paper by She et al. [67]. In the SEM images, specimens had a rough surface and consisted of multi-plane phases. The modified surface is composed of mechanically reinforced micro-pillars with a nano-roughness structure on them. The surface tomography was similar in meso- and micro-meter scale, but on the surface of concrete treated with SC there were more phases in the nanoscale. The researchers proved that the addition of silica can decrease the Ca/Si ratio of cement hydrate in the surface layer, thus improving mechanical properties. Franczak-Balmas in her study [68] showed how roughness is an important factor. She analysed the influence of roughness of the contact surface as a parameter shaping the load-bearing capacity of the joint of the composite concrete elements. In her paper, she proved that mechanical adhesion is a key component of the contact load-bearing capacity because as the surface roughness increases (development of the contact area), load-bearing capacity increases by 60%.

4. Conclusions

The presented studies showed that sawdust in the form of CASD can be used as additive in lightweight aggregate production. CASD can be effectively used in lightweight concrete production, which is proven with the results of physical and mechanical properties tests. The microscopic examination showed good adhesion of the contact points of cement paste and lightweight aggregates. Because of the higher absorbability and porosity caused by the CASD content in concrete, it is necessary to apply anti-moisture treatment on the surface of concrete in the form of hydrophobisation.

Measurement of the contact angle is one of ways of controlling wettability development of hydrophobised building materials. Application of different preparations leads to different wetting and adhesion properties of concrete. Lightweight concrete surface hydrophobisation has been observed to contribute to the formation of different CA. The value of CA grows noticeably on the water-repellent surface, especially with the organic solvent methyl silicone resin (HA2). For non-hydrophobic concrete, the CA values are 3-6 times lower than for the impregnated surface.

Introduction of organo-silicon compounds into the surface zone of lightweight concrete results in a reduction of absorbability which depends on the chemical structure of the preparations. This has the effect of limiting the penetration of corrosive substances into the structure of concrete, i.e. soluble salts, toxic gases, and thus influences its durability.

References

[1] Suliman N. H. et al., "Concrete using sawdust as partial replacement of sand : Is it strong and does not endanger health ?", *MATEC Web of Conferences*, vol. 258, (2019), p. 01015. https://doi.org/10.1051/matecconf/201925801015

[2] Kantautas A. and Vaickelionis G., "Modified sawdust concrete", *Statyba*, vol. 6, no. 2, (Jan. 2000), pp. 113–119. https://doi.org/10.1080/13921525.2000.10531574

[3] Paramasivam P. and Loke Y.O., "Study of sawdust concrete", *International Journal of Cement Composites and Lightweight Concrete*, vol. 2, no. 1, (Mar. 1980), pp. 57–61. https://doi.org/10.1016/0262-5075(80)90008-1

[4] Cheng Y. et al., "The Implementation of Waste Sawdust in Concrete", *Engineering*, vol. 05, no. 12, (Nov. 2013), pp. 943–947. https://doi.org/10.4236/eng.2013.512115

[5] Omar M. F. et al., "Partially Replacement of Cement By Sawdust And Fly Ash in Lightweight Foam Concrete", in IOP Conference Series: Materials Science and Engineering, 2020, vol. 743, no. 1. https://doi.org/10.1088/1757-899X/743/1/012035

[6] Bahtli T. and Ozbay N.S., "Corrosion resistances of C30 concrete: Effect of finely ground bronze sawdust waste", *Materials Chemistry and Physics*, vol. 243, (Mar. 2020), p. 122588. https://doi.org/10.1016/j.matchemphys.2019.122588

[7] Li M. et al., "Mechanical characterization of concrete containing wood shavings as aggregates", *International Journal of Sustainable Built Environment*, vol. 6, no. 2, (Dec. 2017), pp. 587–596. https://doi.org/10.1016/j.ijsbe.2017.12.005

[8] Sudin R. and Swamy N., "Bamboo and wood fibre cement composites for sustainable infrastructure regeneration", in Journal of Materials Science, 2006, vol. 41, no. 21, pp. 6917–6924. https://doi.org/10.1007/s10853-006-0224-3

[9] Chowdhury S. et al., "The incorporation of wood waste ash as a partial cement replacement material for making structural grade concrete: An overview", *Ain Shams Engineering Journal*, vol. 6, no. 2, (Jun. 2015), pp. 429–437. https://doi.org/10.1016/j.asej.2014.11.005

[10] Siddique R., "Utilization of wood ash in concrete manufacturing", *Resources, Conservation and Recycling*, vol. 67, (Oct. 2012), pp. 27–33. https://doi.org/10.1016/j.resconrec.2012.07.004

[11] Chowdhury S. et al., "Strength development in concrete with wood ash blended cement and use of soft computing models to predict strength parameters", *Journal of Advanced Research*, vol. 6, no. 6, (May 2014), pp. 907–913. https://doi.org/10.1016/j.jare.2014.08.006

[12] Drdlová M. et al., "The behavior of cement-bonded wood-chip material under static and impact load", in IOP Conference Series: Materials Science and Engineering, 2018, vol. 379, no. 1, p. 12025. https://doi.org/10.1088/1757-899X/379/1/012025

[13] Coatanlem P. et al., "Lightweight wood chipping concrete durability", *Construction and Building Materials*, vol. 20, no. 9, (Nov. 2006), pp. 776–781. https://doi.org/10.1016/j.conbuildmat.2005.01.057

[14] Kasai Y. et al., "Study on Wood Chip Concrete with Used Timber", *Special Publication*, vol. 179, (Jun. 1998), pp. 905–928.

[15] Chege J. et al., "The effects of pine (Pinus Canariensis) tree bark extract on the properties of fresh and hardened concrete.", *Civil and Environmental Research*, vol. 6, no. 9, (2014), pp. 70–81.

[16] Oba K. M. and Amadi I.G., "A Predictive Mathematical Model for Water Absorption of Sawdust Ash – Sand Concrete", *International Journal of Engineering and Management Research*, vol. 10, no. 01, (Feb. 2020), pp. 33–41. https://doi.org/10.31033/ijemr.10.1.7

[17] Ewaen Ikponmwosa E. et al., "Experimental and numerical investigation of the effect of sawdust ash on the performance of concrete", vol. 5, (2020), p. 15. https://doi.org/10.1007/s41024-020-00081-3

[18] Oyedepo O. J. et al., "Investigation of properties of concrete using sawdust as partial replacement for sand", *Civil and Environmental Research*, vol. 6, no. 2, (2014), pp. 35–42.

[19] Aldred J. M. et al., "The effect of initial moisture content on water transport in concrete containing a hydrophobic admixture", *Magazine of Concrete Research*, vol. 53, no. 2, (Apr. 2001), pp. 127–134. https://doi.org/10.1680/macr.2001.53.2.127

[20] Demirboğa R. and Gül R., "The effects of expanded perlite aggregate, silica fume and fly ash on the thermal conductivity of lightweight concrete", *Cement and Concrete Research*, vol. 33, no. 5, (May 2003), pp. 723–727. https://doi.org/10.1016/S0008-8846(02)01032-3

[21] Kim H. K. et al., "Workability, and mechanical, acoustic and thermal properties of lightweight aggregate concrete with a high volume of entrained air", *Construction and Building Materials*, vol. 29, no. 29, (Apr. 2012), pp. 193–200. https://doi.org/10.1016/j.conbuildmat.2011.08.067

[22] Suchorab Z. et al., "Influence of moisture on heat conductivity coefficient of aerated concrete", *Ecological Chemistry and Engineering S*, vol. 18, no. 1, (2011), pp. 111–120.

[23] Suchorab Z. et al., "Capillary rise phenomenon in aerated concrete. Monitoring and simulations", in Proc. ECOpole 2 (4) (2010), 2010, pp. 285–290.

[24] Lo T. Y. et al., "The effect of aggregate absorption on pore area at interfacial zone of lightweight concrete", *Construction and Building Materials*, vol. 22, no. 4, (Apr. 2008), pp. 623–628. https://doi.org/10.1016/j.conbuildmat.2006.10.011

[25] Tittarelli F., "Oxygen diffusion through hydrophobic cement-based materials", *Cement and Concrete Research*, vol. 39, no. 10, (Oct. 2009), pp. 924–928. https://doi.org/10.1016/j.cemconres.2009.06.021

[26] Suchorab Z. et al., "Free of volatile organic compounds protection against moisture in building materials", *Ecological Chemistry and Engineering S*, vol. 21, no. 3, (Oct. 2014), pp. 401–411. https://doi.org/10.2478/eces-2014-0029

[27] Czarnecki L., "Polymer concretes", *Cement Lime Concrete*, vol. 15 (2), (2010), pp. 63–85.

[28] Baltazar L. et al., "Superficial protection of concrete with epoxy resin impregnations: influence of the substrate roughness and moisture", *Materials and Structures/Materiaux et Constructions*, vol. 48, no. 6, (Jun. 2015), pp. 1931–1946. https://doi.org/10.1617/s11527-014-0284-9

[29] Osterholtz F. D. and Pohl E.R., "Kinetics of the Hydrolysis and Condensation of Organofunctional Alkoxysilanes: A Review", *Journal of Adhesion Science and Technology*, vol. 6, no. 1, (1992), pp. 127–149. https://doi.org/10.1163/156856192X00106

[30] Felekoğlu B., "A method for improving the early strength of pumice concrete blocks by using alkyl alkoxy silane (AAS)", *Construction and Building Materials*, vol. 28, no. 1, (Mar. 2012), pp. 305–310. https://doi.org/10.1016/j.conbuildmat.2011.07.026

[31] Zhu Y. G. et al., "Influence of silane-based water repellent on the durability properties of recycled aggregate concrete", *Cement and Concrete Composites*, vol. 35, no. 1, (Jan. 2013), pp. 32–38. https://doi.org/10.1016/j.cemconcomp.2012.08.008

[32] Nakamura Y. et al., "Surface analysis of silane nanolayer on silica particles using 1H pulse NMR", *Journal of Adhesion Science and Technology*, vol. 25, no. 19, (Jan. 2011), pp. 2703–2716. https://doi.org/10.1163/016942411X556079

[33] Xiong G. et al., "Influence of silane coupling agent on quality of interfacial transition zone between concrete substrate and repair materials", *Cement and Concrete Composites*, vol. 28, no. 1, (Jan. 2006), pp. 97–101. https://doi.org/10.1016/j.cemconcomp.2005.09.004

[34] Klisińska-Kopacz A. and Tilova R., "Effect of hydrophobization treatment on the hydration of repair Roman cement mortars", *Construction and Building Materials*, vol. 35, (Oct. 2012), pp. 735–740. https://doi.org/10.1016/j.conbuildmat.2012.05.002

[35] MacMullen J. et al., "Brick and mortar treatment by cream emulsion for improved water repellence and thermal insulation", *Energy and Buildings*, vol. 43, no. 7, (Jul. 2011), pp. 1560–1565. https://doi.org/10.1016/j.enbuild.2011.02.014

[36] Chmielewska B. et al., "The influence of silane coupling agents on the polymer mortar", *Cement and Concrete Composites*, vol. 28, no. 9, (Oct. 2006), pp. 803–810. https://doi.org/10.1016/j.cemconcomp.2006.04.005

[37] Matziaris K. et al., "Impregnation and super-hydrophobicity of coated porous low-fired clay building materials", in Progress in Organic Coatings, 2011, vol. 72, no. 1–2, pp. 181–192. https://doi.org/10.1016/j.porgcoat.2011.03.012

[38] Rudawska A., "Selected issues on establishing adhesion bonds – homogeneous and hybrid", in Monographs – Lublin University of Technology, Lublin, 2013.

[39] European Committee for Standardization, EN 828:2013-05. Adhesives. Determining wettability by means of measuring the contact angle and critical surface tension of solid. CEN: Brussels, Belgium, 2013.

[40] Lugscheider E. and Bobzin K., "The influence on surface free energy of PVD-coatings", *Surface and Coatings Technology*, vol. 142, (2001), pp. 755–760. https://doi.org/10.1016/S0257-8972(01)01315-9

[41] Baldan A., "Adhesion phenomena in bonded joints", *International Journal of Adhesion and Adhesives*, vol. 38, (2012), pp. 95–116. https://doi.org/10.1016/j.ijadhadh.2012.04.007

[42] Vedantam S. and Panchagnula M.V., "Constitutive modeling of contact angle hysteresis", *Journal of Colloid and Interface Science*, vol. 321, no. 2, (May 2008), pp. 393–400. https://doi.org/10.1016/j.jcis.2008.01.056

[43] Zielecka M., "Methods of contact angle measurement as a tool for characterization of wettability of polymers", *Polimery-W*, vol. 49, (2004), pp. 327–332.

[44] Żenkiewicz M. et al., "Contact angle and surface free energy of electron-beam irradiated polymer composites", *Polimery-W*, vol. 53, (2008), pp. 446–451.

[45] Shang J. et al., "Comparison of different methods to measure contact angles of soil colloids", *Journal of Colloid and Interface Science*, vol. 328, no. 2, (Dec. 2008), pp. 299–307. https://doi.org/10.1016/j.jcis.2008.09.039

[46] Klein N. S. et al., "Evaluation of the wettability of mortar component granular materials through contact angle measurements", *Cement and Concrete Research*, vol. 42, no. 12, (2012), pp. 1611–1620. https://doi.org/10.1016/j.cemconres.2012.09.001

[47] European Committee for Standardization., EN 206+A1:2016-12. Concrete – Part 1: Specification, performance, production and conformity. CEN: Brussels, Belgium, 2016.

[48] Polish Committee for Standardization, PN-B-06265:2004. National supplements PN-EN 206-1:2003 Concrete – Part 1: Specification, performance, production and conformity. PKN: Warsaw, Poland.

[49] European Committee for Standardization., EN 197-1:2012. Cement—Part 1: Composition, Specifications and Conformity Criteria for Common Cements; CEN: Brussels, Belgium, 2012.

[50] Polish Committee for Standardization. and European Committee for Standardization, EN 1936:2010. Natural stone test methods – Determination of real density and apparent density, and of total and open porosity. PKN: Warsaw, Poland, 2010.

[51] Polish Committee for Standardization, PN-EN 1389:2005. Polish National Supplement: PN-EN 206-1:2003 Concrete. Specification, performance, production and conformity. PKN: Warsaw, Poland, 2005.

[52] European Committee for Standardization, EN 12390-7:2019. Testing hardened concrete. Density of hardened concrete. CEN: Brussels, Belgium, 2019.

[53] European Committee for Standardization, EN 12390-3:2019. Testing hardened concrete – Part 3: Compressive strength of test specimens. CEN: Brussels, Belgium, 2019.

[54] Polish Committee for Standardization and Polish Committee for Standardization., PN-B-06250:1988. Ordinary concrete (In Polish). PKN: Warsaw, Poland, 1988.

[55] Rudawska A. and Jacniacka E., "Analysis for determining surface free energy uncertainty by the Owen-Wendt method", *International Journal of Adhesion and Adhesives*, vol. 29, no. 4, (Jun. 2009), pp. 451–457. https://doi.org/10.1016/j.ijadhadh.2008.09.008

[56] Thalmaier G. et al., "Influence of sawdust particle size on fired clay brick properties", *Materiales de Construcción*, vol. 70, no. 338, (Mar. 2020), p. 215. https://doi.org/10.3989/mc.2020.04219

[57] Md Noor N. et al., "Compressive strength, flexural strength and water absorption of concrete containing palm oil kernel shell", in IOP Conf. Series: Materials Science and Engineering 271, 2017.

[58] Castro J. et al., "Effect of sample conditioning on the water absorption of concrete", *Cement and Concrete Composites*, vol. 33, no. 8, (Sep. 2011), pp. 805–813. https://doi.org/10.1016/j.cemconcomp.2011.05.007

[59] Szafraniec M. et al., "Surface Modification of Lightweight Mortars by Nanopolymers to Improve Their Water-Repellency and Durability", *Materials*, vol. 13, no. 6, (Mar. 2020), p. 1350. https://doi.org/10.3390/ma13061350

[60] Suchorab Z. et al., "Mechanical and physical properties of hydrophobized lightweight aggregate concrete with sewage sludge", *Materials*, vol. 9, no. 5, (Apr. 2016), pp. 1–18. https://doi.org/10.3390/ma9050317

[61] Barnat-Hunek D. et al., "Properties of hydrophobised lightweight mortars with expanded cork", *Construction and Building Materials*, vol. 155, (Nov. 2017), pp. 15–25. https://doi.org/10.1016/j.conbuildmat.2017.08.052

[62] Qu Z. and Yu Q.L., "Synthesizing super-hydrophobic ground granulated blast furnace slag to enhance the transport property of lightweight aggregate concrete", *Construction and Building Materials*, vol. 191, (Dec. 2018), pp. 176–186. https://doi.org/10.1016/j.conbuildmat.2018.10.018

[63] Barnat-Hunek D. et al., "Evaluation of the Contact Angle of Hydrophobised Lightweight-Aggregate Concrete with Sewage Sludge", *Ecological Chemistry and Engineering S*, vol. 22, no. 4, (Jan. 2015), pp. 625–635. https://doi.org/10.1515/eces-2015-0037

[64] Lei L. et al., "Fabrication of superhydrophobic concrete used in marine environment with anti-corrosion and stable mechanical properties", *Construction and Building Materials*, vol. 251, (Aug. 2020), p. 118946. https://doi.org/10.1016/j.conbuildmat.2020.118946

[65] Fic S. and Szewczak A., "Hydrophobisation effectiveness of building ceramics, polymeric inorganic ultrasound integrated with the addition of fillers", *Budownictwo i Architektura*, vol. 14, no. 4, (Dec. 2015), pp. 019–027. https://doi.org/10.35784/BUD-ARCH.1517

[66] Yoon H. S. et al., "Thermal transfer and moisture resistances of nano-aerogel-embedded foam concrete", Construction and Building Materials, vol. 236, (Mar. 2020), p. 117575. https://doi.org/10.1016/j.conbuildmat.2019.117575

[67] She W. et al., "Superhydrophobic concrete with enhanced mechanical robustness: Nanohybrid composites, strengthen mechanism and durability evaluation", Construction and Building Materials, vol. 247, (Jun. 2020), p. 118563. https://doi.org/10.1016/j.conbuildmat.2020.118563

[68] Franczak-Balmas D., "Analiza wpływu szorstkości powierzchni styku jako parametru kształtującego nośność styku zespolonych elementów betonowych", *Budownictwo i Architektura*, vol. 16, no. 3, (Dec. 2017), pp. 125–134. https://doi.org/10.24358/Bud-Arch_17_163_12

Crossref
Similarity Check
Powered by iThenticate

Orginal Article

Self-healing cement materials – microscopic techniques

Marta Dudek

Chair of Building Materials Engineering; Faculty of Civil Engineering;
Cracow University of Technology; Warszawska St. 24, 31-155 Cracow, Poland;
marta.dudek@pk.edu.pl (iD) *0000-0003-0658-6922*

Abstract: The article presents a general classification of intelligent materials with self-healing (self-repairing) properties, focusing on self-healing cementitious materials. The purpose of the paper is to describe the prospects of two of the most popular micro-observation techniques, i.e. with the use of an optical and scanning electron microscope. In addition, it describes the advantages of using a tensile stage mounted in the microscope chamber for testing self-healing materials. The advantages and disadvantages of these devices have been characterized, and the results of preliminary research have been provided. The tests include the optical microscopy and scanning electron microscopy observations of the microstructure of cracks before and after the process of healing. They were carried out using ZEISS Discovery V20 optical microscope and ZEISS EVO-MA 10 scanning electron microscope on mortar samples modified with macro capsules filled with polymer. In addition to observations, chemical analysis was performed with the use of an EDS detector. The microscopic observations and chemical analyses provide the basis for assessing the effectiveness of the self-healing process, showing that the crack has been healed. Moreover, the preliminary results of the tests of micro-mechanical properties, carried out with the use of a tensile stage, have been described. The problems of using this research technique are also listed. This study shows the usefulness of this kind of tests for microcapsules for self-healing materials.

Keywords: optical microscopy, scanning electron microscopy, tensile stage, self-healing cementitious materials, micro-mechanical properties

1. Introduction

Intelligent materials are the subjects of many scientific research conducted in various branches of science. According to Takagi [1] "intelligent materials" are materials which are able to react (respond) to external impulses by significantly changing its own properties and obtain expected and effective reaction to such impulses, whereas "smart materials" only have a predictable effect of changing the properties under external impulses. The group of intelligent materials comprises of materials with an ability to change colour, emit light, change shape

and size (also with shape-memory properties), change temperature and density, self-group, self-heal and self-repair.

The research conducted all over the world on self-healing (self-repairing) materials were inspired by the nature, and especially self-healing processes which occur e.g. in human body. For example, injured skin or broken bone has the ability to heal without human intervention. Bearing this in mind, scientists were striving to develop materials with the capability of self-healing in case of damage. These materials are also known as intelligent materials, as they can sense changes, process information and respond to these changes [2]. According to Zwaag [3], self-healing materials are those materials which have negative damage rate at one or several stages of use. It means that damages heal themselves, and as a result, over time there are fewer damages than there were at the beginning. The effectiveness of this process depends on the speed of damage formation and the speed of self-healing. Polymers are the materials which have best self-healing properties. Then, there are ceramic materials, especially cement materials. The most problematic group, in the context of these abilities, are metals [4].

The aim of the self-healing (self-repairing) process of cement materials is to completely or partially recover their original properties or contain destructive processes (for example the propagation of crack) [5]. Self-healing cement materials, due to their fragile nature, are mainly destined to close the crack.

According to RILEM Technical Committee [5], self-healing involves all the processes leading to the recovery of the properties. They are divided into two basic groups:

– Autogenous: a self-healing process is autogenous when it concerns components of materials which have been used to form that material (they were not added for the purpose of obtaining self-healing properties).

– Autonomous: a self-healing process is autonomous when it uses components which have been added for the purpose of obtaining self-healing properties. They can be for example mineral additives, capsules filled with self-healing materials, and many others.

The autogenous self-healing process of concrete consists in filling and sealing cracks caused by chemical reactions with non-hydrated concrete mixture components and carbonation reactions, which are natural reactions for setting of the cement bond. From this point of view, cementitious materials, by their nature, have high self-healing potential. The reason is the hydration process of cement components, which lasts for years, and most of all, presence of non-hydrated or partially hydrated cement grains. When the concrete cracks, these grains react with the moisture, forming additional phases of concrete sealing. However, in the process of autonomous healing, cracks are closed by hydration of mineral substances that were added to the materials for the purpose of obtaining such characteristic. They have pozzolanic and expansive properties, after having reacted with water, and they trigger new products of hydration. On the other hand, activated repair is based on healing properties of components which were added during the production process, for example capsules filled with polymer resin or with bacteria.

2. Materials and Methods

Depending on the aim of self-healing (self-repairing) process, there are different techniques used to verify the effectiveness of that process. If the purpose of the process of recovery of the original properties is to improve the resistance to external environment, the tests that allow to assess the permeability of material are used. Whereas, in case of mechanical

recovery, strength tests are preferable. However, microscopic tests are very important in all of the processes. Their aim is usually to measure occurring cracks, assess the process of cracks propagation over time, and also to assess the self-healing process of the material.

2.1. Optical microscopy

An optical microscope is used to magnify the image, due to its construction consisting of a system of lenses, through which a beam of light is sent. As a result, an enlarged and inverted image is received. The research with the use of optical microscopy is one of the ways to assess the width of the crack during the process of sealing in self-healing materials. This technique is cost-effective and easy to handle. It provides, in comparison to scanning electron microscopy, the possibility of colourful sample observation, which helps to visualize the process of crack sealing. It makes it also possible to observe samples of much greater size. What is more, it provides bigger field of observation, which makes it easier to analyse cracks, the structure of materials, pores and aggregates. In this case, to obtain a good quality of image, a user can operate parameters such as: work distance, magnification, lighting, filters, and distribution of optical elements [5]. Numerous publications indicate that the use of this device is prevalent amongst researchers [6, 7]. Many of them have been using optical microscopes for assessing the effectiveness of sealing cracks in mortars with biological substances closed in lightweight aggregates, and also for the observation of the influence of powdered materials closed in self-healing capsules.

2.2. Scanning electron microscopy

The principle of image formation in scanning electron microscopy is different than in optical microscopy. This technique does not use light beams; the observed sample is scanned by focused high-energy electron beam generated with the use of the electron gun. In this process, electrons interact with atoms in the sample, and the tested material emits a variety of signals recorded by detectors. These signals are secondary electrons, backscattered electrons, and characteristic X-rays. Subsequently, the detectors process them into an image. Secondary electrons are responsible for creating the image with information about the topography of the sample; backscattered electrons, on the other hand, give better phase contrast, while the characteristic X-rays allow for the elemental analysis of the composition. SEM yields much greater magnifications (several to dozen of thousands of times) and at the same time, it maintains the depth of focus and good resolution. Its main disadvantage, in comparison to the optical microscope, is the fact that the image is in shades of grey, which necessitates the use of small and very small samples, which very often also requires a proper preparation, and provides a smaller view. However, it enables more detailed analysis of the material, especially if there is a need to see the elements invisible to the naked eye. It allows also to make a chemical elemental analysis during sample observation by using special detectors. The quality of images is impacted among the others by pressure in the chamber, work distance, material contamination, spot size, scanning speed and accelerate voltage [5].

Due to the size of magnification, scanning electron microscopy is more often used in the research concerning self-healing materials than optical microscopy. The authors of the publication [9] about self-healing concretes modified with capsules used SEM to assess the appearance of capsules and their micro-morphology [10]. In particular, they determined their diameter and layer thickness. The researchers compared the effect of calcium-nitrate

micro-capsules on further concrete strength by modification of the encapsulation method, and they assessed how it affects strength reduction. With this technique, it is possible to estimate the self-healing capabilities of cementitious composites [11], not only by observation of cracks and the area after their sealing, but also by assessment of the chemical elemental composition of healing products with the use of EDX method. In this advanced technique, it is also possible to monitor the process of leaking of the healing substance from capsules, to observe sealing process, and to determine what affects its speed [10].

2.3. Tensile stage mounted in scanning electron microscope

The DEBEN MICROTEST 200N tensile stage is made to be mounted in the scanning electron microscope chamber (Figure 1). It gives the possibility to determine the tensile, compressive and fatigue strength during the simultaneous microstructure observations in SEM. The working range of the device is 200N; it works at a speed from 0.1mm/min to 1.5mm/min. During the test, a graph is drawn which shows the influence of force on elongation or time. It can be used to assign micro-mechanical properties.
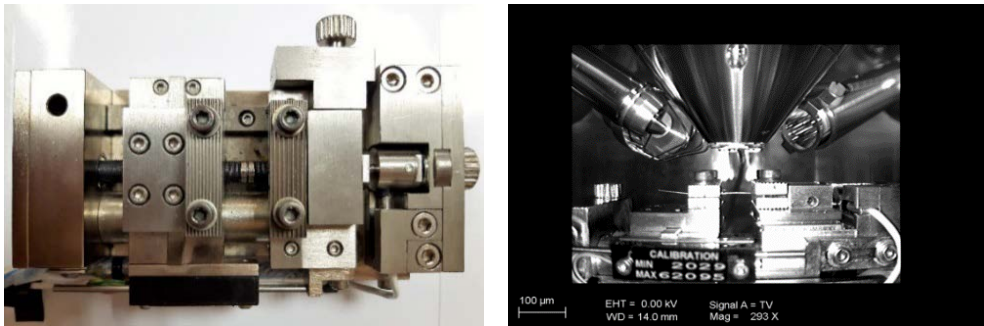
Fig. 1.   Tensile stage – general view (on the left), scanning electron microscope chamber with mounted tensile stage (on the right). *Source:* author's own study

3. Results and discussion

3.1. The results of optical microscopy

This research was performed by means of a ZEISS Discovery V20 optical microscope with magnification up to 345x. The tool has the option to change parameters such as magnification, focus, contrast, and brightness during observations. Luminous methods and contrasts are achieved by LEDs or cold light.

Sample results of the observation of cracks after the healing process are presented in the Figure 2. For the study mortars beams were used (40x40x160mm³), modified with glass capsules filled with polymer. After initiating a crack made with 3-point bending test, the capsule burst, and the healing agent filled the crack. The image on the left shows a sample of the cut mortar with the capsule, while the image on the right shows the bottom of the beam along the crack, where the polymer flows.
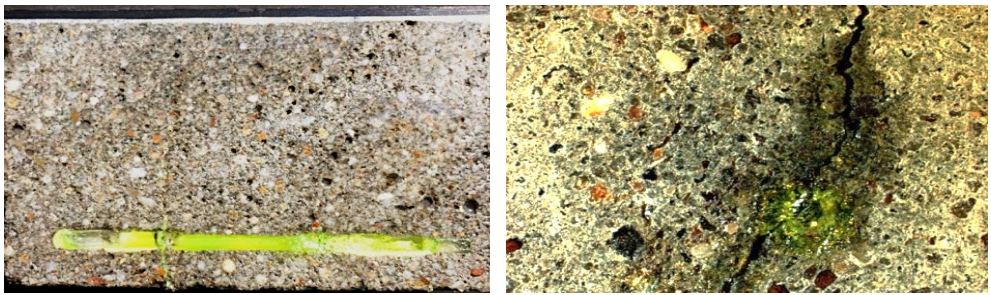
Fig. 2.   On the left: image of a sample of the cement mortar with capsule filled with polymer viewed with optical microscope Zeiss Discovery V20. On the right: crack after healing. Yellow colour indicates the place where polymer leaked from the capsule in the place where the crack occurred. *The source:* author's own study

3.2. The results of electron microscopy

Microstructure observations were carried out on the same samples as with the use of optical microscope (Figure 3) by the author of the paper. For the test, a ZEISS EVO-MA 10 scanning electron microscope was used, equipped with SE, VPSE and BSD detectors, as well as with the EDS Bruker XFLASH 6/30 detector, that facilitates chemical elemental composition analysis (line, point and mapping). The SE and VPSE detectors enable to observe sample topography, depending on high vacuum (SE) or variable vacuum (VPSE) used during the research, whereas BSD detector allows a better contrast while observing the sample in both conditions, which is especially helpful during EDS analysis. Scanning electron microscopy with this device allows for testing the microstructure of materials of a maximum height of 100mm, a diameter up to 230mm and weight not exceeding 0.5kg. The possible magnification enlarges the view from several dozen to a several dozens of thousands of times.

The pictures made by the author during the research show a sample of mortar after pre-cracking and after healing the crack with the polymer that has leaked from the capsule. The images were taken at a magnification of 50x, maintaining a working distance of 16mm. A BSD detector was used, and tests were carried out at accelerating voltage of 20 kV.
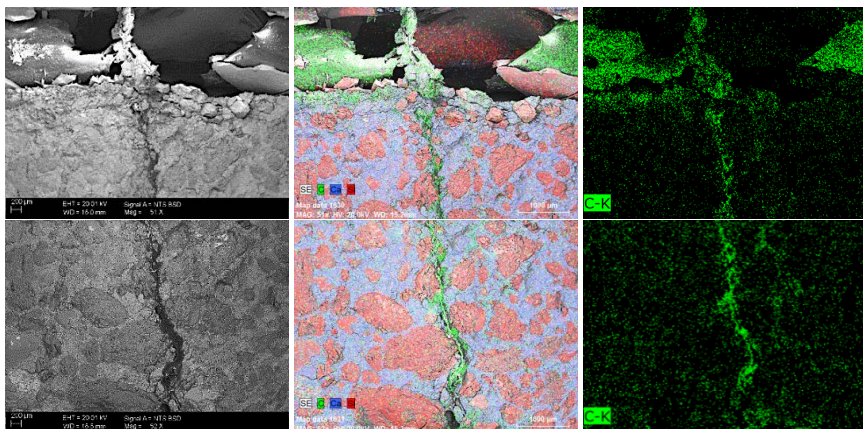
Fig. 3.   SEM image of a part of capsule after the healing process, a visible crack filled with polymer, at 50x magnification. Surface distribution of chemical elements: carbon (green), calcium (blue) and silicon (red). Carbon mapping indicates the crack filled with polymer. The first line shows capsule and the second line the further part of sample along the crack. *Source:* the author's own study

3.3. The results of micro-strength test in scanning electron microscopy by using a tensile stage

For the purpose of the research, vitamin (powder) micro-capsules in shape of oval were stuck with cyanoacrylate glue to previously prepared handles (printed with a 3D printer). Prepared research elements were sprayed with gold to obtain a better visual effect under microscope. Pictures of samples and tests results carried out with the use of a tensile stage are presented in Figure 4-5.
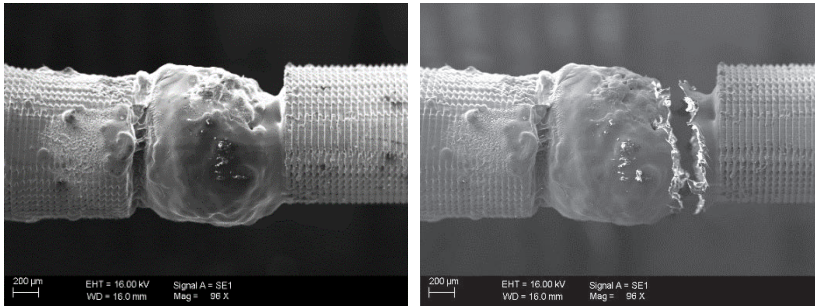
Fig. 4.   SEM images of attached powder micro-capsule installed in a tensile stage (on the left) and micro-cap-
          sule after stretching (on the right). The test was performed at 96x magnification. *Source:* the author's
          own study
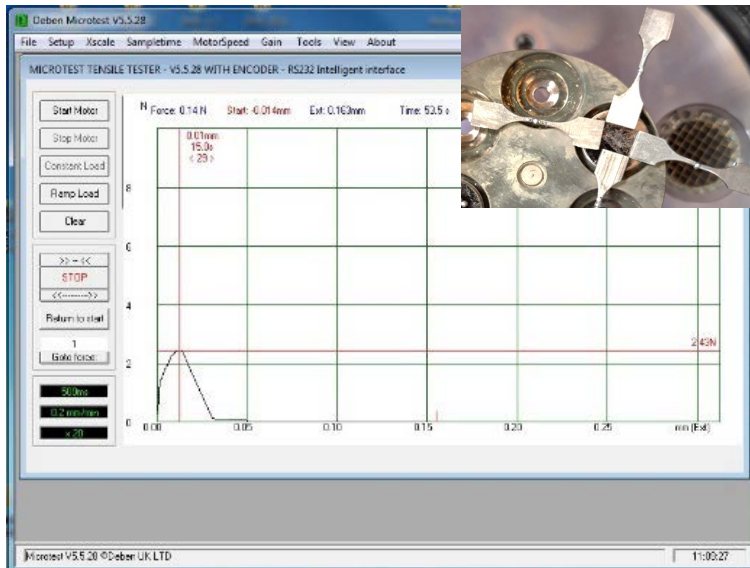
Fig. 5.   The result of tensile strength test of a powder micro-capsule under a tensile stage mounted in the
          microscope chamber. Examination of the impact of the force and elongation of the sample. Photo
          of the sample with 2 cm long handles (micro-capsule attached to handles printed in a 3D printer).
          Source: the author's own study

The research allowed to determine the elongation of the sample and the maximum value of force needed to destroy the element. The video made during the test made it possible to recognize the moment when the first cracks appeared in the material. The destruction was

not very rapid, with the time lag between consecutive cracks, and finally a part of material broke away from the capsule along the line of the cracks. A graph showing impact of force on elongation was obtained, due to which it was possible to determine the tensile strength of the capsule. The maximum force value was 2.43N and elongation was 0.01mm, which gives approximately the strength of 3 MPa.

4. Conclusions

The results of the research described in the article are the basis for assessing the possibility of using an optical microscope and scanning electron microscope with a tensile stage for testing the process of self-healing of cementitious materials. The microscopic observation techniques are commonly used in tests and observations of the materials with self-healing properties. However, every type of material requires to adapt the research to the methodology. Other interesting feature is the possibility to determine micro-mechanical properties of engineering materials, such as other capsules.

In the research described in the paper, the observations were made on mortar beams modified with macro-capsules filled with polymer with the use of both optical and scanning microscopes. By using these research methods, it is possible to visually assess whether a given crack has been sealed. Research with the use of an optical microscope resulted in a preview of a larger part of the sample due to the larger field of view. Scanning microscopy, however, enabled more accurate observations of the crack and the polymer that filled it. The use of chemical analysis has facilitated the assessment of the effectiveness of the healing process. In this case, the polymer marked with the green marker shows exactly where the polymers were distributed in the crack.

The test with the use of a tensile stage was carried out on micro-capsules, in this case on prototype samples in order to better understand the capabilities of the device. It is crucial to determine mechanical strength of both micro- and macro-capsules in self-healing materials. These capsules should break when the material (mortar in this case) is pre-cracked, not before. They should not either be more durable than the material itself. The determination of their mechanical characteristics enables the selection of a suitable material for the carrier of the healing agent.

References

[1]   Takagi T., "Present state and future of the intelligent materials and systems in Japan", *Journal of Intelligent Material Systems and Structure,* no. 10, (1999), pp. 575-581.

[2]   „Polimery są materiałami przyszłości", *Chemia i Biznes.*, no. 3, (2015), Available: https://www.chemiaibiznes.com.pl/aktualnosc/polimery-sa-materialami-przyszlosci [Accessed: 25 Nov 2019]

[3]   Zwaag S. (ed), "Self-healing materials, an alternative approach to 20 centuries of materials science", *Springer Series in Materials Science*, vol. 100, Springer, Dordrecht 2007.

[4]   Hager M.D. et al., (2010). „Self-healing materials", *Advanced Materials*, pp. 5424-543, https://doi.org/10.1002/adma.201003036, quoted after: Zając B., Gołebiowska I., „Procesy odtwórcze w materiałach cementowych", *Inżynieria i Aparatura Chemiczna* vol. 55, no. 3, (2016), pp.112-113.

[5]   Rooij M. et al., *State-of-the-Art Reports, Self-Healing Phenomenain Cement-Based Materials*. Editors Technical Committee 221-SHC: Self-Healing Phenomenain Cement-Based Materials. Springer 2013.

[6]   Tziviloglou E. et al., "Bio-based Self-healing Mortar: An Experimental and Numerical Study", *Journal of Advanced Concrete Technology*, vol. 15, no. 9, (2017), pp. 536-543. https://doi.org/10.3151/jact.15.536

[7]   Alghamri R. Kanellopoulos A. Al-Tabbaa., "Impregnation and encapsulation of lightweight aggregates for self-healing concrete", *Construction and Building Materials,* no. 124, (2016), pp. 910-921. https://doi.org/10.1016/j.conbuildmat.2016.07.143

[8]   Qureshi T.S., Kanellopoulos A., Al-Tabbaa., "Encapsulation of expansive powder minerals within a concentric glass capsule system for self-healing concrete", *Construction and Building Materials,* no. 121, (2016), pp. 629-643. https://doi.org/10.1016/j.conbuildmat.2016.06.030

[9]   Al-Ansari M., et al., "Performance of modified self-healing concrete with calcium nitrate micro-encapsulation", *Construction and Building Materials,* no. 149, (2017), pp. 525-534. https://doi.org/10.1016/j.conbuildmat.2017.05.152

[10]   Dong B. W. et al., "Smart releasing behavior of a chemical self-healing microcapsule in the stimulated concrete pore solution", *Cement and Concrete Composites*, no. 56, (2015), pp .46-50. https://doi.org/10.1016/j.cemconcomp.2014.10.006

[11]   Yildirim G. et al., "A review of intrinsic self-healing capability of engineered cementitious composites: Recovery of transport and mechanical properties", *Construction and Building Materials*, no. 101, (2015), pp. 10-21. https://doi.org/10.1016/j.conbuildmat.2015.10.018

Program of fragmentary revitalization of the historical town of Lyashky Murovani. Murovane Village, Staryi Sambir district in the Lviv Region

Zoriana Lukomska[1], Halyna Lukomska[2], Iryna Shevchuk[3]

[1] Department of Architecture and Urban Planning; Institute of Architecture, Construction and Power Engineering; Ivano-Frankivsk National Technical University of Oil and Gas; Karpatska St. 15, 76019 Ivano-Frankivsk, Ukraine
sorianalukomska@gmail.com (iD) *0000-0002-8769-1830*

[2] Department of Architecture and Urban Planning; Institute of Architecture, Construction and Power Engineering; Ivano-Frankivsk National Technical University of Oil and Gas; Karpatska St. 15, 76019 Ivano-Frankivsk, Ukraine
galia.lukomska@gmail.com (iD) *0000-0001-9252-0094*

[3] Department of Architecture and Urban Planning; Institute of Architecture, Construction and Power Engineering; Ivano-Frankivsk National Technical University of Oil and Gas; Karpatska St. 15, 76019 Ivano-Frankivsk, Ukraine
irashevchuk.mail@gmail.com (iD) *0000-0002-6248-1271*

Abstract: The research uncovers the value and uniqueness of the volumetric planning structure of the historical town of Lyashky Murovani, now known as Murovane Village, Staryi Sambir district in the Lviv region.

Within the town features of Baroque urban planning are found and characteristics of the historical urban development of the location are revealed. The current components of the volumetric and spatial composition of the former city are analysed. A reconstruction scheme of the 17th-century city planning structure was presented, when it consisted of a market square with residential buildings blocks, sacral objects, and a palace and park complex. The study also reveals that the urban object passed through several stages of reconstruction during its development. A fragmentary revitalization program of the historical town into a modern village of Murovane was proposed.

Keywords: historical town, historical planning structure, valuable urban object, palace and park complex, Lyashky Murovani

1. Introduction

The process of researching the architectural and urban heritage of Western Ukraine, brings several problems to the fore. The most prominent ones are the lack of preservation, lack of protection and poor presentation of valuable historic urban ensembles and complexes, of which create the image of cities in the past and are now significant components of such historical cities and settlements. The aforementioned problems are especially related to the settlements that lost their city status during their historical development and consequently decayed or become destroyed. Once magnificent and with glorious history, developed according to the progressive European traditions of city planning, castles, palaces, palace and park complexes, today are experiencing a period of decline and destruction. It is however possible to stop this process, by applying a comprehensive approach to the formation of new positive image of these valuable historical objects.

Today, the key problem is to find ways for preservation and protection of these complexes and their components. The primary task is to display these valuable historical, architectural, and urban complexes in the architectural heritage and urban planning documentation. The next stage is to plan a development strategy and to create regeneration programs of urban objects that would reveal their historical and architectural value, to ensure their coexistence with the contemporary urban area, and to maximize their further protection and conservation [1, 4, 5].

2. Historical, architectural and urban development of Murovane village

This paper presents the historical town of Lyashky Murovani, which is one of the most valuable town-planning objects in the Ukraine. The town stands out because of its unique urban structure of the 17th and 18th centuries, and today is now known as Murovane Village, located in the Staryi Sambir district, in the Lviv region, on the Khyriv – Staryi Sambir route. The urban composition originally consisted of a castle-palace ensemble with a large-scale park, a market square framed with buildings, sacral structures, and probably fortifications (Fig. 1, 2).

Fig. 1.   Liashky Murovani. Austrian military map of Halychyna 1806 – 1869. Fragment

Fig. 2.   Cadastre map of the town Liashky Murovani, 1853. Fragment

Historical references to the existence of a town with a market square in the area around the castle, owned by the Mniszech family, date back to the 16th century. There is also evidence that this town had been granted the Magdeburg rights [3].

The castle was mentioned mostly in historical descriptions. It was located in the northern part of the city on a small hill surrounded by the plain. The castle was built in the mid 16th century by the Tarlo family. In 1592 it was handed over to the Mniszech family, i.e. Jerzy Mniszech, a governor of Sandomierz Province. The castle had a pentagonal plan and was surrounded by three lines of ramparts, the last one of which had three bastions in its three corners. The castles established by Jerzy Mniszech were one of the largest and richest castles in Rus in the 16th century, they boasted powerful construction equipment, fortifications, internal equipment, and opulent decoration. The castle building is characterized by Russian features – it was two stories high and included an underground level. The ramparts, which surrounded the castle, contained large casemates inside. [2].

In addition to the representative purpose, the castle in Lyashky Murovani had a defensive function and stood in the way of frequent invasions of Tatars and the Turks, as was another, similar castle in the neighborhood of Dobromyl. Both castles had military garrisons and served as the last refuge for local settlers during these attacks.

The development of the castle, and later the palace in Lyashky Murovani, is closely connected with many significant historical events and personalities that influenced its further development and formation. Especially Maryna Mniszech, who was born there in circa 1588, who was the upcoming queen of Moscow, and the wife of False Dmitry I.

In the mid 17th century, while under the ownership of Franciszek Bernard Mniszech, the castle was badly damaged by a fire, but was subsequently restored or rebuilt [3].

Probably during this period, the former castle completely lost its defensive function and the Mniszech family's home was transformed into a residential palace, with a predominantly representative function and a completely leveled defense.

During this period, the castle and palace complex acquired even more expressive character, so it could match the Berezhany, Krasiczyn, Pidhirtsi, and Zhovkva castles. It was shaped as a large pentagon, with a spacious courtyard inside and three round towers in each corner outside. The entrance proceeded through a gate in the southwest corner, underneath the clock tower. The tower had several levels and was a dominant feature throughout the composition. The contemporaries admired the majesty of the internal system. The palace had forty-five

rooms and two knight halls with marble floors, which measured sixty feet by forty-five feet. In addition to rich furniture, expensive weapons, gilded cornices, and stucco, the walls were decorated with precious fabrics, paintings, family portraits, and portraits of Polish kings [2].

In the 17th century, bastions surrounded the castle and a large garden was created on the northwest. The plan, which was drawn up in 1734, contains an accurate conception of the palace building and the park (Fig. 3).
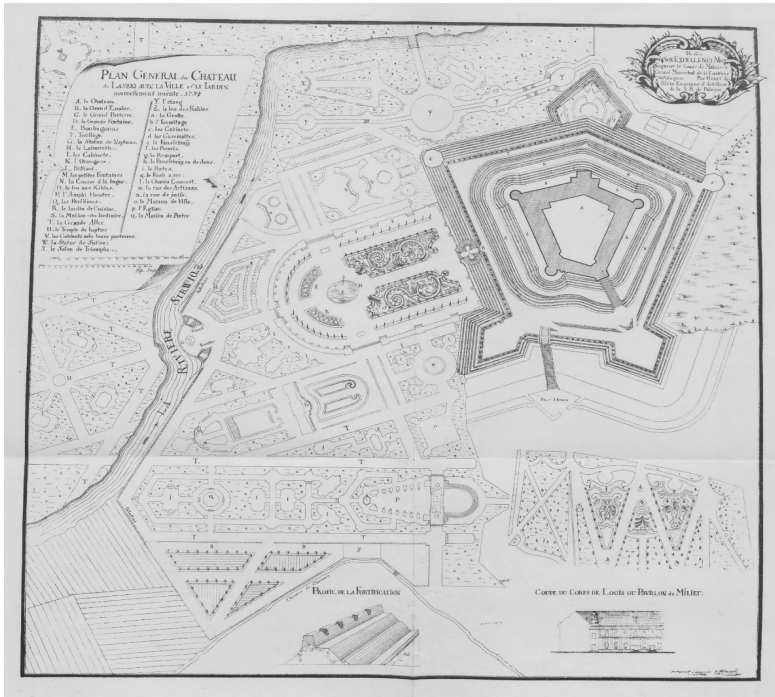
Fig. 3.   General plan of the castle and garden in the town Liashky Murovani, 1734

The park included statues of Neptune and Satire, a large fountain, three water mirrors, two small fountains, beautiful parterres, and flower lawns, which created delicate ornaments inherent in the French garden fashion of the 17th and 18th centuries, such as labyrinths, mysterious shelters hidden in the shadows, pavilions, and grottoes. Broad, straight lanes cut through the park and beautiful green galleries were put up to give shade. An amphitheater and two bowling alleys were also created in the complex. A round arena, which was used for the noble games of knights, was adored by the high society of the time. The park was landscaped with a plethora of hedges, various types of shrubs, flowerbeds, water arrangements, arbors, cabinets, and other decorative elements.

Agreeably, this urban complex could have been compared to the outstanding palace and park complexes of Europe, such as the castle of Vaux-le-Visont near Paris, the Palazzo Barberini in Rome, the Schönbrunn Palace in Vienna, and many others.

The Mniszech family, who owned the complex until 1815, apparently maintained it in its original form. Later the object became the property of Edward Zerboni de Spoletti. After a fire in 1835, the new owner decided not to rebuild the castle. Instead he dismantled the remains and

the materials that survived the fire were traded. During the First World War, the Russian army inflicted the last, devastating blow to this once outstanding complex, which was never rebuilt.

By the end of the 19th century only one part of the complex remained – the one-story tall eastern wing with a magnificent staircase inside, the rest was leveled to the foundations in the first half of the 20th century. Nowadays, only a fragment of just one of the east wing walls remains.

Over time, the historical town Lyashky Murovani lost its status. Today, Murovane Village, located in the Staryi Sambir district, Lviv region, has a volumetric and spatial structure with only a few preserved historical elements.

3. The current state of the urban complex of Murovane Village

By 2018, only several small fragments of the palace walls were preserved, historical ramparts can also be identified from the relief. Unfortunately, the park area had been badly damaged over the centuries (Fig. 4). The structure of the village retained the historical market square, buildings framing the space, and historical parcels (Fig. 5).

Fig. 4.   Views of the relics of the former historical palace complex in the village Murovane. Picture took by the authors in 2018

Fig. 5.   Views at the historical Market Square buildings in the village Murovane. Picture took by the authors in 2018

A series of field surveys and fixations of the preserved elements of the historical urban planning of 17th -18th century was made during the research. The basic identifying elements are: the existence of the valuable elements of the historic castle and palace complex, the Church of the Immaculate Conception and St. Martyr George (mid-18th century), and St. Joseph the Betrothed Church (late 18th century) (Fig. 6), fragments of the historical park, the elements of residential buildings, streets, and squares.

Fig. 6.   Views at the historical churches in the village Murovane. Picture took by the authors in 2018

The study contains a theoretical reconstruction of the planning structure of the historical town Lyashky Murovani (Murovane Village, Staryi Sambir district, Lviv region) (Fig. 7). The source base used for the theoretical reconstruction were historical cartographic materials: a Cadastral map of Lyashky Murovani, 1853 [8], Austrian military maps of Galicia of two

periods 1764 – 1784 and 1806 – 1869 [9, 10], the plan of the castle, town, and garden in Lyashky Murovani 1734 [6], a topo-geodetic survey of the village park in the village of Murovane 2016; historical narrative materials; the current fixation of the object.
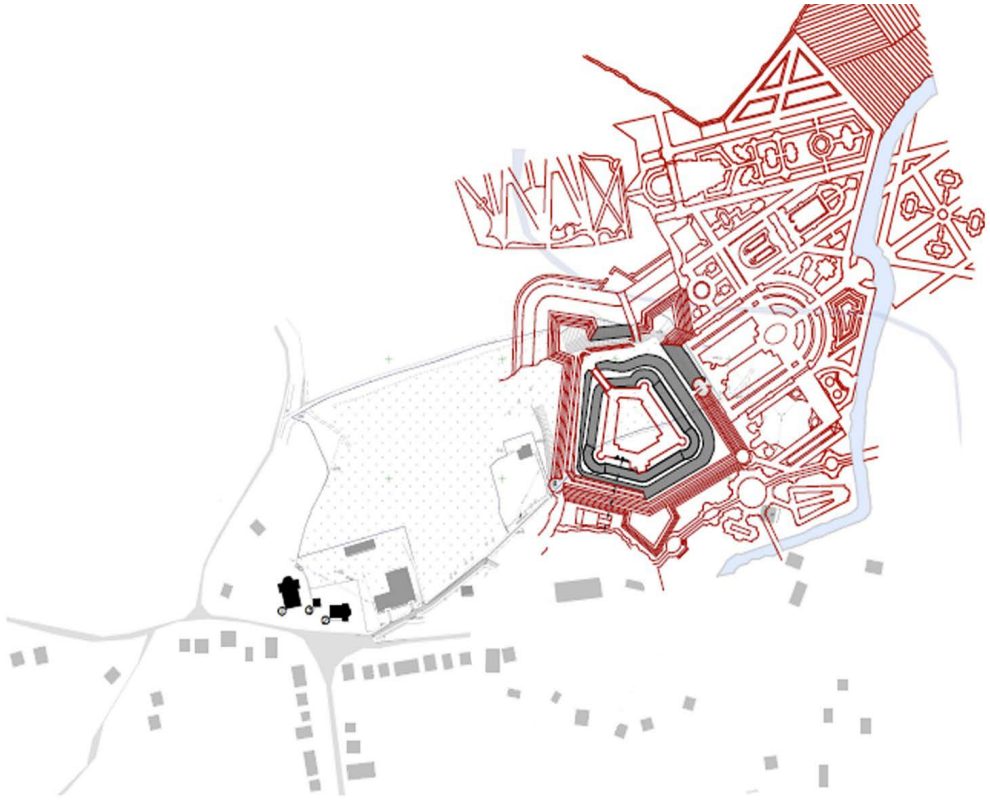
Fig. 7.   The scheme of the theoretical reconstruction of the planning structure of the historical town Liashky Murovani. Notice: missing elements are marked with the red color. Author: I. Shevchuk

The urban composition originally consisted of two equivalent elements: the market square with framing buildings and the palace and park complex, which form a cross-axial composition. The location of the Church of the Immaculate Conception and St. Martyr George (mid-18th century) is an interesting planning feature, located at the intersection of the composite axes. Due to historical circumstances, this compositional unit was supplemented by another sacral building of St. Joseph the Betrothed Church (late 18th century).

The palace and park complex had a dominant role in the composition of the town. The residence of the town owners passed through several stages of development. In time it had transformed from the defensive castle into a palace and park ensemble of the "palazzo in fortezza" type. The regular park was arranged in line with the most up-to-date requirements of the18th-century French landscape architecture. The palace building resembled a large pentagon with a wide courtyard, with three round towers in the corners. The entrance to the palace was located in a gateway clock tower. By the beginning of the 17th century, the palace building, which was built in several stages, had been supplemented by a fortification

system with three bastions, which were reconstructed in the beginning of the 18th century and transformed into a representational element of the park. The spacious composition of the park stretched across 10ha of land. It consisted of several main structural elements, featured by symmetry, rhythm and geometry, especially the main alley with a large fountain and other elements, which formed the main compositional axis. The alley ended with a large staircase which led to the viewing terrace over the Strviazh River. The stairs joined the park with a river and menagerie formed on the opposite bank of the river. The secondary compositional axes were formed on the left- and right-hand side from the main alley. The left compositional axis was parallel to the main alley and constituted a large, straight alleyway devided in the middle by a ring-racing arena and a greenhouse. This axis ended with two small fountains. The other axis comprised an amphitheater, a cabinet system and led towards the river.

The elements of the right compositional axis created a zone of peace, seclusion, and quiet rest. Its main elements were a hermitage, cabinets, and grottoes. This tranquil area was enclosed by a pond from the outside and formed several round dances on its way.

At that time the ensemble consisted of a large alley, parterre, flower beds, lawns, fountains, bowling alleys, trellis, labyrinths, greenhouses, billiards, grottoes, fountains, and water channels. There were over 40 main elements in total, and they were planned according to the clear axial composition and, at the same time, were adapted to the natural conditions. Without doubt, this park could be compared to the most famous European baroque park complexes.

3. Conclusions

The obtained results of the research and fixation work make it possible to suggest the concept of development and regeneration of this historical urban object. The developed concept envisages a fragmentary reproduction of the historical components of Lyashky Murovani within the territory of Murovane, Lviv region. The paper is a symbolic indication of the lost elements of the historical volumetric and planning city centre structure, especially streets, market square, residential buildings; recreation of the historical garden and park composition, the lost palace complex; disclosure and exposure of the preserved authentic underground substance of the palace complex, and the elements of the urban structure for their further exposure. It is also proposed to carry out informational regeneration of this valuable historical town-planning object: the creation of educational sightseeing routes throughout the territory of the historical town of Lyashky Murovani; involvement of this historical urban complex in the cultural tourism programmes of the region; virtual reconstruction of the castle and palace complex, arrangement of the virtual museum dedicated to the development stages of the palace complex; development of the 3D reconstructions and augmented reality programs that would demonstrate the evolution of the city and the castle complex.

The proposals are presented in the form of "The fragmentary reproduction program of the historical town of Lyashky Murovani" (Fig. 8). The proposed program requires three stages of implementation:

I - stage:

– tracing the borders of the lost historical castle and palace structure (16th – 17th century) (1 – on the Fig.8);

– conservation and addition of the preserved stone wall elements of the palace structure 18th century;

– installation of information stands in the village of Murovane (at the village entrance, on the territory of the historical market square, at the beginning of the linden lane, which connected the historic market square and the palace complex) (2 – on the Fig.8);

– creation of the exhibition space (installation of the mobile exhibition pavilions) in the territory of the historical palace and park complex that is almost lost (3 – on the Fig.8);

– development of a map and implementation of excursion route with stops in all significant places of the historical city;

– creation of a multimedia program to play back the spatial composition of the lost palace with the use of holograms.

II – stage:

– fragmentary recreation of the historical bastion (clearance, commissioning, strengthening and exposition of terrestrial fortifications fragments);

– baring and exposure of the underground chamber fragments from the palace and its fortifications;

– tracing the outline of the historical market square (4 – on the Fig.8);

– restoration of the lost amphitheater and its arrangement in order to carry out the art events (film festivals, exhibitions, concerts, etc.) (5 – on the Fig.8);

– symbolic indication of the lost park elements using the sidewalk lightning system;

– recreation and presentation of a fragment of the historic steam alley (historic lawns, flower beds) (6 – on the Fig.8);

– symbolic indication of a historic linden lane using the sidewalk lightning system (7 – on the Fig.8).

III – stage:

– fragmentary restoration of the historical planning structure of the 18th century park (elements of the central alley: walking paths, large fountain, ground lawns, flower beds, ceremonial stairs and observation terrace);

– restoration of the lost park structures and elements (retaining walls, pergolas, park sculptures, small architectural forms, etc.);

– reproduction of the lost park water elements (historical stream systems);

– creation of an environmental museum within the territory of the historic castle and palace complex.
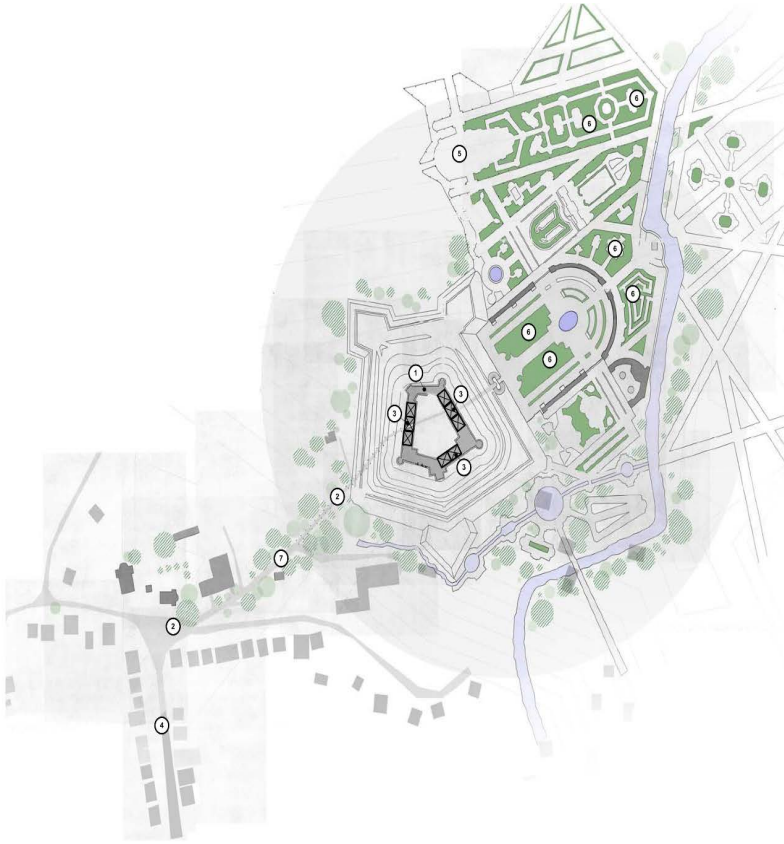
Fig. 8.　　The scheme representing the list of actions aimed at reproduction of the historical town Liashky Murovani. Authors: Z. Lukomska, H. Lukomska

The implementation of the proposed monument protection measures will allow: investigation into the existing technical condition of the historical urban object, elimination of the negative factors that cause the destruction of cultural heritage objects; an increase in the value of the preserved historical buildings by involving them in public life; preservation of the unique historical and urban planning environment and adapt it to modern needs of the society; to mark and partly recreate the lost unique palace and park complex; to convey the historical aspects of the region development to the residents and visitors of the historical city and to begin the process of grounding the proper attitude to the monuments of architecture and history; activation of the development of tourism as one of the main factors for the promotion of Ukrainian urban heritage.

References

[1]　　Bevz M., "Zberezhennia ta regeneratsiia istorychnykh tsentriv mist v zakhidnii ta tsentralno-skhidnii Yevropi", in: *Problemy teoryy y ystoryy arkhytektury Ukrayny*. Sb. nauch. trudov, Vyp. 4, OHASA, Odessa, p. 152-169, 2003.

[2]　　Czolowski A., „Dawne zamki i twerdze na Rusi Halickiej", *Teka Konserwatorska Galicyi wschodniej*, Lviv, 1892, p. 70.

[3]   Loziński W., *Życie polskie w dawnych wiekach*. Lwów, 1921, p. 218.

[4]   Prybieha L., „Istorychne seredovyshche yak pamiatkookhoronna katehoriia", *Ukrainska akademiia mystetstva*, vol. 11, p. 177-185, 2004.

[5]   Prybieha L., „Muzeiefikatsiia obiektiv arkhitekturno-mistobudivnoi spadshchyny: (Metodolohich-nyi aspekt)", *Ukrainska akademiia mystetstva*, vol. 19, p. 159–166, 2012.

[6]   Rodichkina O., *The Old Estates of Ukraine: Knyha-albom*. Mystetstvo, Kyiv, p. 384, 2015.

[7]   Inwentarz z r. 1748 (kopia) oraz inne materialy dotyczace zamku w Laszkach murowanych zebrane przez A. Czolowskiego, available at: https://polona.pl/item/inwentarz-z-r-1748-kopia-oraz-inne-materialy-dotyczace-zamku-w-laszkach-murowanych,MzEyNjA2OTQ/

[8]   Cadastral map of Liashky Murovani, 1853., ZDIAL Ukrainy; F. № 186; op.10, spr.858.

[9]   Henryk Klein, *Plan general du Chateau de Laszki avec la Ville et le Jardin nouvellement invente 1743*. Available: https://polona.pl/item/plan-general-du-chateau-de-laszki-avec-la-ville-et-le-jardin-nouvellement-invente-1734,MzYyMzg0Nzg/ [Access: 12 Dec 2019]

[10] Europe in the XIX. Century, *The Second Military Survey (1806-1869)*, Available: http://mapire.eu/en/map/collection/secondsurvey/?zoom=14&lat=49.39116&lon=25.6154 [Access: 12 Dec 2019]

Crossref
Similarity Check
Powered by iThenticate

Orginal Article

Contemporary challenges of spatial development of local service centres in the suburban areas of Wrocław – example of Czernica, Poland

Piotr Kryczka[1], Katarzyna Chrobak[2]

[1] Department of Urban Planning and Settlement Processes; Faculty of Architecture;
Wrocław University of Science and Technology;
Bolesława Prusa St. 53/55, 50-317 Wrocław, Poland;
piotr.kryczka@pwr.edu.pl (ID) 0000-0001-6735-2658
[2] Department of Urban Planning and Settlement Processes; Faculty of Architecture;
Wrocław University of Science and Technology;
Bolesława Prusa St. 53/55, 50-317 Wrocław, Poland;
katarzyna.chrobak@pwr.edu.pl (ID) 0000-0002-1422-6671

Abstract: The residential anthropopressure in the areas around large urban centres has become an irrefutable fact. According to many analysts, the suburban development is not related to rational land-use, focused on shaping multifunctional settlement units. The paper is a study of a selected case of spatial development of a service function in the suburban area of Wrocław. The article presents the literature on the subject of building systems of service centres, as well as the analysis of planning documents of the Czernica municipality, including their correlation with higher-order planning studies. As a consequence of the above, the spatial structure of the municipality and potential development possibilities of the service centres system were analysed. For this purpose, GIS analyses (in particular, the analysis of building density or spatial accessibility analysis) were carried out. The research constituted an important starting point for shaping guidelines in the area referring to establishing a hierarchical system of service centres. This led to the further debate on shaping the spaces for integration of rural residents connected to local service centres.

Keywords: spatial policy, rural areas, suburban neighbourhoods, spatial accessibility, network analysis

1. Introduction

Spatial development of cities is dictated by the evolution of each of the components of the functional and spatial structure, including the subsystem of services, and as a consequence – its spatial distribution. Analysis of the urban subsystem of services focuses mainly

on economic phenomena by examining theoretical bases of demand and supply (e.g. [1]), service and settlement geography (e.g. [2]), sociology (e.g. [3]), and finally urban planning and spatial planning (e.g. [4], [5]). The last of the indicated analytical ranges is a particular interest of the authors. Shaping land-use in free market conditions is an important element affecting the quality of people's lives, and thus equalizing opportunities in access to basic public goods [6]. In this context, the development of the hierarchy of service centres in the area affected by suburbanisation processes in the Czernica municipality located in the vicinity of Wrocław (a metropolitan city), has been analysed. A multi-functional space is considered to be a service centre, providing access to a diverse typology of services at different scales (cf. [7], [8]). The service centres are functionally diverse at the national, regional and local level. In this paper, a local service centre is understood as a first order element in the hierarchical urban subsystem of services, that provides dwellers accessibility to services (public and commercial). Commonly, it has defined boundaries and urban composition. Sometimes the public space is an element of it. The local service centre is also a part of a larger network system, as connected with higher order service centres, depending on the level of service provided.[1] The subject of research is particularly important in the context of shaping areas affected by intensive housing anthropopressure in the vicinity of large urban centres. The process of migration of the Wrocław population to the suburban area has been observed since the early 1990s. In 1995, the negative migration balance for Wrocław was recorded for the first time, with a positive migration balance in the neighbouring municipalities, of which the Czernica municipality experienced the most dynamic growth [9]. In this period, the process of residential suburbanisation connected with the process of demographic suburbanisation began, followed by economic suburbanisation from the beginning of the 21st century [10].

Along with the dynamic development of suburban settlements, the morphological structure of the village began to undergo changes [11]. The development of housing estates with a mono-functional character was intensified by the development of individual transport, functional ties with Wrocław [10] and spatial policy based on irrational space management. As a result, new housing estates not only do not fit into the traditional structure of the village, but also, inhabited by a homogeneous "urban" community, lead to intensification of social stratification processes [11]. This process is compounded by the lack of public spaces associated with a multi-functional service offer that can gather the "old" and "new" residents of the village. This is especially important when the recent users of services in the city are dissatisfied with the services offered by the village, in which they live, for example due to its non-adaptation to their needs or taste. Ultimately, this state of affairs forces further intensification of contacts with the central city ([12] p.184).

Therefore, the overarching goal of the study is to systematize knowledge in the field of shaping the system of service centres in the areas affected by suburbanisation processes. Service centres, as places integrating local communities, are important elements of spatial development, therefore the auxiliary goal and also the research strategy was to verify the territorial cohesion of shaping the hierarchical system of service centres in the municipality of Czernica. The basis for the purposes of the study is the current spatial policy of the municipality and region in the analysed thematic area. This directly contributed to the continuation of discussions about shaping public space.

---

1   Detailed definitions and a synthetic hierarchy of service centres are presented in the chapter *Systematisation of service centres*.

2. Tools and methods

2.1. State of research

The current analyses of service centres are carried out in relation to different research contexts. In particular, the need to analyse users (their distribution, mobility) and their needs (in the sociological dimension), spatial form, functional program and accessibility (in the various urban and architectural dimensions) should be indicated (see Fig. 1).
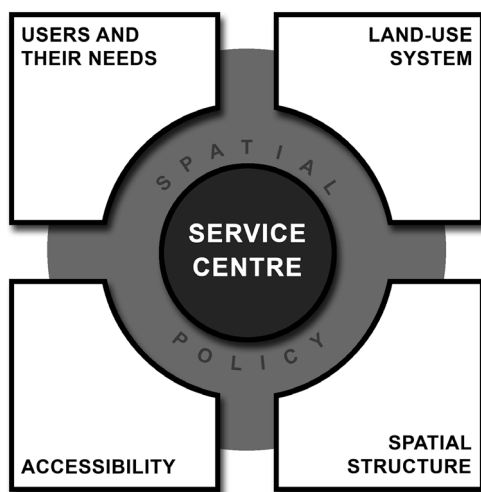
Fig. 1.   Research context of service centres. *Source:* own study

The theoretical background of the analyses is spatial policy, which is shaped by local government units at the voivodeship, region and local levels [13].

The intensification of urban sprawl resulted with more research on the future of rural areas in the context of their relationship with cities. In 2017 OECD released the report related to the challenges of the new rural policy [14]. The report highlights the complementarity of villages and cities, especially when rural areas fall inside the functional urban area. Due to the report, this type of rural area faces problems such as i.a. providing services for residents, while they are mainly concentrated in the core area and also problems in land-use management policy while facing urban core polarisation. While rural and urban territories are interconnected, OECD also underlines a role of urban-rural partnership on the level of regional policy. A salience of interrelationship between rural and urban areas was also noticed by Tacoli [15], where she proved that often a lot of services and facilities in the city relies on the demand from the rural area residents.

A lot of researches indicate the role that retailing and private service sectors have in shaping the spatial structure, the form in which particular area expands and consequently – a cost of travels made by residents [16], [17], [18]. Holden and Norland in their research [19] underline the role of distance between households and local service centres and indicate that accessibility to services is beneficial in the context of energy spent on everyday trips. Ferrell [20] points out that people living in highly accessible areas are more likely to make shorter trips and spend less time in retail-oriented trips. It is especially important while facing

the cost of urban sprawl in the context of households' losses on commuting and returning from the core city [21].

Nevertheless, along with the changes in consumer behaviour, oriented on mobility increase, the spatial distribution of services also had to change to adjust to changeable economic conditions [22]. Fernardes and Chamusca [23] indicate that the spatial distribution of services is mainly the result of decisions made by city dwellers. While the preferences and behaviour patterns change rapidly, service activities have to respond to these changes and according to demand and supply rules – adjust to the new economic conditions [22].

In connection with interactions and interrelationships described above, researchers also underline the necessity to undertake a strategy connected to sustainable development of both urban and rural areas (cf. [24], [25]). 'Sustainable Development in Rural Areas' also used to be one of the planning policy statements in the United Kingdom [26]. In one of their main missions the necessity of providing access to a variety of services and facilities was underlined. This mission could be achieved by planning local service centres in areas of intensive rural development that are accessible by walking, cycling or public transport and also in which the necessity of strengthening the role of particular local service centres was identified. The distribution of services should also promote the idea of mixed-use development to provide community vitality. The document also underlines the role of planning authorities in improvement of accessibility to existing services and facilities such as village shops, petrol stations, post offices or churches, which are very important for village communities. Nick Gallent [27] also underlines that spatial accessibility is a crucial element in rural areas planning, also in the matter of services and facilities distribution. He notices that spatial accessibility has an influence on difficulty of living in rural areas. Thus, he also highlights the necessity of providing transport links between residences and the places of realization of their everyday needs, while pointing out that this action is difficult in areas of dispersed development.

2.2. Methods

The research is based on the example of the Czernica municipality located in the vicinity of Wrocław, where the negative effects of suburbanisation processes have been identified so far [9]. The study is based on comparative and descriptive methods as well as deductive methods with an empirical inference. The study refers to the literature review in the field of shaping the hierarchy of service centres depending on the scale of their availability, which was then correlated with the planning documents of the voivodeship, region and the analysed municipality. In the next step, GIS analyses were carried out to verify the functional and spatial structure of Czernica and the availability and distribution of space users. The analyses were based on available statistical data, open spatial databases and urban inventory carried out in the municipality of Czernica.

3. Systematization of service centres

The systems of functional and spatial organization of service centres have been changing over the years. Today, we interpret primary service centres as places important for the community for economic reasons (e.g. trade and exchange of goods) or social (exchange of thoughts, rest, contemplation). The archetype of public spaces (that could be understood as a part of service centres) can be the Athenian agora or urban markets and squares of the Middle Ages, which idea of space creation was continued for many years [8].

The systematisation of service centres depends on the analytical issues raised. On the one hand, we are talking about territorial systematisation: spatial (on an urban scale) or geographical systematisation (including regional specificity), but also functional systematisation. The latter concerns, in particular the occurrence of dominant functional systems, in this case services, depending on the chosen spatial arrangement [28]. However, the most common specificity of service centre analysis concerns their location in space with the definition of their functional system – then we talk about functional and spatial specificity. Service centres have always been associated with urban thought. Particular attention was paid to them in American models of urban structure, where, among others [29] proposed a concentric model to describe the distribution of social groups in the urban structure centred around the main core, called the Central Business District. The Burgess model was so controversial that subsequent researchers made attempts to describe the urban structure, while also implementing concepts for the distribution of service centres, e.g. the Homer Hoyt sector model [30], and finally the multifocal model created by Chauncy Harris and Edward Ullman [31], which assumes many service centres spatially diversified depending on their location.

The hierarchy of service centres depends on the level of service to residents. There are six degrees of service centres in Polish literature on the subject:

- I° – elemental with the highest access for the society, where the facilities are visited very often (at a distance of up to approx. 500 m);
- II° – proximity of basic residential equipment, where facilities are often used; supports 10-25 thousand population (up to approx. 700 m);
- III° – used periodically, including spatially concentrated services, serving approx. 100,000 residents, accessible both on foot and by public and individual transport;
- IV° – used occasionally, of a high standard, covering a voivodeship centre;
- V° – supra voivodeship centres;
- VI° – state capital [8].

It is worth emphasizing that the development of service centres is different depending on their level of service. In the case of local and communal centres (I-III degree) we are talking about a specific urbanised space, e.g. square or street, while higher-order centres (IV-VI) can include the entire polycentric urbanised structure as such and shape a diverse repertoire of functions in a given unit settlement, which testifies to its rank.

Due to the varied detail of spatial analysis of the location of service centres, centres with the highest level of local service (I-III) are a particularly important aspect of urban space development, also significantly in suburban areas with high susceptibility to monofunctional housing development. It is the local public spaces, called agoras, that have become a special point of research for the Dutch architect Frank van Klingeren, and the idea of modern agora has been thoroughly analysed by Marek Kowicki [4] in urban and rural areas. Service centres, according to these authors, are to be on the one hand a regionalist tool protecting cultural values, but also a spatial context enabling society to meet their own needs – in urban areas, but also in rural areas. "The task of reform of rural areas should start with the implementation of a network of correctly located and designed socio-service centres, which, taking over the functions of agora, market, open-air market, sports and entertainment arena and many other functions, have all the data to act as the main social and main "nodes" conducive to the correct crystallization of the plan."([4]: 22).

4. Spatial policy of local government units

The background of research on the hierarchy of service centres is spatial policy, which in Polish legal conditions applies in particular to local government units – provinces and municipalities. Depending on the scale of the study, spatial policy is the basis for creating a development strategy, and consequently for developing hierarchy of the urban subsystem of service centres. Therefore, the planning documents of the Lower Silesian Voivodeship, regional study for the Functional Area of Wrocław and the study on land use planning of Czernica municipality were analysed.

4.1. Spatial development plan of the Lower Silesian Voivodeship (SDPLSV)

Spatial Development Plan of the Lower Silesian Voivodeship. Prospect until 2020 [32], adequately for the scale of its study, focuses on the hierarchy of service centres in the context of the region. SDPLSV thus indicates the development of Lower Silesia based on the European metropolitan centre (Wrocław), 3 regional centres, 7 sub-regional centres, 2 cross-border centres and other county centres (Fig. 2). Nevertheless, in the diagnosis of the conditions of the settlement zone, it was pointed out that both county and municipality centres, including villages – act as local centres, which constitute "basic service centres for the inhabitants of the region, and their regular distribution in the voivodeship space provides convenient access to basic services; maintaining their hierarchical division into three stages is a factor conducive to spatial cohesion of the region and a condition for maintaining a polycentric layout of the settlement network."([32]: 23).

A graphic reflection of the analysed case of service centres is presented in Figure 2 of the SDPLSV, where the Czernica municipality has not been assigned a clear role in the hierarchy of service centres. The municipality is located in the zone of impact of the Wrocław metropolitan centre within the area of intensification of multi-functional development, as well as between Siechnice and Jelcz-Laskowice – the centres of equilibrating development. It can therefore be concluded that Czernica in the hierarchical system of the voivodeship is to serve residents at the local level, which in the light of the cited literature on the subject and the demographic situation of the municipality corresponds to the first and second degree centres.
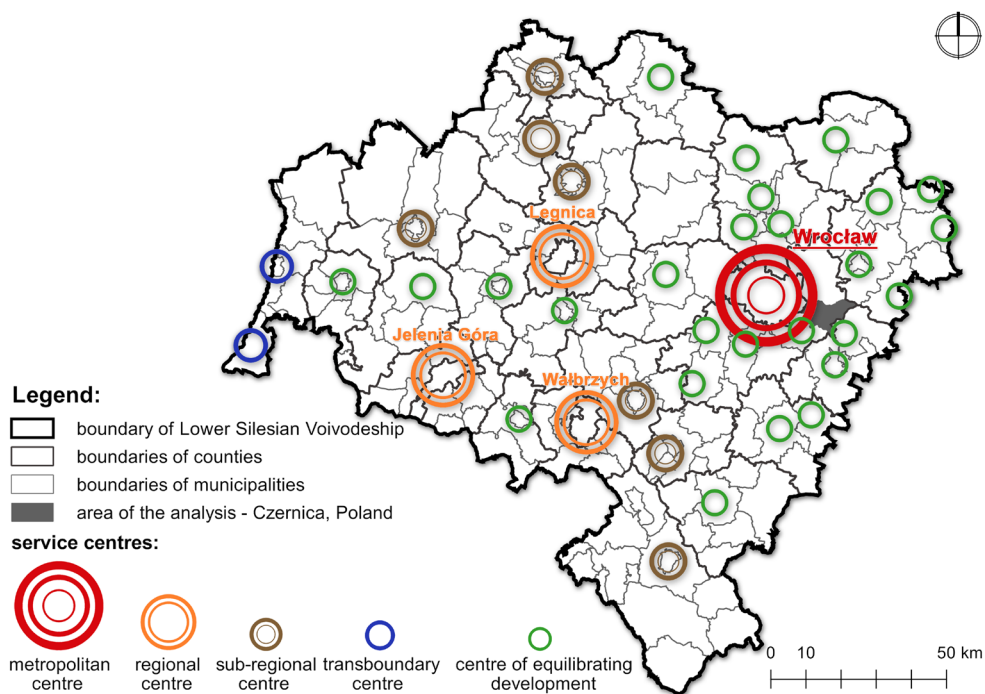
Fig. 2.   Development of service centres in Lower Silesia on the example of Spatial Development Plan for Lower Silesian Voivodeship. Prospect until 2020. *Source:* own study based on [32]

4.2. Functional Cohesion Study in the Functional Area of Wrocław (FCSFAW)

The Act of March 27, 2003 on spatial planning and development does not introduce the obligation to draw up planning documents at the level of the functional area of a larger urban zone. Nevertheless, a Functional Cohesion Study [33] was prepared as part of the Functional Area of Wrocław (FAW). It is a document that thoroughly analyses the functional and spatial phenomena in Wrocław and its areas of influence.

FCSFAW presents an in-depth analysis of the hierarchy of service centres (Fig. 3). It is indicated that in recent years there has been significant transformation of service centres in the FAW. Analysis of the dynamics of demographic changes and the balance of migration, which were carried out as part of FCSFAW, confirm the thesis that the migration of Wrocław residents to suburban areas resulted in significant transformations of towns near Wrocław. The sudden and often uncontrolled spatial development of residential areas did not go hand in hand with the adequate development of service centres serving them. As a result, dozens of villages around Wrocław and larger urban centres in FAW changed their spatial structure. The historical rural structure has been blurred, turning them into spreading housing estates with disturbed composition elements, i.e. inconsistent geometric layout, disturbed hierarchy of importance of elements, chaotic material and blurred borders of the village and their components.
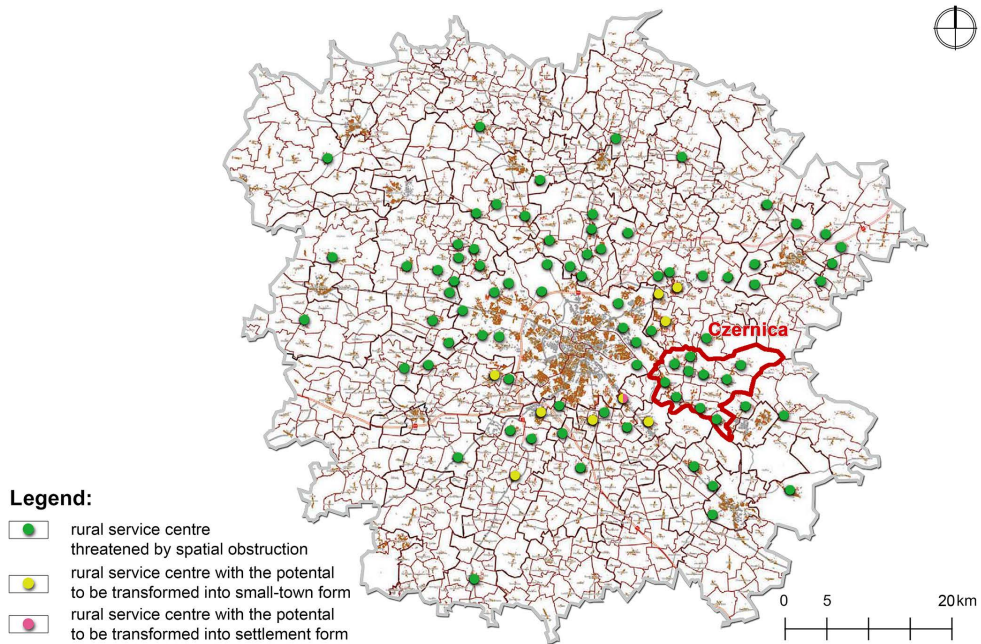
Fig. 3.   Analysis of service centres in FAW. *Source:* own study based on ([33]: 139)

FCSFAW identifies 10 rural service centres threatened by spatial obstruction in the Czernica municipality. These are: Chrząstawa Mała, Chrząstawa Wielka, Czernica, Dobrzykowice, Gajków, Kamieniec Wrocławski, Krzyków, Nadolice Małe, Nadolice Wielkie, and Ratowice

4.3. Study on land use planning of the Czernica municipality

The study on land use planning of the Czernica municipality laconically refers to spatial aspects of the functioning of the hierarchical system of service centres. The study indicates that the density of the residential areas is determined by the index 6.0 km*2*/settlement unit (6.5 km*2*/village council). The functional structure of the existing municipality settlement network has a clear hierarchical system of service centres (Fig. 4):

- the village of Czernica – second level (local) service centre, also fulfilling an administrative function,
- the village of Kamieniec Wrocławski – first level service centre,
- the villages of Nadolice Wielkie and Ratowice – first level service centres – additional,
- the other villages are centres with the level of elementary services.

The nature of the functions of individual villages clearly correlates with the observed dynamics of their growth. Typical agricultural villages, with the exception of the Nadolice Wielkie, have so far been characterized by stagnation of population growth, and the largest population increase was recorded in the village of Kamieniec Wrocławski, which is most affected by urbanisation. It was also pointed out that the location of the primary school was an important element integrating villages so far.

The study on land use planning of the Czernica municipality, in contrast to the Functional Cohesion Study in the Functional Area of Wrocław, designates only 4, not 10 service centres, not indicating potential threats in their functioning.

Fig. 4.   Analysis of hierarchy of service centres in Czernica municipality, Poland. *Source:* own study based on [34]

4.4. Implementation policy of the Czernica municipality in local spatial development plans

Spatial policy contained in the Study on land use planning of the Czernica municipality should be implemented in local spatial development plans, which by definition should clearly describe the target spatial development. There are 142 local spatial development plans in the municipality that cover the municipality in over 81% [35]. In relation to the query of higher-level planning documents, local spatial development plans for the central parts of the village, indicated as possible to shape service centres, were analysed (Fig. 5).

Despite the high planning coverage of the municipality, no local spatial development plan was drawn up for the currently invested area of Czernica village. This is a particularly important area due to the administrative functions occurring here and other accompanying services, which creates high potential in shaping service centres, in particular at a higher hierarchical level. A similar situation occurs in Dobrzykowice, where the central area does not have a local spatial development plan, and its direct vicinity consists mainly of single-family housing as well as covering large areas (almost 53 ha): service buildings – without indicating its specific type (approx. 11 ha) and service buildings related to the location of the university campus (approx. 42 ha). The local plan proposing a university in this area has been in force since 2004 and has not yet been implemented, and the proposed destinations, despite doubts regarding their location aspects, are an important element of the hierarchical system of service centres.

Fig. 5.   Local zoning plans for selected central areas of villages in Czernica municipality, Poland. *Source: own study based on [35]*

The spatial planning situation in Kamieniec Wrocławski, Nadolice Wielkie and Ratowice is similar. The plans almost entirely cover the central areas of these villages and mainly single-family housing with services or multi-family housing are introduced there. In Kamieniec Wrocławski, particular attention is paid to the location of the school and the playground in the vicinity of the park and newly emerging services with a diverse catalogue, as well as the development of residential buildings in their surroundings. In the development plans for Ratowice, strictly residential space is organized around smaller areas designated for service buildings, in particular the existing church and the adjacent store. The plan also marks the existing primary school. A different character of space occurs in Nadolice Wielkie, where the planned service structure is polycentric and implements existing traffic attractors into the functional structure. These are planning units including a local museum, church, manor with a park and a fire station of the Volunteer Fire Department. However, there is a noticeable lack of provision of promising areas constituting the development of these functions in the area of the village.

In the local spatial development plans one can identify the purposes of the areas which prove the potential of shaping the system of service centres. Nevertheless, a negative tendency is to indicate the lack of public spaces (e.g. plazas) in these plans. Lack of this type of way of shaping projects of local plans creates uncertainty about shaping public space enabling integration of the local community.

5. Results

Analysis of planning documents on both a local and regional scale has enabled the identification of a potential hierarchy of service centres in the municipality of Czernica (see Fig. 4). It constituted the basis for further analysis of the spatial structure of the municipality in terms of development opportunities in its area of the service centre system. The verification of the extracted structure was made on the basis of the research context of service centres presented in Chapter 1 (see Fig. 1), on spatial analyses based on GIS software (verification of the distribution of space users and the level of accessibility of selected service centres) and urban inventory (analysis of the functional program and spatial forms of service centres).

One of the indicators that allow analysing the distribution of users in space is the density indicator. In municipalities under pressure of suburbanisation, due to frequent discrepancies in the actual number of inhabitants and the number of registered people (Kajdanek 2011: 49), it is not always accurate to determine the density based on statistical data on the number of people registered in a given registration area. What's more, due to the intense growth of housing, newly completed apartments can only be a potential for an increase in the number of users of a given space. When dealing with areas of intense, often chaotic monofunctional

development, it seems more accurate to analyse the density of housing development, helpful in identifying areas of its rapid growth. The degree of housing density allows the selection of areas predestined to perform specific functions in the spatial structure of the municipality.

The scheme of density of housing development in the municipality of Czernica (Fig. 6) was made using the kernel density tool in ArcGIS software. In this case, each residential building was presented as a single point. Data regarding the arrangement of housing were obtained from the Topographic Objects Database, successively supplemented with OpenStreetMap open resources and orthophotomap data. A search radius of 500 m was adopted.
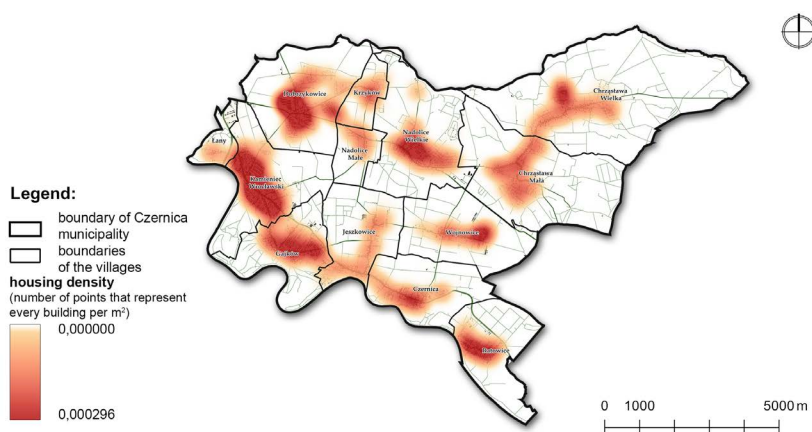
Fig. 6.   Scheme of the housing density in the Czernica municipality based on the kernel density tool. *Source: own study*

The analysis of housing density in the municipality of Czernica allowed to identify the impact of Wrocław on the appearance of new residential buildings in neighbouring municipalities. While in rural municipalities performing traditional functions, buildings develop the most in the village fulfilling an administrative function (residence of the municipality office), in the case of municipalities located in the suburbia zone of a large centre, the most attractive places to live in are located near this centre. In the case of the Czernica municipality, the highest density of housing is characterized by registration precincts located in the immediate vicinity of Wrocław (primarily Dobrzykowice and Kamieniec Wrocławski), and it is in them that new residential develops, often of a similar nature to urban ones, becoming almost a continuation of buildings of Wrocław. These results became the basis for taking into account also the village of Dobrzykowice in further analysis as an area of intensive housing development. At the same time, the seat of the municipality office – the village of Czernica, due to its peripheral location, is characterized by one of the lowest housing density indicators in the municipality.

Analysis of the accessibility of service centres was carried out using the Network Analyst tool in ArcGIS software (Fig. 7). Accessibility of residents to service centres located in five cadastral districts was examined, viz Czernica, Dobrzykowice, Kamieniec Wrocławski, Nadolice Wielkie and Ratowice. First of all, the pedestrian accessibility to selected central points in selected cities was analysed at intervals of up to 10 min, up to 20 min and up to 30 min. For each of the service polygons, the level of service for residents was calculated, understood as the number of single and multi-family residential buildings that fall within a given time range.
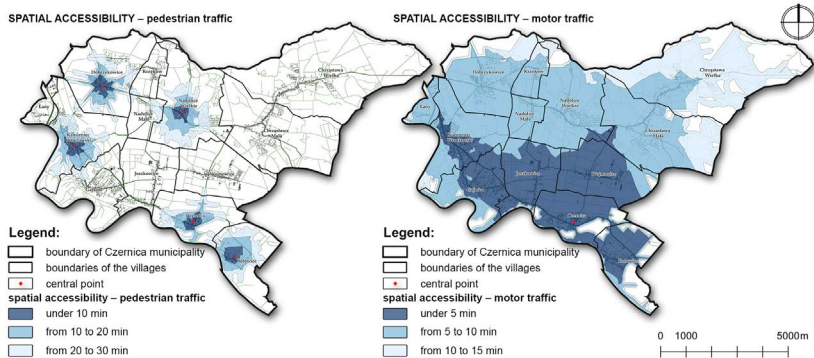
Fig. 7.   Analysis of spatial accessibility in pedestrian traffic to central points located in selected villages and spatial accessibility in motor traffic to a central point located in Czernica. *Source:* own study

For each of the service training grounds, the level of service for residents was calculated, understood as the number of single- and multi-family residential buildings that fall within a given time range (Table 1).

In both, the first and second time zones, the largest percentage of buildings served in the municipality was recorded in the village of Dobrzykowice. First of all, they are single-family buildings and this type of development is being built to the greatest extent in the villages bordering Wrocław. The village of Kamieniec Wrocławski bordering Wrocław has the highest level of service (the highest among the analysed centres in the third time zone) also is connected with a large number of multi-family buildings.

Table 1.   The level of service of residential buildings by central points in selected cities – pedestrian traffic. *Source:* own study

Central location	Number of residential buildings served in accessibility zone		
	single-family	multifamily	total share in residential buildings in the municipality of Czernica
zone up to 10 min			
Czernica	67	11	2%
Dobrzykowice	213	2	5%
Kamieniec Wrocławski	174	3	4%
Nadolice Wielkie	110	0	2%
Ratowice	93	0	2%
zone up to 20 min			
Czernica	178	11	4%
Dobrzykowice	516	2	11%
Kamieniec Wrocławski	468	10	10%
Nadolice Wielkie	265	6	6%
Ratowice	268	0	6%
zone up to 30 min			
Czernica	242	11	5%
Dobrzykowice	642	2	14%
Kamieniec Wrocławski	719	10	16%
Nadolice Wielkie	397	6	9%
Ratowice	274	0	6%

In the village of Czernica the level of service is much lower (each time the lowest or one of the lowest among the analysed). Although already in the first zone includes 11 multi-family buildings, it is still a level of service too low to perform the function of the main municipality centre. Nevertheless, the village of Czernica still has a functional specialization related to its administrative function – the residence of the municipality office. The range of this function is greater, so for the village of Czernica the availability of car traffic was also analysed, in subsequent service zones: up to 5 min, up to 10 min and up to 15 min (Table 2).

Almost 50% of all residential buildings in the municipality are located in the 5-minute zone. In the next zone it is almost 100%. The relatively dense road network means that even the peripheral village of Czernica is accessible by car to residents even in a very short time. However, one should bear in mind the fact that there are numerous difficulties in navigating the road network in suburbs, where congestion increases significantly at the contact with the central city (in this case the city of Wrocław), modifying the obtained spatial accessibility results.

Table 2.   The level of service of residential buildings by central point in Czernica – car traffic. *Source:* own study

accessibility zone	single-family	multifamily	total share in residential buildings in the municipality of Czernica
Zone up to 5 min	2014	24	44%
Zone up to 10 min	4400	37	95%
Zone up to 15 min	4633	37	100%

Therefore, one should try to promote pedestrian traffic by creating places of its absorption and a diversified functional and spatial offer encouraging walking. From the residents' perspective, there will always be a desire to minimize travel time, however, the different specifics of the services accompanying local service centres have different ranges of influence (also in territorial sense) and may even encourage further travel if the functional offer varies significantly.

The urban inventory of central places made in the next step allowed to assess the functional and spatial diversity of places shaped as potential local service centres in the analysed centres (Fig. 8).

Residence of the municipality office – the village of Czernica, has two areas of local centrality. The first, limited by Kolejowa and Wrocławska streets, has a higher degree of specialization and stands out in this respect from the whole municipality. It is associated with the presence of the municipality office, train station and restaurant. The second, with functions typical of rural areas – associated with the presence of a store, school and church, but also a post office, is located in the area of the accumulation of multi-family housing. Despite the greater potential of the first centre, related to its significance for the entire municipality, it requires spatial ordering – primarily revitalization of post-industrial areas located nearby the railway station. It is also important to create traffic generators that allow linking both centres to create a coherent structure.
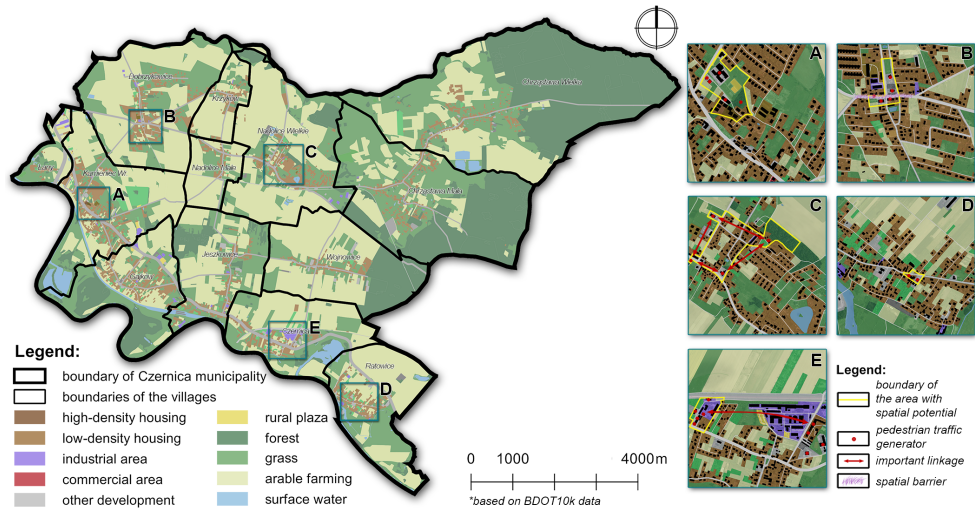
Fig. 8.   Inventory and functional assessment of central places in selected villages of the Czernica municipality.
Source: own study

In the village of Dobrzykowice, the area bounded by Stawowa, Szkolna, Czerwona and Ładna Streets is shaped as the central one. Its functioning is associated with the presence of such service facilities as school, church, store and restaurant. Despite the increased functional offer in relation to the basic unit found in the countryside, it is necessary to increase the readability of the system, which is most disturbed by the presence of a spatial barrier – Wrocławska Street. It is a busy street, an artery with a high technical class and parameters that are not friendly to pedestrians. Its elimination should at the same time increase the representative function of the church situated next to it, which is an important place for the local community.

Another village located in the vicinity of Wrocław – Kamieniec Wrocławski, has a central place in the Palace Park area, associated with the existence of a school, nursery school, clinic, police station, store and pharmacy. These facilities are located chaotically and do not create a coherent spatial structure. That is way the readability of this place must be increased. Due to high housing anthropopressure in this area, it is also necessary to increase the service offer and encase the centre with more services targeted at residents. The park area itself, which is a potentially strong attractor, also needs better spatial organization.

A different character of the space occurs in Nadolice Wielkie, where the service structure is polycentric and concerns the local museum in the southwest, the church in the northwest, the manor and park in the northeast and the fire station in the southeast. This urban equipment is an important traffic generator, and its interconnection can create a potential for a functionally diverse centre.

The village of Ratowice has the poorest service offer. The area that appears to be important for the inhabitants of the village occurs in the area of Wrocławska Street and is associated with the existence of a basic service unit for the village, including a church and a store. For this area, it is necessary to revalorize it in order to maintain its important position for the inhabitants of the village. The example of Ratowice shows how much the functional and spatial diversity of central places changes when it is farther from the borders of Wrocław.

6. Discussion

The analysis confirms the progressive and multi-faceted modifications of the functional and spatial structure of the Czernica municipality caused by the adverse effects of suburbanisation. They constitute a special starting point for undertaking a broader scope of analyses covering a larger number of municipalities neighbouring with Wrocław – in order to further verify the results in relation to the holistic phenomenon of suburbanisation as well as to determine clear conclusions regarding the administrative specificity of municipality and the location of central areas in a more extensive analytical context. Research indicates that special functional and spatial potential is located in the capital of the municipality, but it is not accessible enough in pedestrian traffic to act as a centre with a higher hierarchical level.

Activities in the field of spatial policy in the municipality of Czernica should aim at reducing monofunctional spatial development and striving to enrich the service offer throughout the entire municipality – also within the villages which development potential of service centres is the lowest, but at the same time particularly important for the functioning of local communities. Building a system of service centres should be focused on the successive study of demographic trends and spatial behaviour within the village with identified potential. However, the development of these centres should be based on existing spatial values and traffic attractors – in particular within the villages of Nadolice Wielkie and Dobrzykowice. An important issue of developing a network of services in space is also the need to build the identity of a given place – already at the design stage.

Conducted analyses highlighted the special need for shaping space in relation to spatial development trends. The highest housing density occurring in the direct vicinity of Wrocław and in the capital of the Czernica municipality shows that firstly, activities aimed at implementing the own tasks of municipality in the field of public space should be oriented in these areas. This action is considered to be deliberate while resulting from the highest values of spatial accessibility of these areas.

Building a common identity is possible, among others, by creating places of integration of residents. These structures should encourage people to stay in them through clear development, as well as through a wide range of services meeting the needs of all residents. It is important to eliminate or suppress the impact of disturbing functions that are not adapted in scale to their more intimate and still rural character. They should also be easily accessible, especially for pedestrians, along with access corridors from each part of the village, enclosed with traffic generators, encouraging them to continue their journey.

The newly created structures (Fig. 9) should constitute a bridge between the city and the village, both in the regional and local dimension, but also urban, based on specific design assumptions, and sociological, connecting "old" and "new" village residents. In this context, local spatial development plans will play a particularly important role, as in their current form they would need to be updated to determine more precise records shaping public space and its encapsulating functions. When planning the functional and spatial structure of rural areas under the pressure of intensive urbanisation in the zone of influence of a metropolitan centre, it is necessary to adapt the service offer to a wider and more diverse group of recipients. The traditional approach to village planning should be re-evaluated in the face of new challenges posed by the emergence of new users accustomed to the "urban" lifestyle, entering areas important for local, indigenous communities.
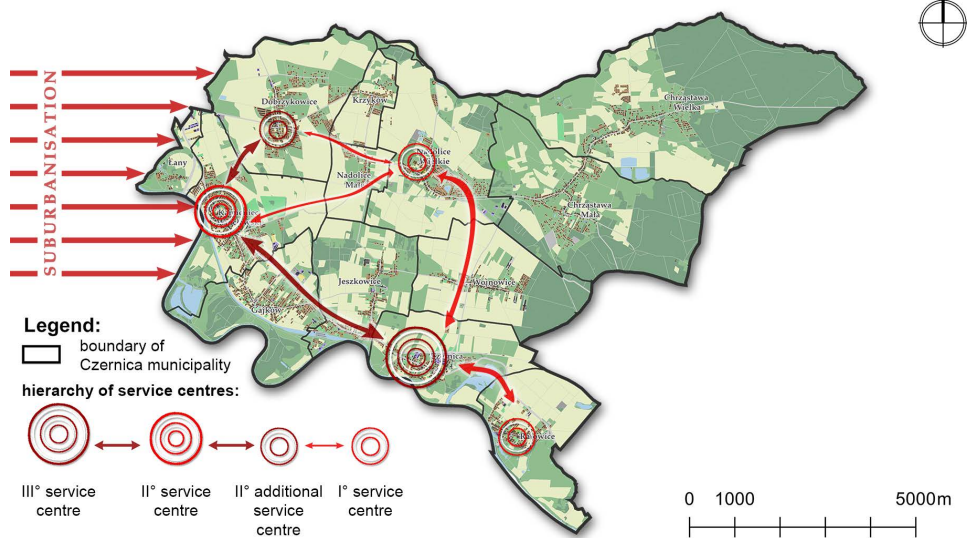
Fig. 9.   The concept of a hierarchical system of service centres in the Czernica municipality. *Source:* own study

Conducted analysis is a part of the current trend of urban planning and design as well as architectural research highlighted in the state of research. Intensive development of Wrocław and its urban sprawl phenomenon resulted in challenges that Czernica municipality must face in planning sustainable development. It is related to the specificity of shaping spatial growth of rural zones in the functional urban area. The conclusions of the OECD report [14] are also appropriate in the analysed municipality. The lack of multifunctional public spaces that provide a diverse catalogue of services for local society in the areas of urban core pressure can be noticed in conducted urban inventory. It should be considered as a negative trend, especially considering the fact that current research indicates the centre-forming role of retailing and private services in the spatial structure. Although, in recent years the crisis in public spaces can be noticed [36]. The patterns in social behaviour are subject to permanent changes [19], [22], [37], thus the accessibility of public space in the context of energy spent on everyday trips will be an important factor for many people. Therefore, the concept of a hierarchical system of service centres in the Czernica municipality based on conclusions of network analysis and urban inventory seems to be justified. Space changes much more slowly than the way it is used, so it also can adapt to economic realities. After all, in the vicinity of valuable public spaces, the economic condition of entities can be intensified. It may have an important impact if the municipality builds a strategy of shaping public spaces and local service centres based on pedestrian traffic generators. The planned hierarchical system of service centres (consistent with current systematization of service centres) and the identification of the areas predisposed to the development of public functions, implements the idea of mixed-use development, as well as indirectly provides the vitality of the local community. A correctly conducted spatial policy and proper implementation of strategic development assumptions play a crucial role in this context. Consequently, the need for further improvement of planning and strategic documents in the Czernica municipality should be indicated. The spatial policy of municipalities should be correlated at the planning level in the functional area and in the voivodeship, but also in smaller – urban design scale [38].

7. Conclusions

The municipality of Czernica, through its proximity to a large urban centre, is exposed to adverse suburbanisation processes, and thus – its negative spatial effects. As indicated in this study, the highest building density in the municipality is correlated with the proximity of Wrocław's administrative borders. In the Czernica municipality, the existence of an unambiguous hierarchical system of service centres has not been identified, even despite the proposals for their creation contained in the rather laconic entries of the Study on land use planning. Their presence is dictated by the location of certain lower-order functions that are not equipped with the appropriate nature of public space development. The analysis carried out for the Czernica municipality shows that the hierarchical system of service centres is disturbed by suburbanisation processes, and the theoretically developed three-level service model is a subject to devaluation processes. It is the result of intensive housing anthropopressure near the borders of the voivodeship city. An additional factor weakening the current structure of the service centre hierarchy is the lack of sufficient functional and spatial potential to create a service system. Monofunctional (residential) development of the space around the city limits prevents development taking into account high spatial accessibility to areas important for society, which are undoubtedly service centres.

In the light of conducted analyses the positive conclusions as well as positive trends in contemporary challenges of spatial development of local service centres in the suburban areas of Wrocław, could be pointed out:

- The spatial development plan of the Lower Silesian Voivodeship correctly indicates the hierarchical system of development of service centres in the regional scale. The need of development of settlement areas in parallel with the need of development of counties and municipality local centres should also be considered as a positive trend.

- In contrast to the spatial development plan of the Lower Silesian Voivodeship, the Functional Cohesion Study in the Functional Area of Wrocław widely diagnoses the trends in service centres, which should be assessed as beneficial. Nevertheless, it is a diagnostic document with no legal force. Therefore, the implementation of its conclusions by the local government units is not required. Moreover, it can be pointed out that guidelines of the Cohesion Study had not been implemented by the Czernica municipality.

- The hierarchical development of service centres in relation to the calculated density of the settlement network was indicated in the study on land use planning of the Czernica municipality. Correlation of development of the service sector with population density is a positive trend.

- Conducted study of the development of service centres in the suburban areas on the example of the Czernica municipality, based on in-depth urban inventory, analysis of the housing density, as well as analysis of spatial accessibility, allowed to indicate the potential development of space (major pedestrian traffic generators, important linkages and current spatial barriers that should be reduced in further spatial development).

- The spatial potential in the development of service centres in suburban areas does not have to be associated with a typical spatial form as a plaza surrounded by service buildings, what was indicated in the analyses. The centres may have a polycentric character, shaped on the basis of pedestrian linkages, where appropriate traffic generators should occur.

Conducted analyses also enabled to define negative conclusions as well as negative trends in contemporary challenges of spatial development of local service centres in the suburban areas of Wrocław:

- There are gaps in the source literature in the case of contemporary development of service centres and their spatial structure. It equals a lack of knowledge that can be implemented within local government units.

- The spatial development plan of the Lower Silesian Voivodeship does not diagnose the special need of development of local service centres in the areas affected by suburbanisation, where the spatial anthropopression related to monofunctional housing development has occurred.

- The study on land use planning of the Czernica municipality does not describe guidelines regarding the specific location and methods of shaping spatial development of local service centres.

- The implementation policy of the Czernica municipality does not provide the necessity of shaping service centres. The regulations included in local plans that are related to the service sector are highly laconic. Moreover, the villages of Dobrzykowice and Czernica do not have local plans that could indicate important public spaces with concomitant services.

- There is a strong necessity of correlation of architectural and urban planning research with sociological research connected to the needs of the users and residents of suburban areas. The results of these researches may widen the functional catalogue and approach to development of public space in the areas affected by suburbanisation, where the specific social groups are combined.

With regard to the above conclusions, attention should be paid to the need to create a service centre system in suburban areas. With regard to the case study of Czernica municipality, the most important (based on the centre-creating municipal functions) is the service centre in Czernica. It shows the highest functional and spatial potential, despite the lower level of service for residents in pedestrian traffic. The second-order centre is located in Kamieniec Wrocławski. It is available for areas located closer to Wrocław, as well as the second-order complementary centre in Dobrzykowice and first order centres in Nadolice Wielkie and Ratowice. The development of local service centres is a significant challenge in contemporary urban planning. On the one hand, it involves the need of ensuring accessibility to services, and on the other hand, the need of shaping public spaces that can integrate the local community.

References

[1] Rosa G. et al., *Współczesna ekonomika usług*. Warszawa: Wydawnictwo Naukowe PWN, 2005.

[2] Ilnicki D., *Przestrzenne zróżnicowanie poziomu rozwoju usług w Polsce: teoretyczne i praktyczne uwarunkowania badań*. Wrocłoaw: Rozprawy Naukowe Instytutu Geografii i Rozwoju Regionalnego Uniwersytetu Wrocławskiego 11, 2009. Available: http://www.geogr.uni.wroc.pl/data/files/publikacje-rozprawy-naukowe-igrr/rozprawy_11.pdf

[3] Kulawiak A., "Społeczne uwarunkowania rozwoju sektora usług w małych miastach: przykład Uniejowa", *Acta Universitatis Lodziensis. Folia Geographica Socio-Oeconomica*, vol. 15, (2013), pp. 115–126.

[4] Kowicki M., *Współczesna agora. Wybrane problemy kształtowania ośrodków usługowych dla małych społeczności lokalnych*. Kraków: Oficyna Wydawnicza Politechniki Krakowskiej.

[5]   Gil-Mastalerczyk J., "The influence of places of worship on the formation and integration of public spaces in the city", *Budownictwo i Architektura*, vol. 16, no. 2, (2017), pp. 031–038. https://doi.org/10.24358/Bud-Arch_17-162_02

[6]   Stettner M., "The quality and conditions of life in Siechnice – social research", *Budownictwo i Architektura*, vol. 15, no. 4, (2016), pp. 087-100. https://doi.org/10.24358/Bud-Arch_16_154_09

[7]   Christaller W., *Die zentralen Orte in Süddeutschland [Central places in southern Germany]*. 1933.

[8]   Damurski Ł. et al., "Wybrane uwarunkowania kształtowania lokalnych centrów usługowych na obszarach zurbanizowanych", *Biuletyn – Polska Akademia Nauk. Komitet Przestrzennego Zagospodarowania Kraju*, no. 271, (2018), pp. 54–74.

[9]   Zathey M., *Wrocławska strefa suburbialna (typescript of doctoral dissertation)*. 2005.

[10] Zathey M., "Zmiany demograficzno-przestrzenne a zrównoważony rozwój Wrocławia", in *Problemy społeczne w przestrzeni Wrocławia / science editor Stanisław Witold Kłopot, Mateusz Błaszczyk, Jacek Pluta*, Warsaw: Scholar Publishing House, 2010, pp. 39–60.

[11] Zathey M., "Struktura przestrzenna i mieszkańcy osiedli podwrocławskich", in *Współczesne formy osadnictwa miejskiego i ich przemiany: XV Seminar on Knowledge about the City: collective work / edited by Iwona Jażdżewska*, 2002, pp. 165–174.

[12] Kajdanek K., *Pomiędzy miastem a wsią. Suburbanizacja na przykładzie osiedli podmiejskich Wrocławia*. Kraków: NOMOS, 2011.

[13] Damurski Ł. et al., "Lokalne centrum usługowe: w poszukiwaniu formy i funkcji", *Przestrzeń Społeczna (Social Space)*, vol. 15, no. 1, (2018), pp. 142–168.

[14] OECD, "New Rural Policy: Linking Up For Growth", Paris, 2017.

[15] Tacoli C., "Rural-urban interactions: A guide to the literature", *Environment and Urbanization*, (1998). https://doi.org/10.1630/095624798101284356

[16] Buliung R. N. and Kanaroglou P.S., "Urban form and household activity-travel behavior", *Growth and Change*, vol. 37, no. 2, (2006), pp. 172–199. https://doi.org/10.1111/j.1468-2257.2006.00314.x

[17] Cervero R. and Duncan M., "Which reduces vehicle travel more: Jobs-housing balance of retail-housing mixing?", *Journal of the American Planning Association*, vol. 72, no. 4, (2006), pp. 475–490. https://doi.org/10.1080/01944360608976767

[18] Gjestland A. et al., "Some aspects of the intraregional spatial distribution of local sector activities", *Annals of Regional Science*, vol. 40, no. 3, (2006), pp. 559–582. https://doi.org/10.1007/s00168-006-0073-7

[19] Holden E. and Norland I.T., "Three challenges for the compact city as a sustainable urban form: Household consumption of energy and transport in eight residential areas in the Greater Oslo Region", *Urban Studies*, vol. 42, no. 12, (2005), pp. 2145–2166. https://doi.org/10.1080/00420980500332064

[20] Ferrell C.E., "Home-Based Teleshoppers and Shopping Travel: Do Teleshoppers Travel Less?", *Transportation Research Record: Journal of the Transportation Research Board*, vol. 1894, no. 1, (2004), pp. 241–248. https://doi.org/10.3141/1894-25

[21] Lityński P. and Hołuj A., "Urban sprawl costs: The valuation of households' losses in Poland", *Journal of Settlements and Spatial Planning*, (2017). https://doi.org/10.24193/JSSP.2017.1.02

[22] Borchert J.G., "Spatial dynamics of retail structure and the venerable retail hierarchy", *GeoJournal*, vol. 45, no. 4, (1998), pp. 327–336. https://doi.org/10.1023/A:1006976407047

[23] Fernandes J. R. and Chamusca P., "Urban policies, planning and retail resilience", *Cities*, vol. 36, (2014), pp. 170–177. https://doi.org/10.1016/j.cities.2012.11.006

[24] Nilsson K. et al., "Strategies for Sustainable Urban Development and Urban-Rural Linkages", *European Journal of Spatial Development*, (2014), pp. 2–26.

[25] Colucci M., Palermo A., Francini M., "The Sustainable Development of Rural Areas", in 2nd International Conference on Civil, Materials and Environmental Sciences (CMES 2015), 2015, pp. 210–211. https://dx.doi.org/10.2991/cmes-15.2015.60

[26] The Office of the Deputy Prime Minister, *Planning policy statement 7: sustainable development in rural areas*. United Kingdom, 2004.

[27] Gallent N. et al., *Introduction to rural planning: Economies, communities and landscapes*. 2015. https://doi.org/10.4324/9781315749280

[28] Palomäki M., "The Functional Centers and Areas in South Bothnia, Helsinki", *Fennia*, vol. 88, (1964), pp. 10–19.

[29] Burgess E.W., "The Growth of the City: An Introduction to a Research Project", in *Urban Ecology*, Boston, MA: Springer US, 2008, pp. 71–78. https://doi.org/10.1007/978-0-387-73412-5_5

[30] Proudfoot M. J. and Hoyt H., "The Structure and Growth of Residential Neighborhoods in American Cities.", *Journal of the American Statistical Association*, (1940). https://doi.org/10.2307/2279683

[31] Harris C. D. and Ullman E.L., "The nature of cities", in *A Geography of Urban Places*, 2014. https://doi.org/10.4324/9781315105352-1

[32] *Uchwała nr XLVIII/1622/2014 Sejmiku Województwa Dolnośląskiego z dnia 27 marca 2014 r. w sprawie zmiany uchwały nr XLVIII/873/2002 Sejmiku Województwa Dolnośląskiego z dnia 30 sierpnia 2002 r. w sprawie uchwalenia Planu Zagospodarowania Przestrzennego Woj*, 2014.

[33] Powiat Wrocławski, *Studium Spójności Funkcjonalnej we Wrocławskim Obszarze Funkcjonalnym*. Wrocł>aw: Powiat Wrocławski, 2015. Available: http://bip.um.wroc.pl/artykul/347/5715/ studium-spojnosci-funkcjonalnej-we- wroclawskim-obszarze-funkcjonalnym

[34] *Uchwała nr VIII/38/2007 Rady Gminy Czernica z dnia 29 czerwca 2007 r. w sprawie przyjęcia studium uwarunkowań i kierunków zagospodarowania przestrzennego gminy Czernica*, 2007.

[35] Powiat Wrocławski, *Spatial Information System of the Wrocławski County*. 2019. Available: https:// serwis.wrosip.pl/imap/?gpmap=gp3 [Accessed: 12 Dec 2019]

[36] Velibeyoglu K. and Gençel Z., "Reconsidering the Planning and Design of Urban Public Spaces in the Information Age : Opportunities & Challenges", *Public Spaces in The Information Age*, (2006).

[37] Skoczylas O., "Transformation of city space and housing estates associated with changes in life-style of inhabitants", *Budownictwo i Architektura*, vol. 15, no. 1, (2016), pp. 143–148. https://doi. org/10.24358/Bud-Arch_16_151_15

[38] Zuziak Z., "On the synergy of urban plan", *Budownictwo i Architektura*, vol. 16, no. 1, (2017), pp. 183–198. https://doi.org/10.24358/Bud-Arch_17_161_16

Crossref
Similarity Check
Powered by iThenticate

Orginal Article

FEM model versus laboratory test of thin-walled steel beams strengthened by CFRP tapes

Katarzyna Rzeszut[1], Ilona Szewczak[2], Patryk Różyło[3]

[1] Institute of Building Engineering; Poznan University of Technology;
Marii Skłodowskiej-Curie St.5, 60-965 Poznań, Poland;
katarzyna.rzeszut@put.poznan.pl (iD) *0000-0002-7134-608X*
[2] Faculty of Civil Engineering and Architecture; Lublin University of Technology;
Nadbystrzycka St. 38 D, 20–618 Lublin, Poland;
i.szewczak@pollub.pl (iD) *0000-0002-4953-0104*
[3] Faculty of Mechanical Engineering; Lublin University of Technology;
Nadbystrzycka St. 38 D, 20–618 Lublin, Poland;
p.rozylo@pollub.pl (iD) *0000-0003-1997-3235*

Abstract: The main aim of the study is to develop the best-suited FEM numerical model of beams made of thin-walled cold-rolled steel profiles retrofitted by CFRP tapes. The FEM model fitting has been carried out based on own laboratory tests conducted on Σ type beams. The CFRP tapes are bonded to the beam at compressed or tensioned flange. The most important part of this study is focused on the investigation of boundary conditions influence in FEM model developed in Abaqus program. Moreover, the numerical models are also tested in terms of different mesh density and type of finite elements. Numerical analyses are carried out using a Newton-Raphson iterative method to solve the non-linear equilibrium equation. In the paper, special attention is paid to the evaluation of the possibility to increase the load capacity by appropriate localisation of CFRP tape.

Keywords: steel thin-walled cold-formed beam, CFRP tape, strengthening

1. Introduction

New technological solutions require a special approach, namely before their introduction to common use, ant that means experimental studies should precede them. Nevertheless, due to the high costs of laboratory tests, they are usually carried out for a very narrow spectrum of cases, while broader analyses are made using the so-called numeric experiment. For this purpose, it is very important to carry out the verification and validation of the FEM numerical model as

well as possible. This problem has recently become extremely important in order to verify the innovative methods of retrofitting the steel thin-walled cold-rolled elements, which have been widely used in civil engineering not only as purlins or rails but also as main structural bearing elements. One can notice that due to very thin walls, these structures are characterised by a limited possibility of reinforcement methods because traditional ones, such as welding or bolted connection, are not very efficient. Therefore, it is necessary to look for a smart and accurate method to overcome the problem of strengthening the existing steel elements with very thin walls.

One of many options is the use of tapes made of carbon fibre reinforced polymers (CFRP); they enable fast and effective reinforcement of the structure practically without limiting the continuity of its operation. CFRP tapes are characterised by excellent mechanical properties such as over ten times higher strength in tension of the tape in fibres direction compared with conventional structural steel grades and high fatigue or corrosion resistance. These properties depend on the type and the orientation of carbon fibres, the type of the epoxy resin, and its percentage share in the final material. The disadvantage of CFRP tapes is low strength in compression, which is approximately 10% of the tensile strength. Strength parameters of FRP materials used to strengthen structures are described in detail in [13]. However, the main advantage of CFRP tape in case of thin-walled structures is the possibility to applicate an adhesive bond between CFRP tape and construction, which allow for an easy and speedy connection without the damage of very thin steel walls. The detailed information on rules of adhesive bonding in steel, aluminium, and composite structures is presented in [9], [8].

Research papers on reinforced steel elements subjected to bending or compression are being presented in scientific reports more and more frequency. Research on steel circular hollow section (CHS) confirms that using CFRP for strengthening deficient columns showed the appropriate impact on rising bearing capacity and reducing stress in the damaged location and preventing local deformation [7]. Also, positive conclusions are drawn from the analysis of the steel squared hollow section (SHS) restrained with CFRP tapes [4]. In addition, as shown in [5], CFRP tapes allow for the reinforcement of corroded steel elements. It was shown that the combined flexural and bearing capacity of the CHS could be significantly increased by adhesively bonding CFRP. The maximum gain in strength was 434%, which was obtained for the most severe 80% corrosion, extended along the full length. In engineering practice, CFRP tapes are used to reinforce steel bridge girders, which is justified by Ardalani et al. in [3], or I-beams used, for example, as floor beams. CFRP materials can also be used to reinforce steel floor beams with holes in the web, as discussed in [1]. In this paper, an experimental study involving four full-scale beams under 6-point bending was carried out. The study was conducted to investigate the ability of CFRP to improve the load-bearing capacity of beams with web opening. As a result, up to 20% increase in the bearing capacity of the elements was achieved. CFRP materials also found application for reinforcement of aluminium structures. In [14], which is based on the example of the pre-stressed aluminium bridge, the authors showed that the application of the extruded CFRP tendon-anchor system provides an improvement of 25%. The abovementioned references indicate the wide use of modern composite materials for reinforcement of various types of steel structures. Still, the use of CFRP composites to strengthen steel structures is incomparably small, in relation to the use of these materials in the reinforcement of concrete or masonry structures. It should be emphasised that there are very few studies on strengthening thin-walled steel structures by CFRP. This fact became

the motivation for the authors to undertake research regarding the strengthening of sigma thin-walled steel elements with CFRP tapes. Authors of this paper paid particular attention to the evaluation of the possibility of increasing the load capacity of the thin-walled beams by appropriate position of CFRP tape. The work involved verification and validation of different FEM numerical models of thin-walled sigma profile strengthen with CFRP tapes using the Abaqus / CAE program and solid or finite shell elements.

2. Laboratory tests

The scope and course of laboratory tests, as well as the obtained test results, were discussed in detail in [11] and [12]. Laboratory tests were carried out on sigma thin-walled, cold-rolled beams. The dimensions of the cross-section of the sigma profile was ∑140x70x2.5. All tested beams were simply supported elements with the span of 2.20 m and loaded by uniformly distributed load using laboratory stand prepared in accordance with the patent [10]. The uniformly distributed load was applied to the sample using steel cables in seven points along the span of the beam. The displacement of each beam was measured using the four displacement gauges – three in the horizontal direction and one in the vertical direction, placed in the middle of the span. In the case of five beams, a measurement of strain was made using six strain electrofusion gauges TENMEX TFs-10, the resistance of 120 Ω ± 0.2%. Experimental studies were carried out in the Laboratory of Civil Engineering, in Lublin University of Technology, in the test machine Zwick & Roel controlling the growth of the load specified by the extending press piston with a speed of 1 mm/min, recording the force at 0.01 s. The scheme of the laboratory stand, the geometry of the cross-section of the tested beams and are shown in Fig. 1.

Fig. 1.   Scheme of the laboratory stand and the geometry of the tested beams. *Source:* own study

On the basis of the σ-ε relationship obtained in laboratory coupon test, the bilinear elastic-plastic material model with strain hardening with Young's modulus (201.8 GPa), Poisson's ratio (0.282), and yield strength (418.5 MPa) was adopted in FEM numerical model (Fig. 2). Lower value of Young's modulus than for the S350 GD steel grade, results from the fact that the samples are made of galvanised steel.
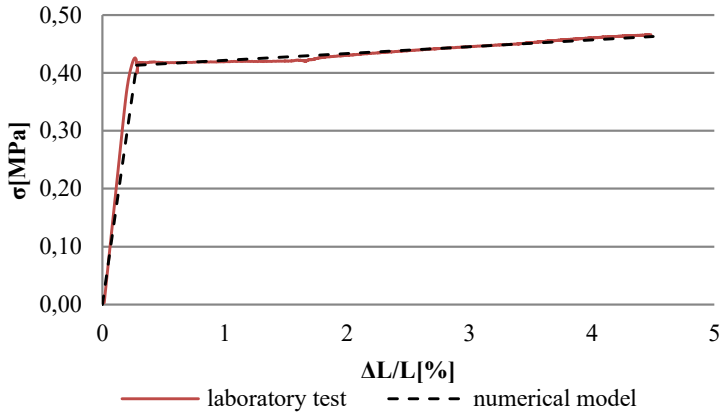
Fig. 2.   Material characteristics of steel: laboratory coupon test; numerical model. Source: own study

The CFRP tapes, with a thickness of 1.2 mm and width of 50 mm, were described as orthotropic material with typical composite materials characteristic such as Young's modulus (165 GPa) and Poisson's ratio (0.308).

3. Numerical model

Various numerical models in FEM program ABAQUS®[1] were developed. In order to select the most suitable one, they were subjected to calibration based on own laboratory test results [11]. Numerical analyses were performed for beams identical to those tested in the laboratory. Namely, for simply supported, subjected to uniformly distributed load elements with the span of 2.20 m and made of Σ140x2.5 cross-section. In the numerical model, the load was defined in the same way as in the experiment, taking into account that the load is transmitted by means of seven steel cables along the length of the beam. Numerical models corresponding to beams tested in the laboratory were considered. Beam "B3" was not reinforced (bare beam). Beam "B4" was reinforced by CFRP tape bonded to the external surface of the tensioned flange, while beam "B1" to the internal surface of the compressed flange. The layout of CFRP tapes in the examined beams adopted in laboratory tests and a numerical model is shown in Fig. 3.
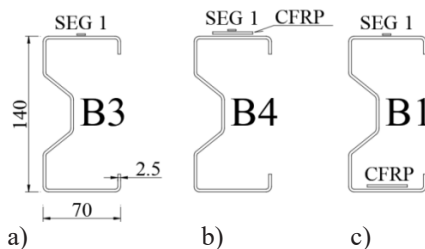

Fig. 3.   Layout of CFRP tapes on the examined thin-walled beams a) bare beams, b) CFRP tape bonded to the tensioned flange, c) CFRP tape bonded to the compressed flange. *Source:* own study

Connection between the CFRP tapes and the corresponding plane (the lower and upper flange) of the beam was modelled using a numerical TIE-type connection. Another method of modelling adhesive connection can be found in [6]. The developed numerical models were different in terms of boundary conditions, the type of finite element (FE) and mesh size. The summary of the analysed numerical models is presented in Tab. 1.

Table 1.   Summary of the analysed numerical models. *Source:* own study

No.	Acronym of num. model	Type of boundary conditions	Type of FE	Number of FE/ nodes
1.	*Abaqus solid B3p*	Non-deform. shell el. R3D4	SOLID C3D8R	45000/61404
2.	*Abaqus solid B3k*	Displacement constraints	SOLID C3D8R	45000/61404
3.	*Abaqus shell B3l.p*	Non-deform. shell el. R3D4	SHELL S4R	46200/46878
4.	*Abaqus shell B3l.k*	Displacement constraints	SHELL S4R	46200/46878
5.	*Abaqus shell B3k.p*	Non-deform. shell el. R3D4	SHELL S8R	46200/139955
6.	*Abaqus shell 3k.k*	Displacement constraints	SHELL S8R	46200/139955

Each of the MES models has been prepared, taking into account the contact properties in the tangent and normal direction, between the beam and supports.

In the numerical models, the supports were modelled in two ways, each of which described so-called fork support. In the first method, the supports were modelled by using displacement constraints imposed at the points No. 1-5 located on the contour in the plane created by the partition of the element. At points No. 1, 2, 3, and 4 transfers displacements U_x were constrained and at point No. 5 – longitudinal displacement U_y was constrained. At all this points rotation was free (Fig. 4a). In the second model, the supports were modelled using non-deformable shell elements of the R3D4 type (Fig. 4b).

Thin-walled sigma beams ware modelled using three different types of finite element, namely, a solid element with a linear shape function of the C3D8R type with 3 translational degrees of freedom in each of the 8 nodes per one finite element. Next, the shell element of S4R type with a linear shape function (four-node type with reduced integration), and finally, a shell element of S8R type with a square shape function was used.

The analysis of the influence of mesh size was made only for the numerical model No. 4 (*Abaqus shell B3l.k*) changing the size of the finite element from 5 mm to 7.5 mm. The model with a finite element size of 7.5 mm had 24 400 elements and 24862 nodes and was marked with the acronym *Abaqus shell B3l.k.g*. The next stage of the analysis consisted of removing the mesh density on the rounded corners of the profile, which resulted in the creation of a cross-section with sharp edges. This model had 21 200 elements and 21 665 nodes and was marked with the acronyms *Abaqus shell B3l.k.k*.

In order to reflect laboratory tests of beams B1 and B4, numerical models No. 1 and No. 4, were extended by the numerical modelling of CFRP tapes. In all numerical models, CFRP tapes were modelled as shell finite elements of the S8R type, which contains 6 degrees of freedom, in each of the 8 nodes per finite element. The number of finite elements was 1 040 and the number of computational nodes was 1 254. Connection between the CFRP tape and the corresponding beam surface was modelled using a "TIE" type numerical connector which preserves the constant distance between points lying on two adjacent surfaces and constraint rotations between these points.
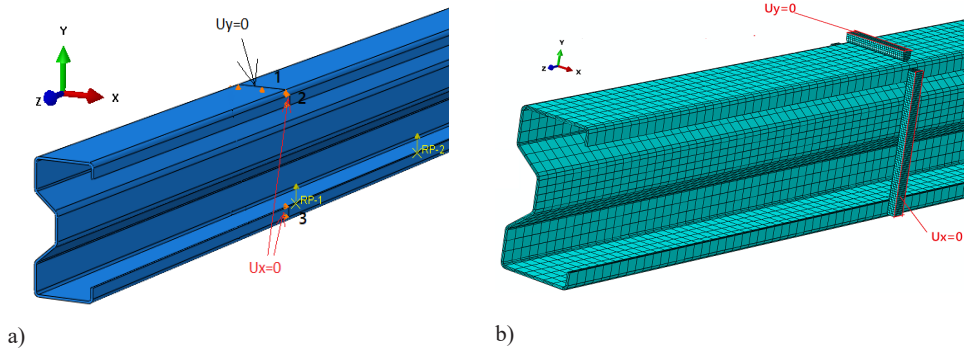
Fig. 4. Numerical models of the support a) displacement constraints: U_y, U_x. b) non-deformable shell elements R3D4 and displacement constraints: U_y, U_x. *Source:* own study

Another parameter that has a decisive influence on numerical results is the size of the mesh in the numerical model. In order to investigate this effect, the mesh size analysis was performed for a numerical model with S4R shell finite elements, linear shape function and supports modelled as displacement constraints. As it was mentioned above, the size of the mesh was changed from 5 mm (Abaqus shell B3l.k) to 7.5 mm (Abaqus shell B3l.k.g). The next modification was to remove the increase mesh density on the rounded surfaces of the element. Thus, a simplified model was created with a finite element size of 7.5 mm and constant mesh density (Abaqus shell B3l.k.k). Various mesh configuration in numerical models are presented in Fig. 5.
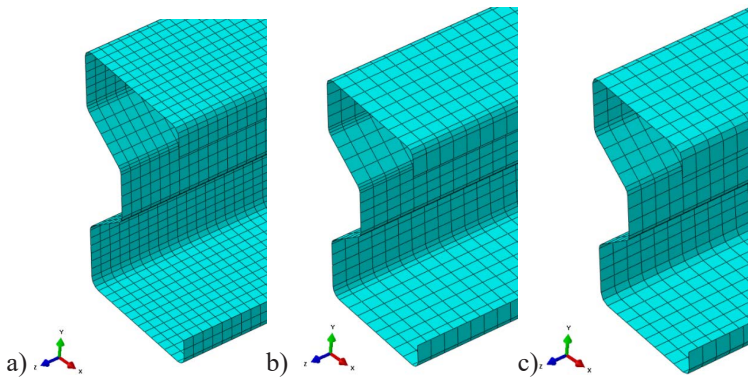
Fig. 5. Various mesh configuration in numerical models: a) *Abaqus shell B3l.k*, b) *Abaqus shell B3l.k.g*, c) *Abaqus shell B3l.k.k. Source:* own study

The non-linear studies are carried out by solving the equilibrium equation. The Newton-Raphson iterative method is used for both stable and unstable post-buckling responses.

4. Results of numerical analysis versus laboratory test

As mentioned before, in order to find the best representation of the real structural behaviour, numerical models differing in terms of modelling boundary conditions, mesh density and finite element types have been developed. FEM model quality assessment was conducted by

comparison of strain measured during laboratory tests by electrofusion strain gauge SEG 1, SEG 2, placed in the middle of the beam span, in the centre of the tensile or compressed flange respectively, with results obtained from the FEM analysis. Unfortunately, due to the significant rotation of the beam, the displacement measurement was not reliable, because the induction gauges did not remain in constant contact with one measuring point (Fig. 6).
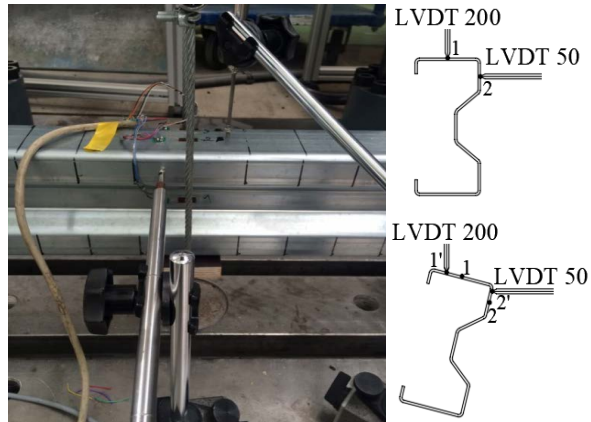
Fig. 6.   Displacement measurements details. *Source:* own study

Therefore, this parameter was not taking into account during the evaluation of the numerical model.

Comparison of the *P-ε* relationship for different numerical models (see Tab. 1) and laboratory test (plot *B3*) for the bare beam (without reinforcement) shows Fig. 7.
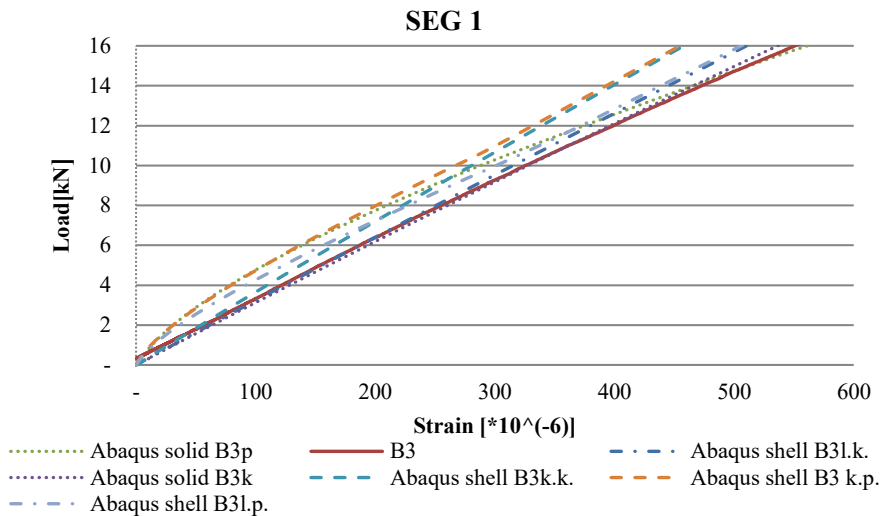
Fig. 7.   The *P-ε* (load – strain) relationship for the bare beam (SEG 1 readout) for laboratory specimen and various numerical models. *Source:* own study

The analysis of the obtained results shows that the highest compliance with the results of laboratory tests was obtained for two numerical models. Namely, for the numerical modelled using solid FE with a linear shape function (*Abaqus solid B3k*) and for a numerical model with shell FE and linear shape function (*Abaqus shell B3l.k*). In these two models, supports were modelled by using displacement constraints. One can notice that the numerical model (*Abaqus solid B3k*) shows compatibility over the whole equilibrium path while the numerical model (*Abaqus solid B3k*) loses its convergence at a higher load level. Noteworthy is also the numerical model (*Abaqus solid B3p*) with solid FE and the supports in the form of non-deformable shell elements R3D4. This model is characterised by very good convergence for the maximum load value. However, the worst compatibility is observed in the case of a beam modelled by shell-type FE with a square shape function and supports in the form of non-deformable shell elements R3D4 (*Abaqus shell B3k.p*).

Based on the above observations, three models were selected for further analysis (*Abaqus solid B3k*, A*baqus solid B3p and Abaqus shell B3l.k*). Thus, in the case of beams strengthened with CFRP tape, the validation and verification were limited only to three numerical models. In Fig. 5 the relationship *P*-ε (load – strain) for the beam strengthened with CFRP tapes based on SEG 1 laboratory readout and results obtained for selected numerical models is presented.

In Fig. 8a the plot *B4* refers to the beam strengthened with CFRP tapes bonded to the tensioned flange tested in the laboratory and the other plots illustrate the response of the beam strengthened in the same way for three representative numerical models (*Abaqus solid B4k, Abaqus solid B4p, Abaqus shell B4l.k*). Fig. 8b presents the strain values read from SEG 1 for beams strengthened with CFRP tape at compressed flange (B1) and analogous numerical model (*Abaqus solid B1k, Abaqus solid B1p, Abaqus shell B1l.k*).

One can notice that in case of the beams strengthened with CFRP tapes at the tensioned or compressed flange the highest compliance with the results of laboratory tests occurs for numerical models with shell or solid FE and displacement constraints (*Abaqus shell B1l.k, Abaqus solid B1k, Abaqus shell B4l.k and Abaqus solid B4k*). This conclusion coincides with the observations made for unreinforced beams. Surprisingly, the most complex numerical model (*Abaqus solid B1p and Abaqus solid B4p*) in the initial phase of the work of the beam provides results that deviate from the laboratory tests.
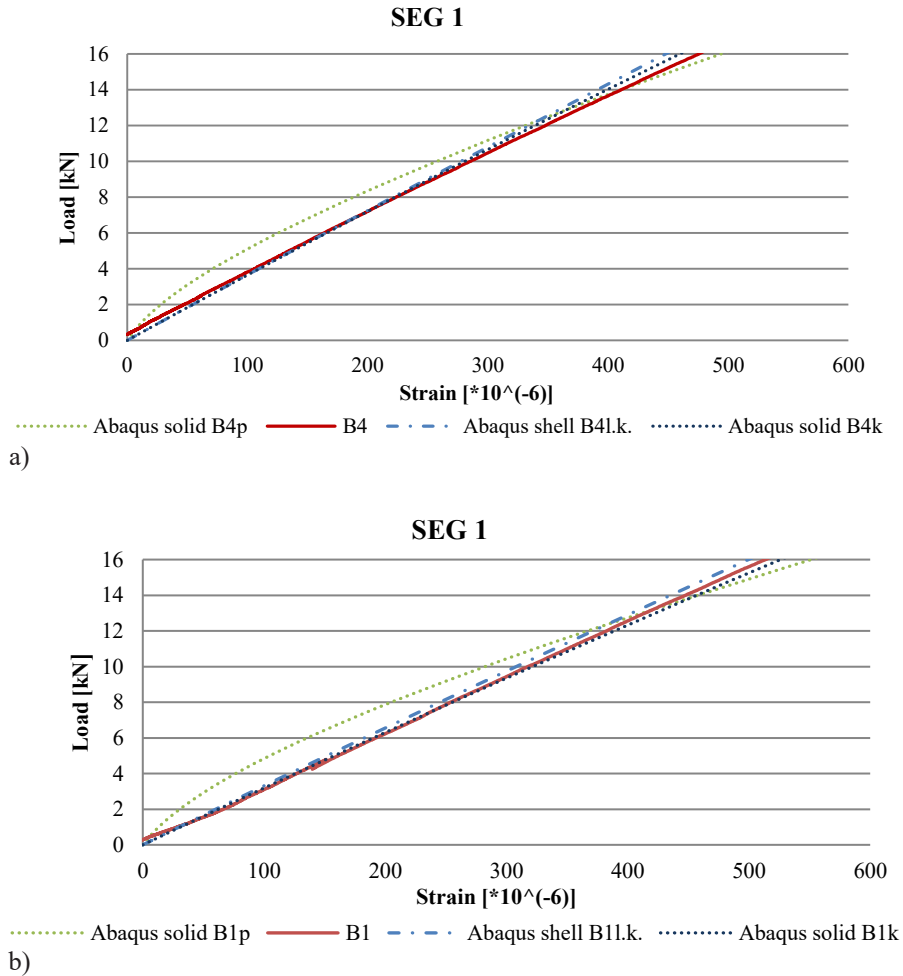
Fig. 8.   The load – strain relationship (SEG 1 readout) for laboratory specimen and various numerical models for the strengthen beam: a) at the tensioned flange, b) at the compressed flange. *Source:* own study

The force – strain relationship obtained for the bare beams for different mesh size in numerical model and SEG 1 readout in laboratory tests is presented in Fig. 9. For the beam restrained by CFRP tape bonded to the tensioned flange (B4) the mesh size analysis (Fig. 10) was performed for the numerical model (*Abaqus shell B4 l.k.k, Abaqus shell B4l.k*). Analogous, the force – strain relationship for beams reinforced with CFRP tape at compressed flange (B1) and the numerical model (*Abaqus shell B1l.k.k, Abaqus shell B1 l.k*) is shown in Fig. 11.

Fig. 9.   The force – strain relation obtained from the numerical model and SEG 1 readout for the bare beams
           for different mesh size. *Source:* own study

Fig. 10.   The force – strain relation obtained from the numerical model and SEG 1 readout for the beams
           reinforced at the tensioned flange. *Source:* own study
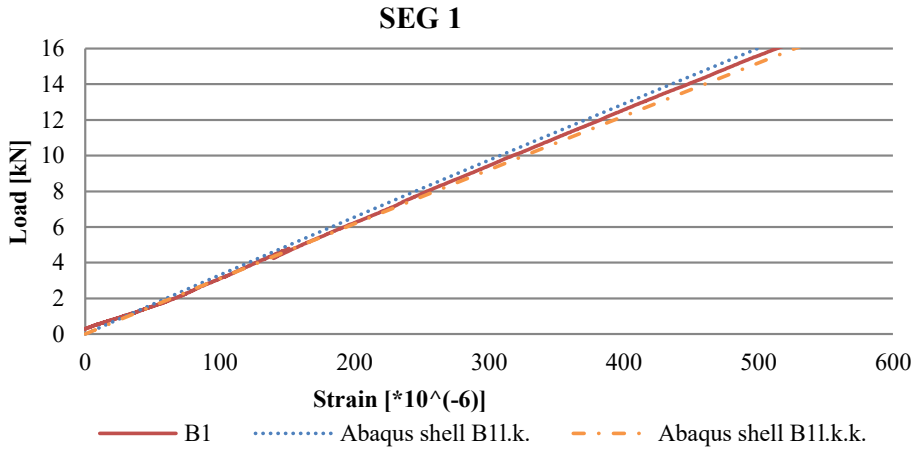
SEG 1

Fig. 11.   The force – strain relation obtained from the numerical model and SEG 1 readout for the beams reinforced at compressed flange. Source: own study

The force – strain relationship obtained for the bare beams and the beams reinforced at the tensioned flange for different mesh size in the numerical model and SEG 2 readout in laboratory tests is presented in Fig. 12 and 13.

SEG 2
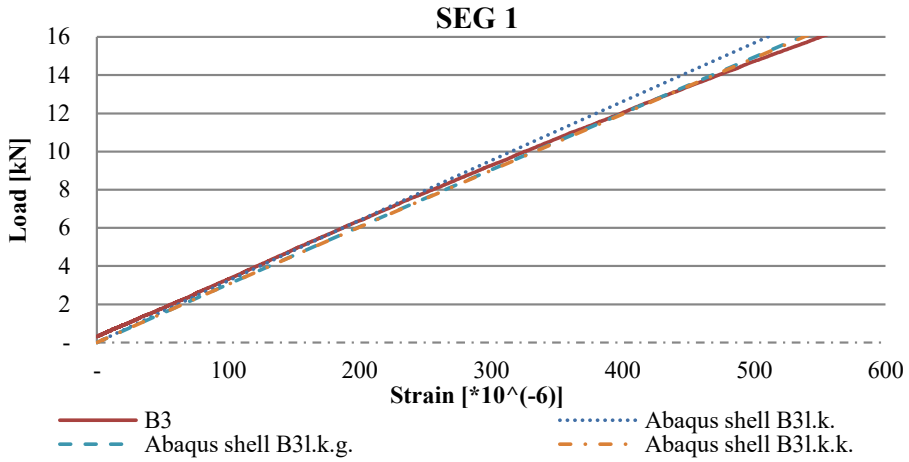

Fig. 12.   The force – strain relation obtained from the numerical model and SEG 2 readout for the bare beams for different mesh size. *Source:* own study
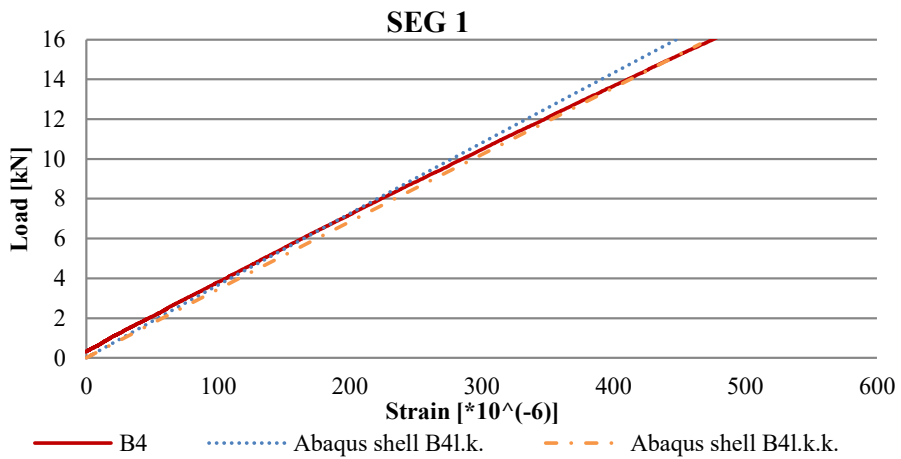
Fig. 13. The force – strain relation obtained from the numerical model and SEG 1 readout for the beams reinforced at the tensioned flange. *Source:* own study.
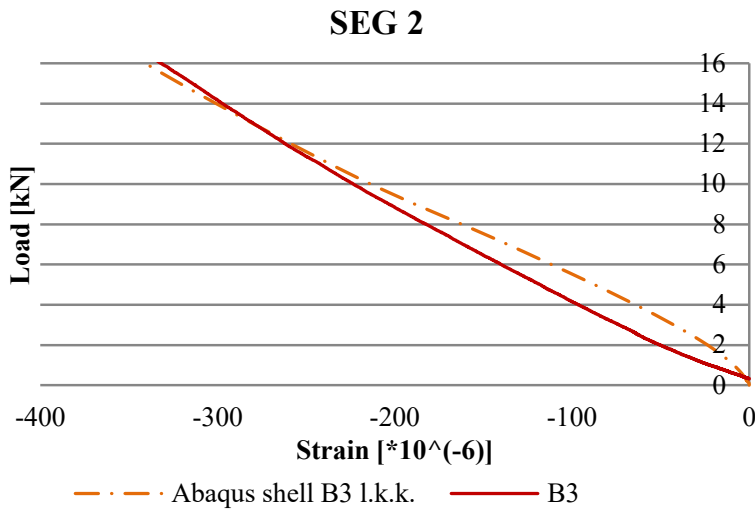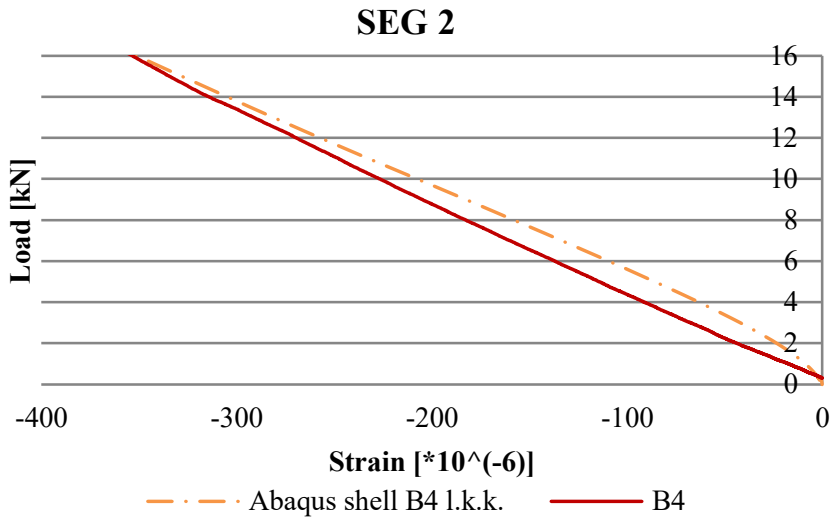
5. Concluding remarks

The research presented in the paper is of a pilot nature and is part of a more extensive program. The primary purpose of the work was to check the efficiency of strengthening sigma beams using CRP tape in the context of laboratory and numerical tests. The primary conclusion of the presented article highlights the difficulties associated with the analysis of the field of displacement and deformation of beams subjected to significant rotation.

The original purpose of the laboratory tests was to analyse beams that undergo significant rotation. Unfortunately, the used laboratory stand made it impossible and eliminate the possibility to carry out the experiment until the damage. Therefore, in order to track the behaviour of the beam reinforced with CFRP tapes over the entire load range. A numerical model was created to reproduce the laboratory conditions as accurately as possible by introducing the appropriate contact and non-linear analysis.

Conducted analyses allowed to conclude that the results most similar to laboratory tests were obtained for the model with supports modelled in a simplified way by using displacement constraints. Numerical model with supports modelled as non-deformable shell elements produced significant discrepancies, which is surprising, because it faithfully reflects the real laboratory conditions. Based on the obtained results, it can be stated that laboratory tests most accurately describe the numerical model (*Abaqus shell B3l.k.k, Abaqus shell B4l.k.k, Abaqus shell B1l.k.k*). This was unexpected because it is the least detailed numerical model. It should be noted that the above results of numerical research concerned beams without geometrical imperfections, which in the real thin-walled section can significantly affect the results.

In terms of the discrete models used, the C3D8R model was based on correlations of the results obtained with experimental studies (the use of the C3D20R mesh) in this case gave less convergent results, although it is this mesh that usually allows to obtain better qualitative and quantitative results. In the case of C3D8R mesh, 3 elements were applied to the thickness of the structure, allowing to create a neutral layer. Probably, it would have been better to use

the C3D20R mesh; however, less convergence of results was obtained for such test model than the C3D8R finally used with 3 elements on the thickness of the structure. Thus, it was found that in the case of static analysis, the least appropriate is the shell model with a square shape function.

References

[1]   Altaee M.J., Cunningham L., Gillie M., "Experimental investigation of CFRP-strengthened steel beams with web openings", *Journal of Constructional Steel Research*, Vol. 138/November 2017, pp.750-760. https://doi.org/10.1016/j.jcsr.2017.08.023

[2]   App 1 to PN-90/B-03200 "Stability parameters of structure", *Konstrukcje stalowe. Obliczenia statyczne i projektowanie.*

[3]   Ardalani G.T., Showkati H., Teymourlouei H.E., Firouzsalari S.E., "The performance of plate girders reinforced with CFRP plates of various lengths", *Thin-Walled Structures*, Vol. 120/ November 2017, pp.105-115. https://doi.org/10.1016/j.tws.2017.08.015

[4]   Bambach M.R., "Strengthening of thin-walled (hollow) steel sections using fibre-reinforced polymer (FRP) composites", in *Rehabilitation of Metallic Civil Infrastructure Using Fiber Reinforced Polymer (FRP) Composites Types Properties and Testing Methods*, eds. M. Karbhari, 2014, pp.140–168. https://doi.org/10.1533/9780857096654.2.140

[5]   Elchalakani M. et al., "CFRP strengthening and rehabilitation of corroded steel pipelines under direct indentation", *Thin-Walled Structures*, Vol. 119/ October 2017, p.510-521. https://doi.org/10.1016/j.tws.2017.06.013

[6]   Kawecki B., Podgórski J., „Analiza pracy wspornikowej belki kompozytowej z uwzględnieniem różnej grubości i lokalizacji spoiny klejowej wykonanej z materiału sprężysto-idealnie plastycznego", *Budownictwo i Architektura*, 15(4), 2016, pp. 195-208. https://doi.org/10.24358/Bud-Arch_16_154_19

[7]   Masoumeh K. et al., "Structural behaviors of deficient steel CHS short columns strengthened using CFRP", *Journal of Constructional Steel Research*, Vol. 138/ November 2017, pp.555-564. https://doi.org/10.1016/j.conbuildmat.2016.09.099

[8]   Pasternak H., Ciupack Y., "Eurocode – Based design rules for adhesive bonded joints", *Conference paper, Eurosteel 2011,* August 31 – September 2, 2011, Budapest, pp. 717-722.

[9]   Piekarczyk M., Grec R., "Application of adhesive bonding in steel and aluminium structures", *Archives of Civil Engineering,* LVIII, 3, 2012, pp. 309-329.

[10]   Pieńko M., Robak A., "Stand for testing deformations of evenly loaded horizontal elements", Lublin University of Technology, 2015, Patent Application (21) 410025.

[11]   Rzeszut K., Szewczak I., "Experimental Studies of Sigma Thin-Walled Beams Strengthen by CFRP Tapes", *International Journal of Civil, Environmental, Structural, Construction and Architectural Engineering*, Vol.11/2017, No.7, pp.888-895. ISNI:0000000091950263

[12]   Rzeszut K., Szewczak I., Różyło P., "Issues of thin-walled sigma beams strengthened by CFRP tape in context of experimental and numerical study", *Engineering Transaction*, vol. 66/2018, no. 1, pp. 79–91.

[13]   Technical report, „FRP Reinforcement in RC structures", Bulletin 40, September 2007. Available: https://www.iranfrp.ir/wp-content/uploads/2018/12/40-FRP-reinforcement-in-RC-structures_0-1.pdf [Access: 16 Jan 2020]

[14]   Zhu P. et al., "Structural analyses of extruded CFRP tendon-anchor system and applications in thin-walled aluminium/CFRP bridge", *Thin-Walled Structures*, Vol. 127/ June 2018, p.556-573. https://doi.org/10.1016/j.tws.2018.02.0294

Report on laboratory tests of sandstone and porphyry for rock fracture analysis

Jakub Gontarz[1], Jacek Szulej[2]

[1] *Department of Structural Mechanics; Faculty of Civil Engineering; Lublin University of Technology;*
Nadbystrzycka St. 40, 20-618 Lublin, Poland;
j.gontarz@pollub.pl (iD) *0000-0002-6900-6158*

[2] *Department of Structural Mechanics; Faculty of Civil Engineering; Lublin University of Technology;*
Nadbystrzycka St. 40, 20-618 Lublin, Poland;
j.szulej@pollub.pl (iD) *0000-0003-4745-7705*

Abstract: The paper presents the results of mechanical tests of three types of rocks from Polish stone mines. Compression tests of cubic samples, three-point bending tests of beams, bending of beams with a notch, and testing of tensile strength using the quasi-Brazilian method were performed. Based on the tests, the compressive strength, tensile strength, Young's modulus, and Poisson's ratios were determined. The stress intensity factor and critical strain energy release rate in mode I were determined from the bending test of the notched beams. The determined values were used as parameters of computer models, which allowed to verify the authors' method of predicting the crack propagation in the Abaqus FEA system.

Keywords: sandstone, porphyry, laboratory tests, fracture mechanics

1. Introduction

In this research, a series of laboratory tests on two types of sandstone and one type of porphyry were performed. The purpose was to obtain rock material parameters, based on which the authors would develop own method of determining the direction of crack propagation of brittle materials, such as rocks, in the Abaqus FEA system using the X-FEM method. Extended Finite Element Method is a method of simulating fracture that does not depend on the elements' mesh. Elements can break anywhere – this is allowed by the appropriate modification of the shape function. The authors used the Abaqus User Subroutine, a tool that is provided by Abaqus, to modify the calculation procedure. The description of own subroutine and the results of these analyzes will be published in the future. To properly verify the created method, several laboratory tests had to be performed. The paper

presents the procedures and test results for required rock mechanical parameters. The tests described here are not innovative, however obtaining material parameters is necessary to verify computer analyzes. The authors also hope that the results presented in this work will help other scientists in their future research.

The choice of rock material was determined by the author's previous analysis [1], where the maximum force of pulling out the anchor from rocks mentioned above was investigated. New mining rescue technology without the use of explosives was initially developed in research commissioned by the KOMAG Institute of Mining Technology. A scheme of this study was presented in the author's previous paper [2], which also contains a summary of similar laboratory tests of different types of rocks. Some of the material parameters for the selected sandstone types (for example – "Brenna" sandstone) were described in work [3] by Tomiczek and [4] by Łukasiak. The analysis of the microstructure of sandstone is especially interesting. Finally, an example of research dealing with a similar subject to this one is [5], where the well-known "Szydłowiec" sandstone was studied.

2. Description of materials and selection of tests

Three types of rocks were tested: grey-coloured sandstone from the "Braciszów" mine, light or pink porphyry from the "Zalas" mine, and sandstone from the "Brenna" mine, similar to the "Braciszów" sandstone.

In the Abaqus system, selected mechanical parameters are required to simulate the crack using the simplest criterion for maximum principal stresses. Values of Young's modulus and Poisson's ratio are required, for elastic materials to which rocks belong, regardless of the cracking criterion. Therefore, cube compression tests were performed with the measurement of horizontal and vertical strain to obtain these parameters. To simulate the fracture in Abaqus, it is required to provide the stress at which the crack will occur. In the simplest case, this stress value is equivalent to the tensile strength. Therefore, three-point bending tests and a quasi-Brazilian test, i.e. tensile force during splitting cubic samples, were performed. Also, the beams were examined using the same quasi-Brazilian method, and the results were compared to the cubes. The analysis also requires providing critical strain energy release rate in mode I. The authors determined the stress intensity factor in mode I K_{IC} through a three-point bending test of beams with notches. Compressive strength using cubes was also tested.

3. Description of the mechanical parameters tests

3.1. Compression test of cubic samples

The authors performed uniaxial compression tests for all described materials. 14 cubic samples of "Braciszów" sandstone (samples K1c-K14c), 10 samples of "Zalas" porphyry (K1z-K10z), and 12 samples of "Brenna" sandstone (K1b-K12b) were tested. For various reasons, the results of not all samples were used to calculate Young's modulus and Poisson's ratio. Samples of "Braciszów" sandstone and porphyry were about 7×7×7 cm, and samples of "Brenna" sandstone were about 10×10×10 cm. Unfortunately, the samples had irregular dimensions, because most of them were obtained from small fragments of cones obtained during the anchor pull-out test.

The samples were initially tested on the MTS 319.25 testing machine, with the measurement of vertical and horizontal deformations. The "Braciszów" sandstone and "Zalas" porphyry

were tested first. Vertical displacements in one direction were determined using a displacement transducer (fig. 2a), measuring the change in sample height during the test. Horizontal displacements (perpendicular to the direction of the compressive force) were measured with a clip-on extensometer measuring the change in distance between the steel plates adhered to the samples. This test was carried out using low force to avoid destruction of the samples and measuring instruments. Then, after removing the measuring devices, the samples were loaded for destruction on a WalterBai testing machine.

It turned out that measuring only two displacements is insufficient to obtain accurate results. For this reason, the next samples from the "Brenna" sandstone were tested using strain gauges. Two vertical and two horizontal strain gauges were glued on opposite sides (fig. 1a, fig. 2b). Changes in displacement in both directions were determined as the arithmetic mean of the strain gauge pair.
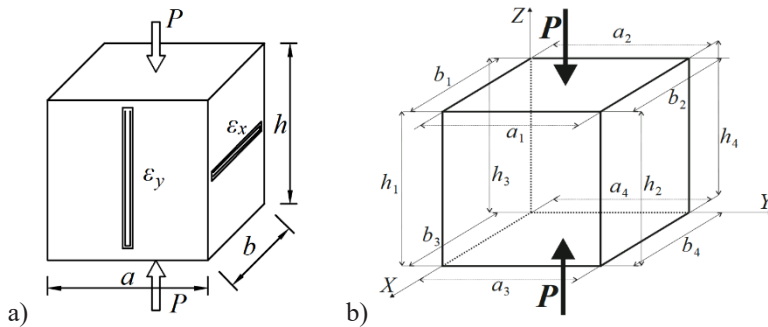
Fig. 1.   Cubic sample. a) assembly method of strain gauges, b) sample dimensions: $a = (a_1+a_2+a_3+a_4)/4$, $b = (b_1+b_2+b_3+b_4)/4$, $h = (h_1+h_2+h_3+h_4)/4$. *Source:* own study

The dimensions of the samples were determined as the average of the length of each of the four edges of a given dimension. Sample photos from the tests are shown in fig. 2.
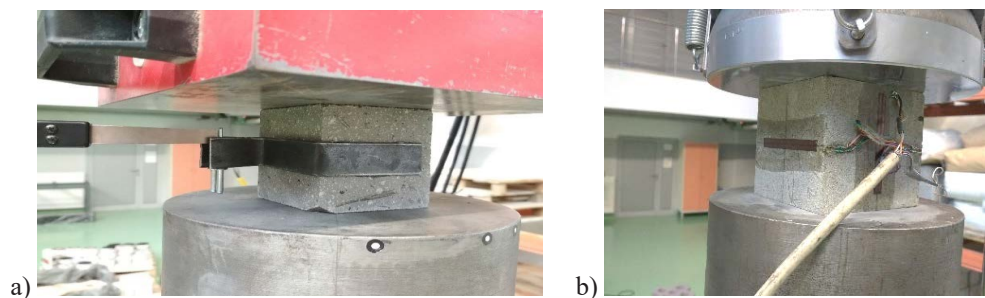
Fig. 2.   Compression test of cubic samples. a) test of "Braciszów" sandstone with the extensometer and displacement transducer, b) test of "Brenna" sandstone with strain gauges. *Source:* own study

In Table 1, Table 2 and Table 3 a, b, h – averaged dimensions of samples in accordance with fig. 1, A – cross-sectional area of the sample: $A = a \times b$, P – maximum force registered by the MTS system, f_c – compressive strength calculated based on the formula: $f_c = P / A$, E – Young's modulus, v – Poisson's ratio determined according to the procedure described later.

Table 1. Dimensions of the samples and results obtained in the uniaxial compression test for "Braciszów" sandstone. *Source:* own study

Sample	h [mm]	a [mm]	b [mm]	A [cm²]	P [kN]	f_c [MPa]	λ [kN/mm]	E [GPa]	v [-]
K1c	69.54	69.70	70.19	48.92	922.6	188.604	-	-	-
K2c	69.60	69.64	69.56	48.44	986.7	203.703	1080.05	15.519	0.208
K3c	68.01	69.86	69.73	48.71	813.5	166.997	1189.51	16.606	0.205
K4c	69.78	69.69	69.67	48.55	1025.2	211.166	705.23	10.136	0.120
K5c	69.86	69.68	69.63	48.52	1081.8	222.960	-	-	-
K6c	69.81	69.80	69.84	48.74	1087.6	223.137	1052.79	15.078	0.130
K7c	69.76	69.74	69.83	48.70	974.1	200.037	987.82	14.150	0.291
K8c	69.78	70.03	69.74	48.84	1001.5	205.069	1733.37	24.768	-
K9c	69.92	69.95	69.99	48.96	968.1	197.741	1353.51	19.331	0.261
K10c	70.11	70.06	69.88	48.95	1002.7	204.823	-	-	-
K11c	87.57	86.86	87.47	75.97	1069.0	140.706	-	-	-
K12c	86.40	84.61	86.89	73.52	1096.7	149.171	-	-	-
K13c	86.18	87.34	84.63	73.91	1326.6	179.490	889.49	10.371	-
K14c	87.14	86.90	87.84	76.33	974.3	127.645	-	-	-
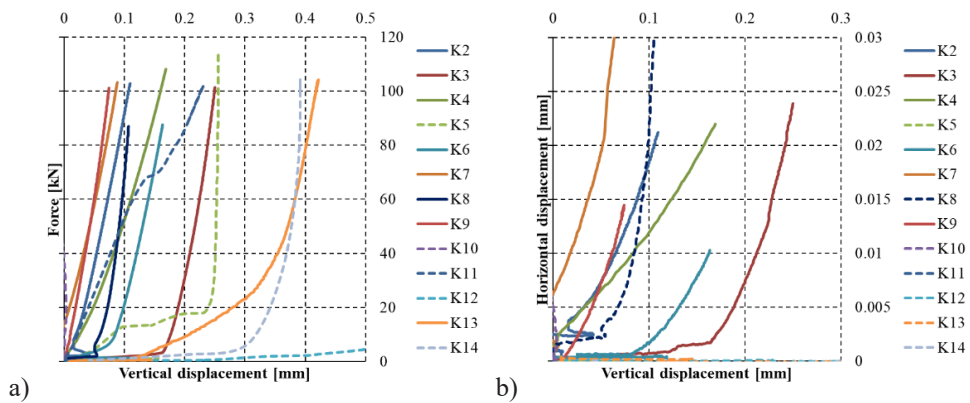
Fig. 3. Graphs of the uniaxial compression test for "Braciszów" sandstone: a) the relationship of force and vertical displacement, b) the relationship of horizontal and vertical displacement. *Source:* own study

Table 2. Dimensions of the samples and results obtained in the uniaxial compression test for "Zalas" porphyry. *Source:* own study

Sample	h [mm]	a [mm]	b [mm]	A [cm²]	P [kN]	f_c [MPa]	λ [kN/mm]	E [GPa]	v [-]
K1z	70.53	70.17	70.16	48.92	1047.3	212.738	883.70	12.661	-
K2z	70.19	70.31	70.20	48.44	980.5	198.673	830.82	11.816	-
K3z	69.98	69.88	70.06	48.71	839.6	171.500	684.55	9.786	-
K4z	70.10	70.60	69.95	48.55	1185.5	240.046	-	-	-
K5z	70.17	70.32	70.12	48.52	1160.7	235.379	1260.10	17.937	-
K6z	70.61	70.05	70.06	48.74	988.7	201.444	580.58	8.353	-
K7z	70.37	70.33	70.09	48.70	752.9	152.741	872.36	12.453	-
K8z	70.06	70.23	70.00	48.84	1328.2	270.183	1115.48	15.897	-
K9z	69.90	69.79	69.90	48.96	904.7	185.440	977.65	14.008	-
K10z	70.26	69.74	70.13	48.95	935.4	191.254	-	-	-

Fig. 4. Graphs of the uniaxial compression test for "Zalas" porphyry: a) the relationship of force and vertical displacement, b) the relationship of horizontal and vertical displacement. *Source:* own study

Table 3. Dimensions of the samples and results obtained in the uniaxial compression test for "Brenna" sandstone. *Source:* own study

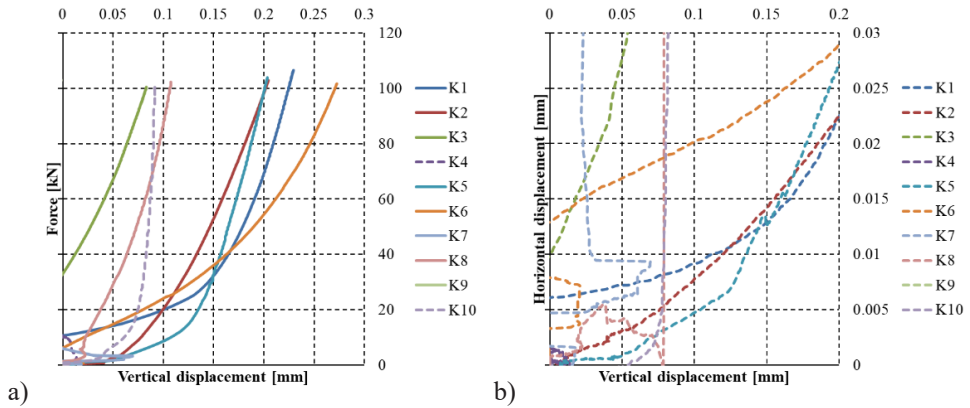| Sample	h [mm]	a [mm]	b [mm]	A [cm^2]	P [kN]	f_c [MPa]	λ [kN/mm]	E [GPa]	v [-]
K1b	95.25	89.95	89.08	80.12	-	-	1087.35	12.927	0.188
K2b	89.40	89.47	87.34	78.15	-	-	1027.62	11.756	-
K3b	89.81	92.98	87.18	81.06	-	-	1560.06	17.286	0.131
K4b	90.20	89.37	87.40	78.11	-	-	1113.70	12.861	0.175
K5b	95.01	90.82	88.79	80.64	-	-	1042.78	12.286	0.141
K6b	91.58	90.22	88.04	79.42	-	-	1556.30	17.945	-
K7b	92.04	88.94	90.25	80.26	-	-	962.00	11.032	0.106
K8b	93.84	90.60	88.40	80.09	860.7	107.469	-	-	-
K9b	93.08	89.42	88.53	79.16	704.5	89.001	-	-	-
K10b	93.83	88.86	90.43	80.36	888.6	110.583	-	-	-
K11b	86.99	73.38	90.10	66.11	472.6	71.486	-	-	-
K12b	95.99	114.87	84.51	97.07	818.1	84.275	-	-	-
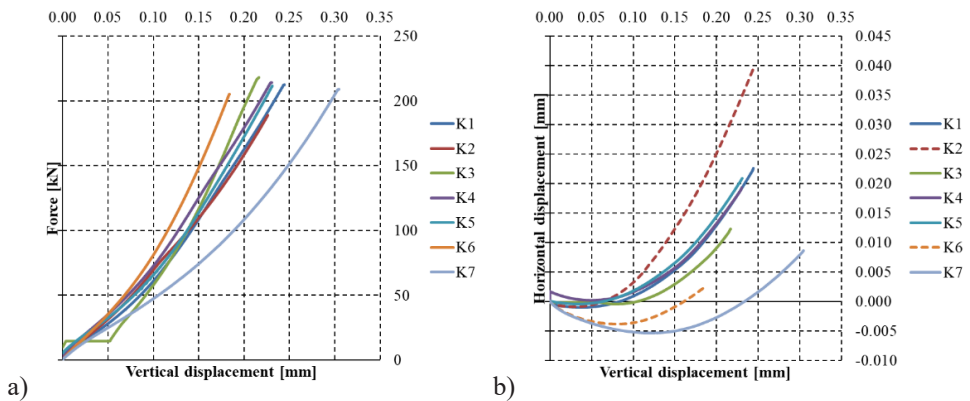
Fig. 5. Graphs of the uniaxial compression test for "Brenna" sandstone. a) the relationship of force and vertical displacement, b) the relationship of horizontal and vertical displacement. *Source:* own study

The results in the diagrams marked with a dashed line were not taken into account because either they are too different from the others, or the test was carried out incorrectly. The graphs presented in fig. 3a, fig. 4a, and fig. 5a are the dependencies of the change of the compressive force on the vertical displacement (reading from the displacement transducer for "Braciszów" sandstone and porphyry, or average from vertical strain gauges for "Brenna" sandstone). Young's modulus E was calculated from the following formula:

$$E = \frac{h \cdot \lambda}{A} \tag{1}$$

where λ is the slope of the force dependence curve for vertical displacements in an area where there is a constant increase close to linear, assuming that in the sample during the test there is a uniaxial and homogeneous stress state and a homogeneous strain state. For example, λ for "Brenna" sandstone is the ratio of force difference to displacement difference read in the range from 100 kN to 200 kN of force, because in this range there was a linear increase of displacement (see fig. 6a).

The graphs in fig. 3b, fig. 4b, and fig. 5b are the dependencies between the horizontal displacement (recorded by the clip-on extensometer, or as the average of horizontal strain gauges), and vertical displacement, the same as when calculating Young's modulus. Poisson's ratio ν is determined as the slope of this curve. As before, only parts of the charts that are close to the linear function were considered.

The average value of the tensile strength f_c obtained from the tests for individual rock types was:

- "Braciszów" sandstone – 187.232 MPa with a standard deviation of 30.315 MPa, which is 16.19% f_c,
- "Zalas" porphyry – 210.338 MPa with a standard deviation of 38.056 MPa, which is 18.09% f_c,
- "Brenna" sandstone – 92.563 MPa with a standard deviation of 16.375 MPa, which is 17.69% f_c.

The average value of Young's modulus E was obtained as follows:

- "Braciszów" sandstone – 15.745 GPa with a standard deviation of 4.757 GPa, which is 30.21% E,
- "Zalas" porphyry – 12.863 GPa with a standard deviation of 3.312 GPa, which is 25.75% E,
- "Brenna" sandstone – 13.727 GPa with a standard deviation of 2.741 GPa, which is 19.97% E.

For the average value of Poisson's ratio ν results are presented below:

- "Braciszów" sandstone – 0.203 with a standard deviation of 0.068, which is 33.73% ν,
- "Brenna" sandstone – 0.148 with a standard deviation of 0.033, which is 22.45% ν.

Poisson's ratio for "Zalas" porphyry was not designated, because all results from tests were incorrect. The remaining results also lack in accuracy. The most accurate results are compressive strength results, but the error is still around 17%. The reason for this is the large heterogeneity of the tested materials. Rocks of this type have a lot of local weakening in the form of linear inclusions. Examples of these inclusions are shown below. Fig. 6a shows a beam with local weakening and fig. 6b shows the effect of the weakening on the Brazilian test.
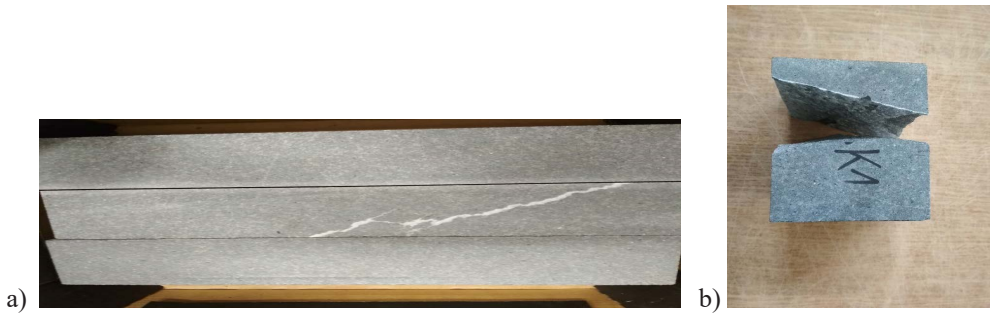
Fig. 6.   a) Beam with local weakening, b) the effect of the weakening on the Brazilian test. *Source:* own study

The results for Young's modulus and Poisson's ratio are even more dispersed because they were affected by the displacement reading. However, there is a clear advantage of measurements with pairs of strain gauges over readings from one horizontal and vertical direction, besides with less accurate devices than strain gauges.

Apart from the heterogeneity of the material and the inaccuracy of the results from the devices for measuring displacements and strains, another reason for such differences may be the orthotropic of rocks. Sandstone is a sedimentary rock and is a layered material, which means that it has different parameters of compressive strength and deformability in different directions. Unfortunately, it was not possible to identify the stratification of materials based on the inspection of the available samples, as it would be required to know in which orientation the material was acquired from the rock block. It was also impossible to differentiate between the results which were compressed perpendicularly to the layers and the ones that were compressed parallel to the layers, because the layers in the cubic sample could arrange at any angle. For these reasons, the authors treat these materials as isotropic for future works.

3.2. Beam bending test

Tensile strength by use of a 3-point beam bending test was made only for "Brenna" sandstone. For the other two materials, tensile strength was calculated only using the method that involved splitting cubes. All available beams for these two materials were used to determine the stress intensity factor.

To determine the tensile strength, 4 beams (B1b-B4b) with cross-sectional dimensions of approximately 10×10 cm and different support spacing were tested. The diagram for determining the tensile strength from this test is shown in fig. 7a. The test was performed on the MTS 319.25 testing machine.
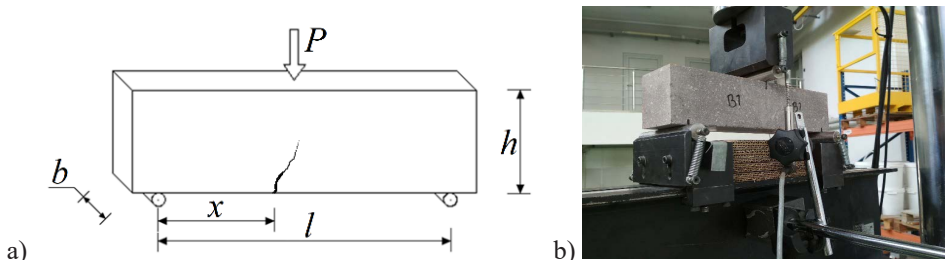

Fig. 7.   3-point beam bending test. a) scheme of the test, b) photo taken during the test. *Source:* own study

Since the samples did not crack in the middle of the width, the value of the bending moment M at the place where the crack appeared was calculated from the bellow equation:

$$M = \frac{P \cdot l}{4} \cdot \frac{2 \cdot x}{l} = \frac{P \cdot x}{2} \tag{2}$$

Where: h – means the height of the sample, b – means width, l – the distance between supports, x – the distance between crack initiation location, and the nearest support, P – the maximum vertical force applied in the centre of the sample, read from the testing machine. The sample dimensions and calculation results are shown in Table 4. $A = a \times b$ – a cross-section of the sample, $W = bh^2 / 6$ – section modulus, $f_t = M / W$ – tensile strength.

Table 4. Dimensions of the samples and results obtained in a 3-point beam bending test for "Brenna" sandstone. *Source:* own study

Sample	h [mm]	b [mm]	L [mm]	x [mm]	P [kN]	A [cm²]	W [cm³]	M [kNcm]	f_t [MPa]
B1b	90.79	89.42	360	160	3.9099	81.18	122.84	31.279	2.546
B2b	95.98	89.94	340	145	0.3946	86.32	138.08	2.861	0.207
B3b	98.20	89.29	340	130	7.3348	87.68	143.50	47.676	3.322
B4b	98.14	90.65	320	130	14.2594	88.96	145.50	92.686	6.370

The above calculations show that the average tensile strength for "Brenna" sandstone was 3.112 MPa with a standard deviation of 2.544 MPa, which is 81.78% of f_t. This dispersion is too large to take this result as correct.

3.3. Determination of stress intensity factor

Critical stress intensity factor in mode I, designated as K_{Ic}, is a material constant that determines the magnitude of the stress at the crack tip in the case of tensile loads working perpendicular to the crack surface. There are several methods for determining this factor [6]. The authors conducted a three-point bending test. This test was performed on specimens with a notch in the centre of its width and was executed on the MTS 319.25 testing machine. The test operation diagram is shown in fig. 8a. There were 6 samples of "Braciszów" sandstone (named N1c-N6c), 5 samples of "Zalas" porphyry (N1z-N5z) and 3 samples of "Brenna" sandstone (N1b-N3b). The samples were tested on the MTS 319.25 testing machine.
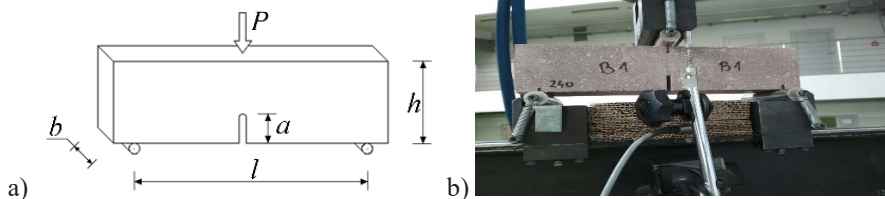

Fig. 8. 3-point beam bending test with a notch. a) scheme of the test, b) photo taken during the test. *Source:* own study

There are many methods of calculating this stress intensity factor [7], [8]. The authors used the equation proposed by Brown and Srawley [9] because it allows any spacing of supports when other methods require spacings 4 times longer than the sample height.

$$K_{Ic} = \frac{3P_c l \sqrt{\pi a}}{2h^2 b} \left[1.090 - 1.735 \frac{a}{h} + 8.28 \left(\frac{a}{h} \right)^2 - 14.18 \left(\frac{a}{h} \right)^3 + 14.57 \left(\frac{a}{h} \right)^4 \right] \qquad (3)$$

In this equation and fig. 8a P_c is the destructive force, l – the spacing of supports, a – length of the notch, h – the height of the beam, b – the width of the beam. The results obtained from the test are presented in Table 5, Table 6, and Table 7.

Table 5. Dimensions of the samples and results obtained in a 3-point beam bending test with a notch for "Braciszów" sandstone. *Source:* own study

Sample	h [mm]	b [mm]	a [mm]	l [mm]	P [kN]	K_{Ic} [N/mm$^{3/2}$]
N1c	70.44	69.99	25	300	6.041	76.618
N2c	69.55	70.17	25	300	4.613	60.182
N3c	69.79	69.87	25	300	5.362	69.673
N4c	70.45	70.88	25	240	7.249	72.597
N5c	68.63	69.67	25	240	6.299	68.437
N6c	70.18	70.28	25	240	6.629	67.596

Table 6. Dimensions of the samples and results obtained in a 3-point beam bending test with a notch for "Zalas" porphyry. *Source:* own study

Sample	h [mm]	b [mm]	a [mm]	l [mm]	P [kN]	K_{Ic} [N/mm$^{3/2}$]
N1z	70.06	70.20	25	300	4.633	59.524
N2z	69.15	70.22	25	300	4.403	58.888
N3z	69.75	69.91	25	300	3.764	49.087
N4z	69.86	69.71	25	300	5.490	71.017
N5z	69.95	69.88	25	300	5.578	72.225

Table 7. Dimensions of the samples and results obtained in a 3-point beam bending test with a notch for "Brenna" sandstone. *Source:* own study

Sample	h [mm]	b [mm]	a [mm]	l [mm]	P [kN]	K_{Ic} [N/mm$^{3/2}$]
N1b	93.70	90.22	25	320	4.211	22.963
N2b	87.48	120.15	25	400	4.275	25.464
N3b	88.17	120.94	25	240	8.179	28.538

From the above results, the average values of stress intensity factors were determined:
- "Braciszów" sandstone – 69.184 N/mm$^{3/2}$ with a standard deviation of 5.500 N/mm$^{3/2}$, which is 7.95% K_{Ic},
- "Zalas" porphyry – 55.833 N/mm$^{3/2}$ with a standard deviation of 5.851 N/mm$^{3/2}$, which is 10.48% K_{Ic},
- "Brenna" sandstone – 25.655 N/mm$^{3/2}$ with a standard deviation of 2.792 N/mm$^{3/2}$, which is 10.88% K_{Ic}.

Also, the authors determined the critical strain energy release rate $G_{Ic} = K_{Ic}^2 / E$ [6], which is 303.995 N/m for "Braciszów" sandstone, 242.344 N/m for "Zalas" porphyry and 47.946 N/m for "Brenna" sandstone.

3.4. Tensile during splitting test

Due to the lack of a sufficient number of beams, it was decided to use most of the beams for three-point bending test of beams with notches, and determine the tensile strength using the quasi-Brazilian method. 7 cubic samples 7×7×7 cm of "Braciszów" sandstone (T1c-T7c), 7 samples of "Zalas" porphyry (T1z-T7z), and 6 samples 9×9×9 cm of "Brenna" sandstone (T1b-T6b) were used. Also, the authors used unusual 7×7 cm samples with much longer width (about 14 cm to 17 cm), which below is referred to as beams. The authors wanted to check if beams could also be used as samples for the Brazilian test. 12 beam samples of "Braciszów" sandstone (T8c-T19c) and 10 samples of "Zalas" porphyry (T8z-T17z) were tested. The beams were obtained from halves of destroyed beams used in 3-point bending tests. No "Brenna" sandstone beams were tested. The samples were loaded on a WalterBai testing machine.

For the purpose that samples were cuboids, the calculation method described in previous authors' paper [10] was used. Typically, cylindrical samples are tested using this method, but in this case, cuboid samples was the only option. Because there is no analytical solution when compressing a cuboid with two balancing linear loads, as in the case of a cylinder, the stress field was numerically determined using FEM. The authors wanted to find the dependence between the tensile stresses that appear in the centre of the sample and the value of the force applied to the sample. This ratio will be named as χ and is determined for 1 cm of load length. Computer simulations showed that χ equals 0.069 for 9×9×9 cm samples, 0.088 for 7×7×7 cm samples, and about 0.070 for beam samples. It turns out that this ratio changes significantly when the width a is less than 1.5 of h. When this width is greater than 1.5, then this ratio does not change much, so the authors decided to leave the value of 0.070 for all beams. The scheme of this task is shown in fig. 9a.
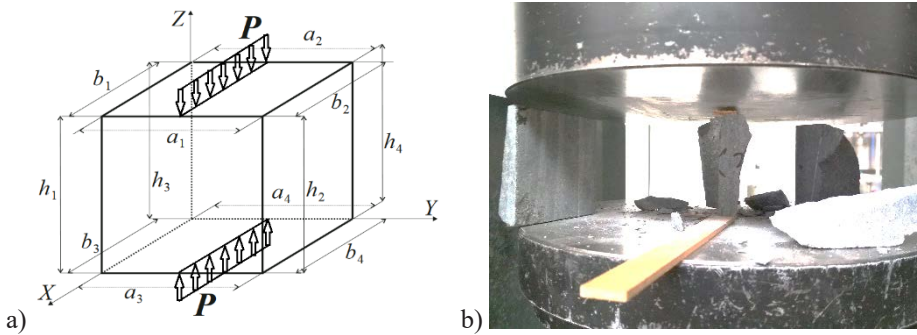
Fig. 9.   Splitting test performed on cuboid samples. a) scheme of the test, b) photo was taken after one of the tests. *Source:* own study

Also, it was assumed that the value of tensile strength is greater than the determined maximum value of tensile stresses because in the middle of the sample there are also compressive stresses that affect the strength of the material. The ratio of tensile stress to tensile strength is marked as ρ, and for the Ottosen-Podgórski criterion, it is calculated as follows:

$$\rho = \frac{\sigma_{max}}{f_t} = \frac{\sqrt{1+4\cdot\gamma^2}-1}{2\cdot\gamma^2}, \text{ where } \gamma = \frac{\kappa}{\eta} \tag{4}$$

κ is the ratio between vertical (compressive) stresses and horizontal (tensile) stresses in the middle of the sample which for 9×9×9 cm samples is 3.263, for 7×7×7 cm samples is

3.241 and for beam samples is 2.687. This value also changes insignificantly when the width of the sample is greater than 1.5 of the height.

η is the ratio of the compressive strength to tensile strength f_c / f_t, and it was calculated by iterations. After one calculation of the tensile strength from this method, the ratio η changed and is substituted to the formula up to the moment where this ratio does not change. The tensile strength f_t was calculated from the following formula:

$$f_t = \frac{\sigma_{max}}{\rho}, \text{ where } \sigma_{max} = q \cdot \chi, q = \frac{P}{b} \tag{5}$$

σ_{max} are maximum tensile stresses that occur in the middle of the sample, q is the load obtained from the machine, distributed on the depth of the sample. The results from all calculations are presented in Table 8, Table 9, and Table 10.

Table 8. Dimensions of the samples and results obtained in the splitting test performed on cuboid samples for "Braciszów" sandstone. *Source:* own study

Sample	h [mm]	a [mm]	b [mm]	P [kN]	q [kN/m]	σ_{max} [MPa]	f_t [MPa]
T1c	68.20	69.92	69.75	98.7	1415.104	12.474	12.687
T2c	69.71	69.69	69.88	153.4	2195.113	19.349	19.680
T3c	69.44	70.17	63.27	155.8	2462.462	21.706	22.077
T4c	69.72	69.80	70.13	82.3	1173.577	10.345	10.522
T5c	69.70	69.85	69.65	55.7	799.770	7.050	7.170
T6c	69.65	69.73	69.52	58.7	844.392	7.443	7.570
T7c	69.58	69.65	69.54	40.3	579.502	5.108	5.195
T8c	70.77	173.50	70.06	77.7	1109.010	7.772	7.845
T9c	70.49	174.50	70.11	80.1	1142.450	8.006	8.081
T10c	69.58	175.50	70.48	88.5	1255.675	8.799	8.882
T11c	69.53	176.50	69.87	77.5	1109.242	7.773	7.846
T12c	69.77	177.50	70.01	87.7	1252.723	8.779	8.861
T13c	69.77	178.50	69.79	57.2	819.572	5.743	5.797
T14c	70.58	137.00	70.69	41.1	581.432	4.075	4.113
T15c	70.53	138.00	70.81	70.0	988.526	6.927	6.993
T16c	68.74	139.00	69.81	31.4	449.792	3.152	3.182
T17c	68.51	140.00	69.58	57.1	820.697	5.751	5.805
T18c	70.24	141.00	70.32	62.3	885.981	6.209	6.267
T19c	70.10	142.00	70.27	77.9	1108.660	7.769	7.842

The first three tests of "Braciszów" sandstone (T1c-T3c) were performed using a 1.5 cm wide fiberboard pad. It turns out that this width is too broad because samples were splitting in two planes, not in one, which can be seen in fig. 9. This width is one-fifth of the sample width, which caused that the load was too wide and worked at two points, not as a concentrated load. These results were therefore omitted because the destructive force was much higher than the others. All other tests were performed using the 0.7 cm pad.

Table 9. Dimensions of the samples and results obtained in the splitting test performed on cuboid samples for "Zalas" porphyry. *Source:* own study

Sample	h [mm]	a [mm]	b [mm]	P [kN]	q [kN/m]	σ_max [MPa]	f_t [MPa]
T1z	70.52	69.50	70.24	102.0	1452.216	12.801	13.061
T2z	70.21	70.10	69.89	72.8	1041.674	9.182	9.368
T3z	68.84	70.39	70.31	59.0	839.201	7.397	7.547
T4z	70.14	70.38	72.92	64.8	888.645	7.833	7.992
T5z	69.92	70.21	69.58	54.5	783.243	6.904	7.044
T6z	70.12	69.99	70.02	75.2	1073.941	9.467	9.659
T7z	70.17	70.35	69.89	83.0	1187.665	10.469	10.681
T8z	70.09	173.50	70.19	67.1	956.045	6.700	6.760
T9z	70.31	173.50	70.24	90.0	1281.276	8.979	9.060
T10z	69.47	173.50	70.13	44.9	640.217	4.486	4.527
T11z	69.69	173.50	70.16	56.8	809.636	5.674	5.725
T12z	69.86	173.50	70.19	73.7	1050.082	7.359	7.425
T13z	69.83	173.50	70.10	64.3	917.326	6.428	6.486
T14z	69.92	137.00	69.52	77.9	1120.541	7.852	7.923
T15z	70.20	138.00	69.63	80.7	1159.066	8.122	8.196
T16z	70.03	139.00	69.91	93.6	1338.960	9.383	9.467
T17z	70.07	140.00	70.08	89.3	1274.213	8.929	9.010

Table 10. Dimensions of the samples and results obtained in the splitting test performed on cuboid samples for "Brenna" sandstone. *Source:* own study

Sample	h [mm]	a [mm]	b [mm]	P [kN]	q [kN/m]	σ_max [MPa]	f_t [MPa]
T1b	95.22	106.96	88.80	44.8	504.505	3.497	3.541
T2b	95.18	107.46	88.82	45.9	516.776	3.582	3.627
T3b	95.21	105.96	90.61	29.3	323.364	2.241	2.270
T4b	94.92	107.63	88.36	51.1	578.332	4.009	4.059
T5b	90.02	96.56	83.23	30.6	367.656	2.548	2.581
T6b	94.26	105.03	90.75	41.1	452.905	3.139	3.179

From the above results, the average values of tensile stresses using solely cubic samples are presented below:

- "Braciszów" sandstone – 7.614 MPa with a standard deviation of 2.199 MPa, which is 28.87% f_t,
- "Zalas" porphyry – 9.336 MPa with a standard deviation of 2.084 MPa, which is 22.32% f_t,
- "Brenna" sandstone – 3.209 MPa with a standard deviation of 0.676 MPa, which is 21.07% f_t.

The result for "Brenna" sandstone is almost the same as obtained from the 3-point bending test, which was 3.111 MPa. This proves that results obtained by this quasi-Brazilian method are correct, but the spread of results is extensive. The next important thing is the results from splitting the beam samples.

- "Braciszów" sandstone – 6.793 MPa with a standard deviation of 1.813 MPa, which is 26.68% f_t,

- "Zalas" porphyry – 7.458 MPa with a standard deviation of 1.537 MPa, which is 20.61% f_t.

These results are 10-20% lower than obtained from cubes, which means that they probably cannot be considered correct.

4. Summary

The determination of material parameters and verification of the physical and numerical model is an integral part of a correctly performed computer simulation. The research described in the article is an example of the solution to an important problem of determining the mechanical properties of the modelled material. The results described in the paper are presented in Table 11.

Table 11. Summary of all determined results. *Source:* own study

Material	f_c [MPa]	f_t [MPa]	E [GPa]	ν [-]	K_{Ic} [N/mm$^{3/2}$]	G_{Ic} [N/m]
"Braciszów" sandstone	187.232	7.614	15.745	0.203	69.184	303.995
"Zalas" porphyry	210.338	9.336	12.863	-	55.833	242.344
"Brenna" sandstone	92.562	3.209	13.727	0.148	25.655	47.946

"Braciszów" sandstone and "Zalas" porphyry turned out to be materials with the highest parameters. "Brenna" sandstone is a weaker material, with lower fracture energy and lower tensile and compressive strength, even though it did not have any local weakening, unlike the "Braciszów" sandstone. Porphyry turned out to be the most durable material, which was to be expected. In addition to obtaining material parameters based on tests, several conclusions were made:

- Sandstone and porphyry are very heterogeneous materials with local weaknesses, which leads to a large spread of results,
- The uniaxial compression of cubes using a pair of strain gauges allows for much more accurate results than when using a single reading from external devices,
- Author's method of calculating tensile strength during splitting gives satisfying results,
- The use of beams in the above method is not recommended,
- When testing small samples using the Brazilian method, it is advisable to use a narrow pad (not larger than 10% of the sample width).

The obtained material parameters will be used to verify the authors' method of crack direction prediction in the Abaqus FEA system. The authors hope that the results presented in work will also be useful for other researchers that use rocks in their studies.

References

[1]   Gontarz J. et al., "Comparison between numerical analysis and actual results for a pull-out test," *Engineering Transactions*, vol. 67, no. 3, (2019), pp. 311–331. https://doi.org/10.24423/EngTrans.1005.20190815

[2]   Gontarz J. et al., "Podsumowanie badań laboratoryjnych piaskowca pod kątem analizy wyrywania kotwy," *Budownictwo i Architektura*, vol. 16, no. 3, (2017), pp. 113–123. https://doi.org/10.24358/Bud-Arch_17_163_11

[3] Tomiczek K., "O różnicach w zachowaniu się skał w warunkach jednoosiowego rozciągania i ściskania," *Górnictwo i Geoinżynieria*, vol. 3, no. 1, (2007), pp. 543–554.

[4] Łukasiak D., "Zmienność wytrzymałościowa piaskowców godulskich z Brennej w warunkach jednoosiowego ściskania," *Górnictwo i Geoinżynieria*, vol. R. 34, z. 2, (2010), pp. 435–441.

[5] Kłopotowska A., "Resistance of szydłowiecki sandstone to salt crystallization in terms of structural strengthening," *Górnictwo i Geoinżynieria*, vol. 35, no. 2, (2011), pp. 341–347.

[6] Mier J. G. M. van, *Fracture processes of concrete*. CRC Press, 1996.

[7] Bower A.F., *Applied mechanics of solids*. CRC Press, 2010. Available: https://www.crcpress.com/Applied-Mechanics-of-Solids/Bower/p/book/9781439802472 [Access: 15 Jan 2020]

[8] Elices M. et al., "The cohesive zone model: advantages, limitations and challenges," *Engineering fracture mechanics*, vol. 69, no. 2, (2002), pp. 137–163. https://doi.org/10.1016/S0013-7944(01)00083-2

[9] Brown W. F. and Srawley J.E., *Plane Strain Crack Toughness Testing of High Strength Metallic Materials*. Philadelphia: ASTM International, 1966. https://doi.org/10.1520/STP410-EB Available: http://www.astm.org/doiLink.cgi?STP410-EB [Access: 15 Jan 2020]

[10] Gontarz J. and Podgórski J., "Explanation of the mechanism of destruction of the cylindrical sample in the Brazilian test," in *Advances in Mechanics : Theoretical, Computational and Interdisciplinary Issues*, Kleiber M. et al. Eds. Gdańsk: Boca Raton, 2016, pp. 479–483.

Impact of curing conditions for concrete on its mechanical properties

Joanna Witkowska-Dobrev[1], Olga Szlachetka[2], Paulina Spiek[3]

[1] Warsaw University of Life Sciences – SGGW;
Nowoursynowska St. 166 , 02-787 Warsaw, Poland;
joanna_witkowska@sggw.edu.pl (iD) *0000-0001-6613-5037*
[2] Warsaw University of Life Sciences – SGGW;
Nowoursynowska St. 166, 02-787 Warsaw, Poland;
olga_szlachetka@sggw.edu.pl (iD) *0000-0002-1195-3603*
[3] Warsaw University of Life Sciences – SGGW;
Nowoursynowska St. 166, 02-787 Warsaw, Poland;
paulina_spiek@sggw.edu.pl

Abstract: This paper aims to present the results of compressive strength tests of concrete specimens, prepared according to two recipes, after 2, 7 and 28 days of maturing in four different environments. The concrete specimens had the same w/c ratio, the same amount of aggregate of particular fractions, the addition of a superplasticizer, but they differed in the cement type. In one recipe, the Portland cement CEM I 32.5R was used, in the other – pozzolanic ash cement CEM IV/B(V) 32.5R-LH/NA. Concrete specimens with dimensions of 100 x 100 x 100 mm made according to both recipes were placed in individual ripening environments: in cuvettes with water, soaked and wrapped with construction foil, left in room conditions in the laboratory, placed outside the laboratory and being exposed to the atmospheric conditions. The obtained compressive strength results confirmed that the best way of curing concrete is the wet cure (in cuvettes with water). It has been proven that the choice of proper curing method is key in terms of compressive strength.

Keywords: concrete care, compressive strength, Portland cement, pozzolanic cement

1. Introduction

Concrete consists of products of simple physical and chemical structure, however, the course of concrete mix production requires great attention and accuracy [1] [2]. Mistakes made at the initial stage of concrete mix production may have negative consequences at subsequent stages of construction. Therefore, the basic procedure to be performed in the early period of concrete "life" is its maintenance. Its main purpose is to ensure optimal thermal and moisture conditions for the maturing concrete and to protect it from the harmful effects of atmospheric

conditions, so as to minimise plastic shrinkage, ensure appropriate strength and durability of the surface zone, minimise thermal stress and protect it from freezing, vibrations, impacts and damage [3].

It is highly recommended to start the process of proper care as early as possible. Otherwise, there will be negative irreversible processes, which the subsequent care will not be able to eliminate (Fig. 1).
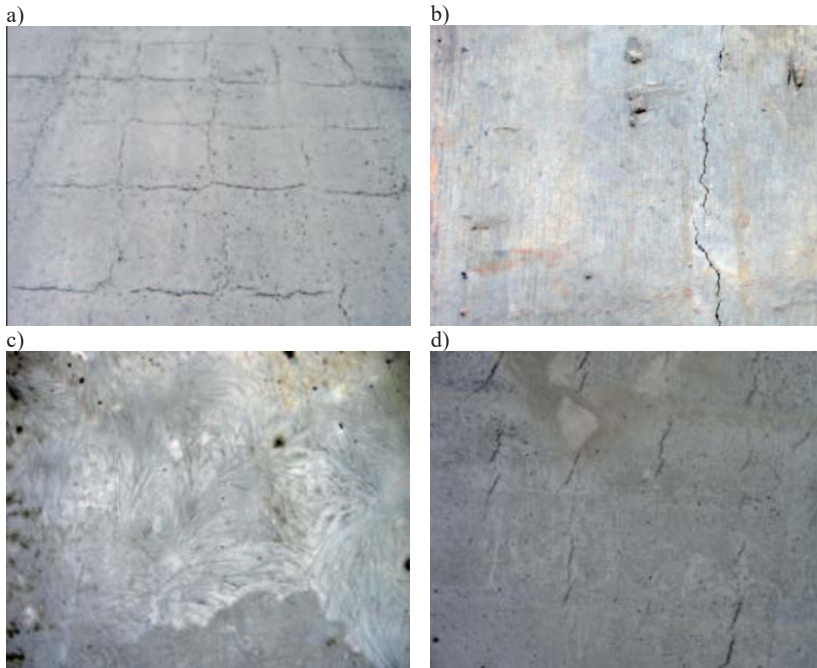

Fig. 1.   Effects of poor concrete care: a) cracks in the bridge slab due to plastic shrinkage, b) cracking of the tank wall due to contraction of the hardening, c) damage to the concrete surface due to freezing of fresh concrete, d) scratches in the bridge slab due to vibrations from the adjacent bay during concreting. *Source:* [4]

The basic methods of concrete care during the summer are [5]:
- sprinkling the concrete surface with water (wet care),
- laying wet mats on the concrete surface and keeping them moist,
- covering the surface of wet concrete with construction foil,
- coating the concrete surface with care products with specific properties,
- concreting in tents ensuring proper temperature and humidity,

In the winter season, the care consists in [5] [6]:
- securing the concrete element with heat-protective materials, e.g. polystyrene foam, mineral wool, bubble wrap,
- concrete heating by air, steam, heating mats, electric current, infrared heaters or electromagnetic field,

● concrete in tents to ensure proper temperature and humidity,

● using special formworks.

proper care is also affected by admixtures of various kinds which have the task to modify properties of a concrete mix and/or a hardened concrete, so as to facilitate placing concrete in winter or in high temperatures. When the concrete is being made in winter, aerating admixtures are applied which enable introducing tiny air bubbles during mixing, hence improving the concrete frost resistance. Still, though less frequently due to the progress in the concrete manufacturing technologies, admixtures are applied in winter which accelerate the concrete bonding and hardening.

If the concrete is placed in high temperatures, when – for example – layers of the concrete being placed must bond to each other, retarding admixtures are applied which have to retard the cement bonding process, hence prolong the liquidity period of a concrete mix [7].

The above mentioned measures, especially in the case of "winter" care, can be applied individually or in combination depending on the prevailing conditions.

The improper cure negatively affects the concrete properties, especially its compressive strength. For example, lack of the frost protection retards the hydration process in the concrete and reduces assumed utility properties of the concrete, including compressive strength, and can also evoke exfoliation of the concrete surface as well as scratching and cracking. Increased temperature in the initial phase of concrete maturation, in turn, speeds up the cement hydration process which results in shorter concrete bonding time and faster strength development – what can result in lower compressive strength. Fast evaporation of water from the concrete mix can be also a reason for plastic shrinkage cracking [5].

The problem of improper concrete care and concrete samples taken at the construction site, were pointed out in the paper [8]. As the authors show, the problem of improper sample care, i.e. inconsistent with the standard, often occurs [9]. Improper care of concrete samples often results from the inability to guarantee the required storage conditions or is caused by negligence (Fig. 2). This results in underestimation of the measured compressive strength.

Fig. 2.   Incorrect storage of concrete samples. *Source:* [8]

The pace of the compressive strength increase depends on many factors – apart from the content of the concrete mix, curing conditions are important.

The aim of the research was to check the influence of the care method on the compressive strength of ordinary concrete samples based on Portland cement and pozzolanic ash.

2. Materials and methods

So as not to restrict the investigations to one particular case, the batches were made for two concrete mix formulas using different types of cements, in aim to highlight the fact that modification of the concrete mix content through the change of the cement type can positively or negatively affect properties of the hardened concrete depending on the way of curing. For one recipe CEM I 32.5R cement was selected. This formula obtained the symbol R1. For the second one, CEM IV/B (V) 32.5R – LH/NA cement was used and this formula was named R2. CEM I 32.5R is produced by the Ożarów S.A. cement plant, while CEM IV/B (V) 32.5R – LH/NA is a pozzolanic cement from Lafarge. The compression strength classes of cement after 28 days are defined by the 32.5R symbol. The letter R indicates early high strength, the LH symbol indicates low hydration heat and the NA symbol indicates low alkali oxide content.

CEM I 32.5R according to [10] is characterized by moderate hydration heat, moderate dynamics of early strength build-up, wide compatibility and moderate dynamics of cooperation with chemical admixtures for concrete and mortar. Whereas CEM IV/B (V) 32.5R – LH/NA according to the manufacturer [11] is characterized by stable strength increase and increased strength during long periods of maturation. Due to low hydration heat this cement reduces the risk of shrinkage cracks. It is also characterized by good plasticity, workability and pumpability of the concrete mix. Average values of physical and chemical properties of the cements according to the manufacturers' data are presented in Tab. 1.

Table 1.   Physical and chemical properties of the cements. *Source:* [10], [11]

Physical/chemical property	CEM I 32.5R	CEM IV/B (V) 32.5R – LH/NA
Specific surface	3300 cm^2/g	4303 cm^2/g
Start of bonding time	210 min	266 min
End of bonding time	300 min	363 min
Compressive strength after 2 days acc. to PN-EN 196-1	21 MPa	14.1 MPa
Compressive strength after 28 days acc. to PN-EN 196-1	45 MPa	38.5 MPa
Specific density	3.05 g/cm^3	2.71 g/cm^3
Water demand	26 %	32.3 %
Sulfate content (as SO_3)	3.17 %	2.71 %
Chloride content (as Cl_-)	0.080 %	0.061 %
Alkali content (as Na_2O_{eq})	0.78 %	1.53 %

The strength class was assumed as C20/25 and the exposure class – XC1. The composition of formulas (Tab. 2) was selected so that the consistency was malleable, i.e. that according to the slump test [1] [12] the fresh concrete had the consistency class S2 and the so-called bleeding phenomenon, i.e. occurrence of water on the sample surfaces caused by separation of concrete components, did not occur.

Table 2. Components of concrete mixes. *Source:* [14]

Ingredient	Amount [kg/m^3]	
	Formula 1 (R1)	Formula 2 (R2)
CEM I 32.5R	280	-
CEM IV/B(V) 32.5R – LH/NA	-	280
Fractional aggregate 0-0.125 mm	40.8	40.8
Fractional aggregate 0.125-0.25 mm	40.8	40.8
Fractional aggregate 0.25-0.5 mm	97.15	97.15
Fractional aggregate 0.5-1 mm	198.75	198.75
Fractional aggregate 1-2 mm	377.5	377.5
Fractional aggregate 2-4 mm	163	163
Fractional aggregate 4-8 mm	510	510
Fractional aggregate 8-16 mm	612	612
Water	140	140
CHRYSO®Optima185 superplasticizer	0.0616	0.039

In aim to make both mixes, a coarse-grained natural aggregate with maximum grain diameter D_{max} = 16 mm was used. It was composed of two aggregate sets: fine, of fraction $0 \div 2$ mm, and coarse, of fraction $2 \div 16$ mm. The percentage of individual fractions in the given mix was: 2% of the fraction $0 \div 0.125$ mm, 2% of the fraction $0.125 \div 0.5$ mm, 7% of the fraction $0.125 \div 0.5$ mm, 9% of the fraction $0.5 \div 1$ mm, 18% of the fraction $1 \div 2$ mm, 8% of the fraction $2 \div 4$ mm, 25% of the fraction $4 \div 8$ mm and 30% of the fraction $8 \div 16$ mm. The obtained fines curve of the aggregate falls between the limit curves (Fig. 3). The super-plasticizer CHRYSO®Optima 185 was added to both mixes. It is an agent reducing water content and produced from modified polycarboxylates and phosphonates. It prolongs the period of maintenance of a given consistency and influences good workability of a concrete mix without bonding retardation effect [13]. The ingredients of the recipes were then mixed in a mechanical mixer (concrete mixer). At first, sand and gravel was poured, then a half of water, then the cement. The agent was added to the remaining half of water and the water was poured gradually till a homogeneous mass was obtained.
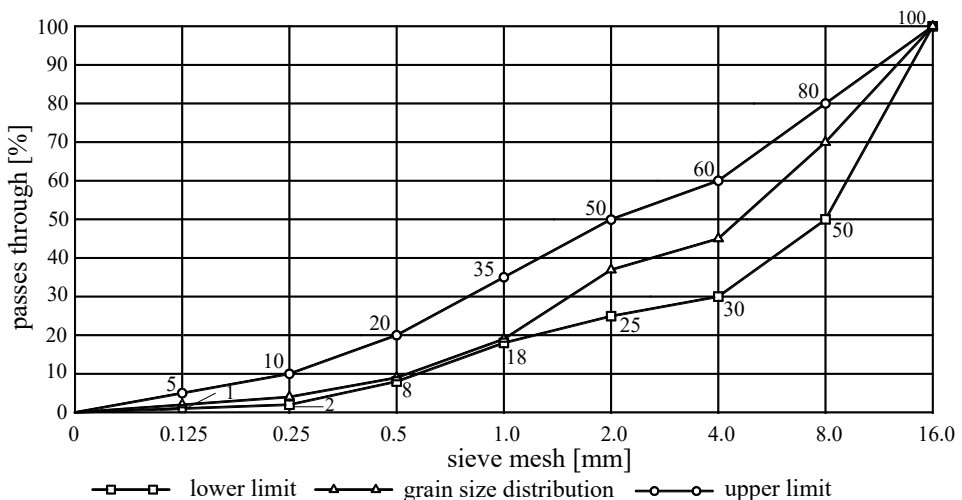

Fig. 3. Upper and lower limit curves of grain size and grain size distribution curve of aggregate. *Source:* Author's own study

The samples were formed in 100x100x100 mm moulds. After forming, the samples were stored for 24 ± 4 hours in a laboratory at 20 ± 2 °C and 40 % humidity. After this time the cubes were disassembled and placed in appropriate ripening environments. Concrete samples were stored: in water trays (A), soaked and wrapped in building film (B), in dry "room" conditions in the laboratory room (C) and in weather conditions outside the laboratory (D). The maturation conditions of the samples are shown in Tab. 3.

Maintenance in water sought to prevent drying shrinkage. It is used at high temperatures, strong sunshine and strong and warm winds to avoid drying out. As a consequence of this type of care, the hydration process may be disturbed.

The curing by soaking and wrapping in construction foil was designed to ensure that the heat released by the hardening concrete is maintained and to prevent water evaporation from the concrete. Unfortunately, this type of care can cause discoloration due to uneven condensation of water vapour on the surface of the membrane adjacent to the concrete.

Table 3. Maturation conditions of samples. *Source:* Author's own study

Description of ripening environment	Description of sample storage environment	Temperature [°C]	Humidity [%]
A	in water according to PN-EN 12390-2 [9]	20 ± 2	100
B	in the laboratory, soaked and wrapped in construction foil	20 ± 8	around 80
C	in a laboratory in a "room" environment	20 ± 5	around 40
D	outside the laboratory building in atmospheric conditions (September 2018) [15]	max. 29 min. 3 average 16	max. 91 min. 56 average 73
		number of rainy days 10	

Samples stored in room temperature in the laboratory were not exposed to changes in thermal and humidity conditions, while samples stored outside the laboratory were exposed to random thermal and humidity conditions depending on the prevailing weather (temperature, humidity, rain). Adequate control over them was lacking.

3. Research results and analysis

Compressive strength tests were performed after 2, 7 and 28 days according to the standard [16]. The value of strength was determined according to the formula:

$$f_{c,cube(150mm)} = 0.95 \cdot f_{c,cube(100mm)} \tag{1}$$

In Tabs 4-5, apart from the ratio of average compression strength after 2 days to average compressive strength after 28 days, which is a measure of the development of concrete strength, the ratio of average compression strength after 7 days to average compression strength after 28 days is shown.

Table 4. Compressive strength ratio $f_{cm,2}/f_{cm,28}$ and $f_{cm,7}/f_{cm,28}$ and density of hardened concrete after 2, 7 and 28 days of curing in different conditions samples for R1 formula. *Source:* Author's own study

Formula R1		Care			
		A	B	C	D
Compressive strength (f_{cm}) in MPa after:	2 days	28.7	28.3	24.3	24.0
	7 days	33.0	32.5	29.8	31.9
	28 days	**43.5**	**36.6**	**36.2**	**39.2**
Relation	$f_{cm,2}/f_{cm,28}$	0.66	0.77	0.67	0.61
	$f_{cm,7}/f_{cm,28}$	0.76	0.89	0.82	0.81
Endurance development		fast	fast	fast	fast
Density ρ kg/m^3 in	2 days	2360.9	2352.4	2314.4	2346.8
	7 days	2334.9	2337.5	2337.3	2348.4
	28 days	2354.7	2342.0	2284.3	2319.2

Although as per the standard classification according to the parameter $f_{cm,2}/f_{cm,28}$ the development of strength for samples made in accordance with both formulas and stored in all analysed ripening environments can be assessed as fast, because always $f_{cm,2}/f_{cm,28} > 0.5$, however this parameter assumed different values depending on the type of cement and care. After analysis of the value of the parameter $f_{cm,2}/f_{cm,28}$, it can be seen that the care method has a greater influence on the development of strength in the case of formula R2 – the value of this parameter ranges from 0.57 for wet care (in water) to 0.81 for dry care in an indoor environment.

Table 5. Compressive strength ratio $f_{cm,2}/f_{cm,28}$ and $f_{cm,7}/f_{cm,28}$ and density of hardened concrete after 2, 7 and 28 days of curing in different conditions samples for R2 formula. *Source:* Author's own study

Formula R2		Care			
		A	B	C	D
Compressive strength (f_{cm}) in MPa after:	2 days	25.5	25.9	26.9	26.3
	7 days	37.0	35.7	30.5	30.2
	28 days	**44.6**	**40.3**	**33.2**	**38.9**
Relation	$f_{cm,2}/f_{cm,28}$	0.57	0.64	0.81	0.68
	$f_{cm,7}/f_{cm,28}$	0.83	0.89	0.92	0.78
Endurance development		fast	fast	fast	fast
Density ρ kg/m^3 in	2 days	2378.3	2317.4	2319.2	2329.1
	7 days	2335.9	2331.8	2303.8	2302.3
	28 days	2397.9	2328.5	2307.4	2357.0

The development of compressive strength is faster with R1 for wet care (A) and film care (B), while for dry room care (C) and weathering (D), R2 concrete has a faster strength development. However, after 28 days it was the samples according to the R1 formula that reached higher compressive strength values than those made according to the R2 formula under storage conditions C and D. This is due to the type of cement used. The effect of the used type of cement on the increase in compression strength is highlighted by comparison of the ratios $f_{cm,2}/f_{cm,28}$ and $f_{cm,7}/f_{cm,28}$. In the case of wet care (in water) the ratio $f_{cm,7}/f_{cm,28}$ informs that after 7 days the strength development for R2 samples is faster, although the ratio $f_{cm,2}/f_{cm,28}$ for R1 was higher than for R2. Eventually, the samples from R2 formula reached a higher compressive strength value. For foil care the ratio $f_{cm,7}/f_{cm,28}$ is the same for both formulas, although also the ratio $f_{cm,2}/f_{cm,28}$ for R1 was higher than for R2. Cement in R2 formula has lower hydration heat, therefore, in undisturbed care conditions, and as such can be considered

conditions A and B, in the first 2 days the strength gain was at a lower level. For dry indoor care, the $f_{cm,7}/f_{cm,28}$ ratio is still higher for R2 formulation samples as was the case with the $f_{cm,2}/f_{cm,28}$, ratio, but the final value of compression strength, i.e. after 28 days, is 3 MPa lower for samples made according to this formula than for R1 formulation samples. For weathering treatment the ratio $f_{cm,7}/f_{cm,28}$ for R1 is higher than for R2, although for this treatment the ratio $f_{cm,2}/f_{cm,28}$ was higher for R2.

To sum up, samples with ash cement with low hydration heat due to ash content are more exposed to temperature fluctuations. As the temperature increases, the hydration process accelerates and the strength of the young concrete increases, but this ultimately negatively affects the final compression strength. The cement hydration can progress properly only if the water amount in the mixture is greater than the amount of already bonded water.

The highest compressive strength after 28 days is achieved with samples stored in water. In the case of film care – for samples with CEM I 32.5R cement the difference in compressive strength after 28 days is 7.3 MPa compared to samples stored in water, and for samples with CEM IV/B (V) 32.5R – LH/NA the difference is 4.5 MPa.

It is worth noting that the values of compressive strength after 28 days for the samples based on the R1 formula stored in the foil and stored under room temperature conditions are practically the same, whereas in the case of the samples based on the R2 formula, there is a clear difference between the values of compressive strength after 28 days concerning the samples maintained in the foil and stored under room temperature conditions – by 7.5 MPa (see Fig. 4). This is, as indicated earlier, due to the type of cement used.
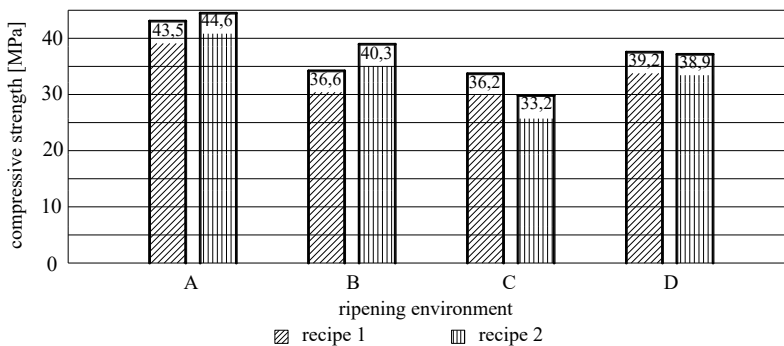

Fig. 4.　Compressive strength value of samples after 28 days of care in given environments. *Source:* Author's own study

However, the compressive strength values of the samples from the two formulae, when stored outdoors in the weather after 2, 7 and 28 days, do not differ much from each other. The compressive strength after 28 days is higher for this treatment than for room temperature care and for R1 than for foil care. This was caused by the favorable conditions for accelerated hydration – the average daily outdoor temperature remained at the level of 18-22 °C for 12 days and was lower than 10 °C for only 4 days, similarly, the average daily humidity – for only 3 days was lower than 60 % [15]. It is worth emphasizing that in the case of these maturation conditions, the results obtained are closely related to the conditions occurring outside the laboratory in a given month.

4. Conclusion

The use of cement of even the best quality may become irrelevant if it is not properly cared for. In the case of water, foil and weathering treatments, concrete with CEM IV/B (V) 32.5R – LH/NA cement has a higher compressive strength. Only in the case of samples stored under dry conditions in a laboratory room, the samples with CEM I 32.5R had a higher compressive strength, this was due to the relatively low air humidity maintained at about 40 %, to which, as it turns out, pozzolanic ash cement with low hydration heat is sensitive.

The analysis of the obtained results indicates that for both types of concrete tested the best way of care from the point of view of the compressive strength value is wet care, which is quite an obvious conclusion. The lowest compression strength values were obtained for samples maintained in dry conditions (inside the laboratory). This is due to the evaporation of more water from the samples.

In summary, it can clearly be stated that both the composition of the concrete mixture and the way the concrete is cared for are crucial with regard to the compressive strength after 28 days.

On a construction site, after removal from moulds, the test specimens should be cured in water at a temperature 20 ± 2 °C. Loss of moisture and deviations from the required temperature should be avoided at all stages of transport of the specimens to laboratory. The most advantageous way is packing the specimens in plastic bags containing water or, if a transport distance is not large, wrapping the specimens in a foil to protect them against dehydration.

Literature

[1]   *PN-EN 206+A1:2016-12 Concrete. Specification, performance, production and conformity.*

[2]   „Beton według normy PN-EN 206 wraz z krajowym uzupełnieniem PN-B-06265", Górażdże Heidelberg Cement Group Directory.

[3]   *PN-EN 13670:2011 Execution of concrete structures.*

[4]   Bajorek G., "Pielęgnacja betonu", *Technologie*, July-September 2016, pp. 48-50.

[5]   Giergiczny Z., "Pielęgnacja betonu – niedoceniany problem", Available: http://www.inzynierbudownictwa.pl/technika,materialy_i_technologie,artykul,pielegnacja_betonu___niedoceniany_problem,9527 [Accessed: 8 Mar 2020]

[6]   „Właściwa pielęgnacja betonu zimą", Available: https://www.budownictwo360.pl/blog/Wlasciwa-pielegnacja-betonu-zima [Accessed: 8 Mar 2020]

[7]   Szruba M., "Domieszki i dodatki do betonów", *Nowoczesne Budownictwo Inżynieryjne*, March-April 2017, pp. 46-50.

[8]   Fiks K. and Prostak K., "Wpływ warunków pielęgnacji na ocenę wytrzymałości betonu na ściskanie", *Autostrady Magazine*, 8-9/2017, 2017, pp. 24-28.

[9]   *PN-EN 12390-2:2019-07 Testing hardened concrete. Part 2: Making and curing specimens for strength tests.*

[10] IBDiM Technical Recommendation No RT/2016-02-0170 from Feb 9th, 2016. Available: http://ozarow.com.pl/cement-portlandzki-32-5-r/ [Accessed: 7 Jul 2018]

[11] Product card. Ash Puccolate cement CEM IV/B (V) 32.5R – LH/NA. Available: https://www.lafarge.pl/sites/poland/files/atoms/files/karta_produktowa_cementu_cem_iv_b_v_32.5_r_-_lh_na.pdf [Accessed: 7 Jul 2018]

[12] *PN-EN 12350-2:2019-07 Testing fresh concrete. Part 2: Slump test.*

[13] Product card. CHRYSO®Optima 185. Available: https://www.chryso.pl/p/8064/3/3029/pl [Accessed: 7 Jul 2018]

[14] Spiek P., "Ocena wytrzymałości betonu zwykłego w różnych warunkach jego pielęgnacji i przechowywania". BEng thesis, Warsaw University of Life Sciences – SGGW, 2019.

[15] Institute of Meteorology and Water Management – National Research Institute, *Metrological data*. Available: https://dane.imgw.pl/data/dane_pomiarowo_obserwacyjne/dane_meteorologiczne/ [Accessed: 2 Feb 2019]

[16] *PN-EN 12390-3:2019-07 Testing hardened concrete. Part 3: Compressive strength of test specimens.*

Crossref
Similarity Check
Powered by iThenticate

Geometry of the cycling track

Maciej Tomasz Solarczyk

Department of Concrete Structures; Faculty of Civil and Environmental Engineering;
Gdansk University of Technology; Gabriela Narutowicza St. 11/12, 80-233 Gdańsk, Poland;
maciej.solarczyk@pg.edu.pl (iD) *0000-0001-6070-0736*

The paper describes the problems related to shaping of the geometry of the cycling track. The method of selection of the angle at the track curve is presented. Issues related to the selection of the appropriate transition curve and the superelevation section along the transition curve are presented. Reference to the recommendations presented in the literature and scientific papers has been made. Special attention to the need of consideration of the subjective feelings of the cyclist is paid. The paper describes the guidelines of the International Cycling Union (UCI) on shaping the geometry of the cycling track.

Keywords: geometry of cycling track; track cycling; transition curve

1. Introduction

Cycling tracks are facilities where track cycling competitions are held. They are oval in shape, with a characteristic significant inclination of the track on a horizontal curve often reaching 45°. During the competition, there are two types of races on the cycling track: sprint and endurance. Fig. 1 shows a view of the Olympic velodrome in London.

Fig. 1.   View of the Olympic Velodrome in London; author of the picture: Tom Green

Among the scientific articles published in recent years on track cycling, the most dominant are those on mathematical modelling of the cyclist's movement on the track, improving the aerodynamic position of the cyclist on the bike, improving the geometry of the bike, improving training methods and improving indoor conditions (such as temperature, humidity, ventilation) to enable athletes to improve their performance. The article [1] presents the results of measurements of air speed and turbulence during a simulated chase race taking place on the cycling track. It describes how the resistance and turbulence of air changes during the ride of one cyclist after another. In the publication [2], the authors presented a continuous mathematical model for the simulation of cycling on a track, which includes calculated angles of slip and steering wheel turns. Model validation was provided by data from a power meter, wheel speed and timekeeper obtained from two different studies and from eight athletes. In the paper [3] the authors described a model which is useful for the analysis of cycling track physics and can be used to predict performance depending on the bike efficiency, type of tyre and conditions on site, in a racing scenario. In [4] the author describes the way of designing the architectural structure of the cycling track in London, in such a way as to provide increased temperature and ventilation for the participants to compete, while minimizing these factors for the public. The article [5] analyses the current knowledge on the reaction to acute or chronic exposure to altitude associated with single and multiple sprints, among others in track cycling. It is only a small extract from current scientific topics in track cycling. However, there are few publications on track geometry construction in the literature. Physical, psychological and equipment aspects are analyzed in detail. Many scientists strive to improve and refine known methods, in line with the idea of small profits, enabling cyclists to beat more records. This article collects guidelines for cycling track geometry and presents directions for further research to improve sports performance, but in the new variant – by shaping track geometry (an approach rarely seen in the scientific literature so far).

As it was written in [6], the text devoted to the velodrome for the London XXX Olympics 2012: *the exact geometry of the cycling track is a strict secret.*

In recent years a number of cycling tracks have been built around the world. The most important of these facilities (tracks for the Olympic Games and the World Championships) were designed by two constructors: Ronald Vincent Webb and Ralph Schürmann.

The article presents problems related to the selection of cycling track geometry, discusses the guidelines of the International Cycling Union (franc. UCI: Union Cycliste Internationale), describes and critically assesses the opinions presented in [7].

2. International Cycling Union (UCI) Guidelines

The guidelines of the International Cycling Union concerning the geometry of the cycling track are quite scarce and leave considerable freedom in the choice of solutions for the designer of the object. According to document [8] (translated into Polish in [9]), the construction of the cycling track itself is entirely the responsibility of the designer: The stability and resistance of the materials and fixings which make up the structure of the velodrome shall meet the legislation regarding construction and safety of the country in which it is built and shall take account of specific geological and climatic conditions. These elements, along with general compliance of the construction and construction materials with technical standards and good practice, remain the exclusive responsibility of (…) engineers (…).

The UCI guidelines [8] for the category 1 facility (thus the track for the Olympic Games and the World Championships) specify:

● the length of the track: 250 m,

- the width of the track: 7 – 8 m,
- horizontal curve radius: 19 – 25 m,
- minimum safety speed: 85 – 110 km/h.

Moreover, in [8] important data from the point of view of track geometry are presented:

- the inner edge of the track shall consist of two curves connected by two parallel straight lines,
- entrance and exit of the curves shall be designed so that the transition is gradual,
- the banking of the track shall be determined by taking into account the radius of the curves and the maximum speeds achieved in the various disciplines,
- the width of the track must be constant throughout its length,
- at any point on the track, a cross section of the track surface must present a straight line.

This is a series of generally formulated guidelines, thanks to which the designer of the object has considerable freedom in choosing the transition curve and the superelevation section on the horizontal curve of the cycling track. Fig. 2 shows a diagram of the construction of the cycling track. In the guidelines [8], it is given additionally:

- the length of the track shall be measured 20 cm above the inner edge of the track (the upper edge of the blue band). This line is called the "track measurement line" and is black on a light or white background or white on a dark background,
- a red line, known as the "sprinters' line" shall be marked out 85 cm from the inner edge of the track,
- a blue line, known as the "stayers' line" shall be drawn at one third of the total width of the track or 2.45 m (whichever is the greater) from the inner edge of the track,
- the width of the infield (blue track) must be at least 10% of the track width. The slope of the infield is between 6° and 12°,
- the minimum width of the safety zone including the infield is 4 m for 250 m tracks,
- a fence at least 120 cm high must be made along the inside edge of the safety zone,
- the outside edge of the track is to be surrounded by a safety fence with a total height of 90 cm.
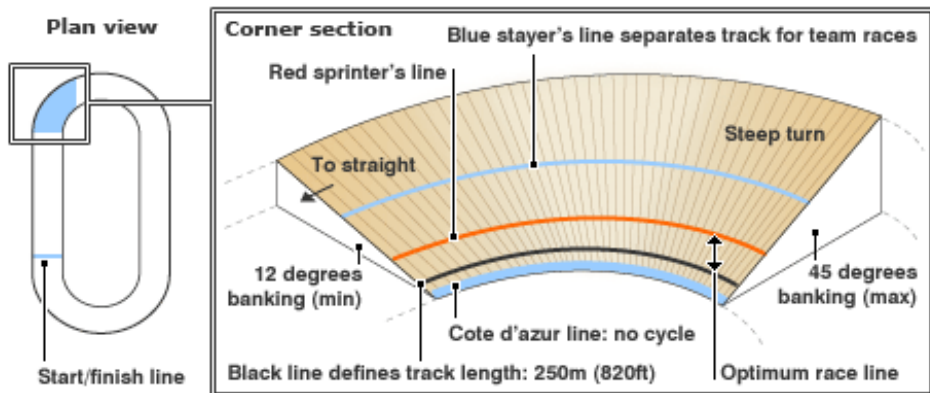

Fig. 2.   Scheme of the construction of the cycling track; source: www.bbc.com, access: 20.08.2015

It is worth noting the necessity of very precise track length measurement, after point 3.6. 074 in [8]: the tolerance of flatness for the track surface shall be 5 mm over 2 metres, after [10] (page 118): track length is measured with an accuracy of 0,005 m and in [11] (page 72): if the track length exceeds 250 m by more than 0,0012 m, the track will be rejected by the controlling UCI representative (it should be stressed that track cycling times are measured with an accuracy of one thousandth of a second).

3. Construction of the track on a horizontal curve

Using the relation given in [10] (page 119), the slope of the track in the horizontal curve is calculated from the formula:

$$\tan \alpha = \frac{V^2}{gR} \, [°] \tag{1}$$

where: V – design speed, $g = 9,81$ m/s^2 – acceleration value, R – horizontal curve radius of the cycling track.

For category 1 track, the size of the gradient at which the cyclist will move on a horizontal curve in a position perpendicular (forming a right angle) to the track surface in a range is obtained:

$$\alpha = 66,3° \div 78,7° \tag{2}$$

Fig. 3 shows a schematic diagram of the forces during horizontal curve riding. During the ride, the cyclist is able to tilt the bike in either direction. Therefore, the friction of the tyre against the track surface should be considered. In [10], it was proposed (based on the experience of Foerster) that the cyclist should have an optimal, safe inclination of up to 30° in both directions without fear of slipping. This issue is presented in fig. 4. Because:

$$\alpha - 30° = 78,7° - 30° = 48,7° \approx 45° \tag{3}$$

it can be considered that the inclination of the horizontal curve on most of the cycling tracks has been chosen in the way given above.
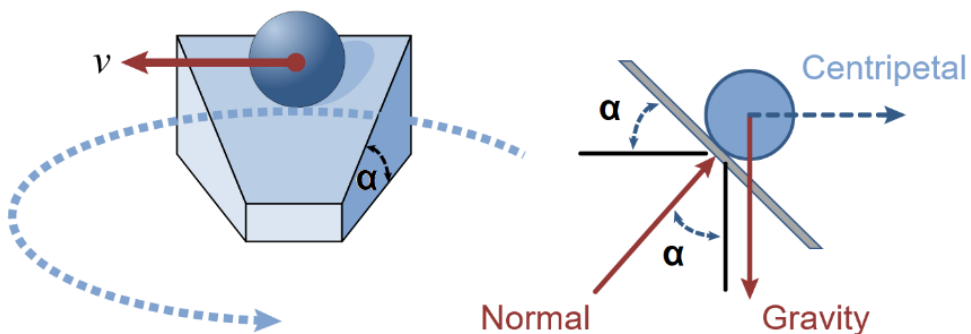

Fig. 3.   Diagram of force applied to a cyclist when riding in a horizontal curve; source: en.wikipedia.org, accessed 20.08.2015
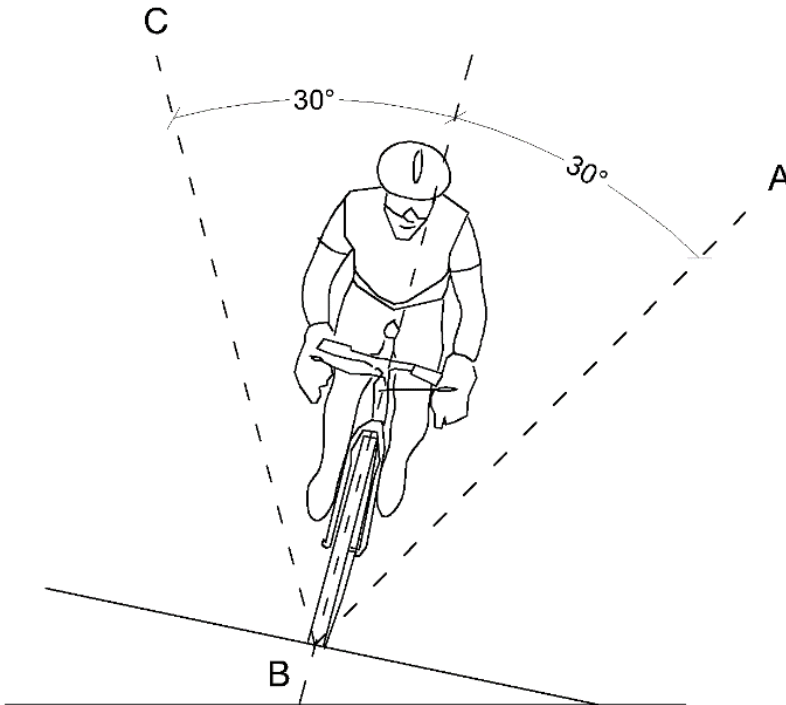
Fig. 4.   Permitted and safe inclination of the cyclist on the track to a position within AB or BC; source: own
           elaboration

Ronald Vincent Webb (Australian Cycling Track Designer, designer of tracks for the 1988 Seoul XXIV Olympics, the 2000 Sydney XXVII Olympics, the 2004 Athens XXVIII Olympics, or the XXX Olympics in London in 2012), in his article in [11] (pages 70 – 73) noted that the above considerations about riding in a horizontal curve are fully consistent for four-wheeled vehicles, e.g. cars, because they are then subjected to forces like in Figure 3, where only the frictional force is omitted. Next, the designer notes that unfortunately, through the years, many cycle tracks have been built in this style. The problem arises because a competition cyclist is on two wheels, and the rider's centre of gravity, balance and friction will be constantly changing, due to aggressive riding or sudden changes of direction within a large field of competitors. Speeds will vary accordingly and sometimes he or she will be riding slowly. The above remarks of Ronald Webb are shown in fig. 4, where the cyclist can be seen leaning to the left of the centre of gravity axis of his bike because of the vigorous pressure on the pedals. This is a frequent phenomenon among racers on the track, so it cannot be omitted when considering its geometry.

Fig. 5 shows an example of a cross-section through the track in a straight section and in a horizontal curve. Fig. 6 shows an example of a cycling track geometry modelled in Autodesk AutoCAD 2015 (educational license).
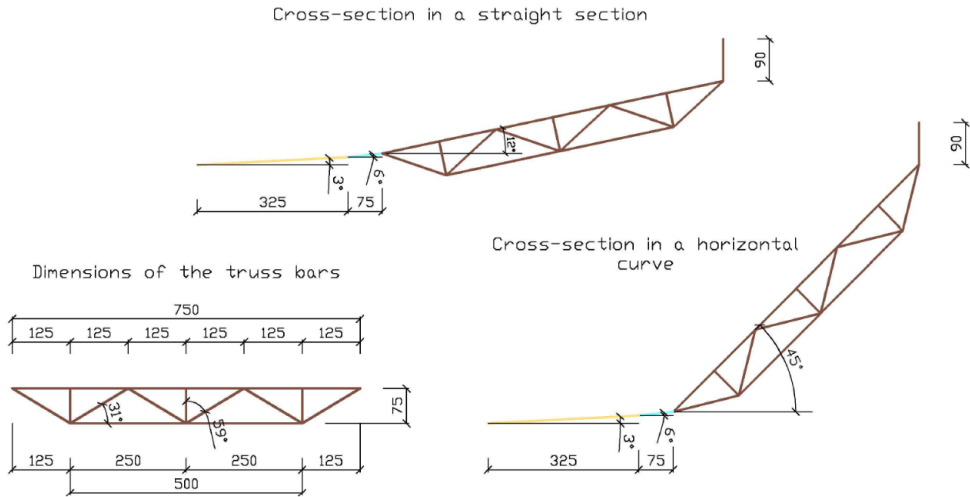
Fig. 5. Cross-section through the exemplary track in a straight section and a horizontal arch; source: own elaboration
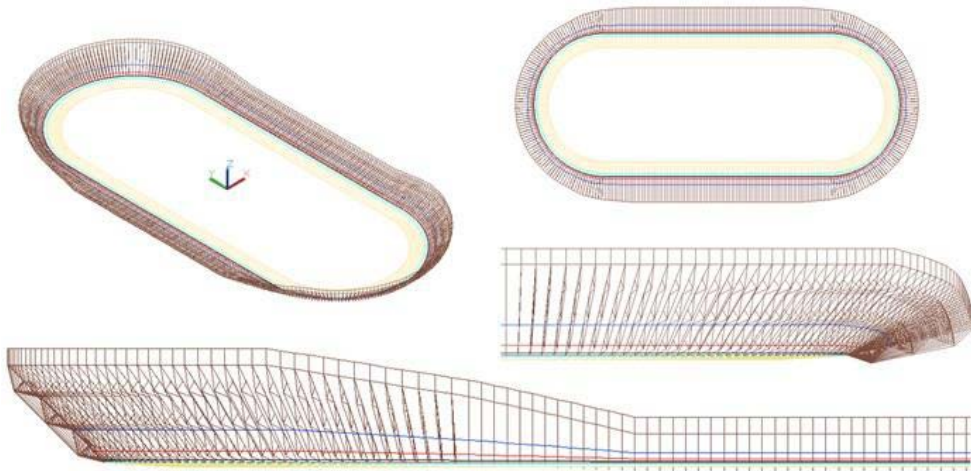

Fig. 6. Cycling track geometry designed in Autodesk AutoCAD 2015 program (educational license); source: own elaboration

4. Cycling track transition curve

The issue of designing the geometry of the cycling track is complex. The secret of the success of famous velodrome designers Ronald Webb and Ralph Schürmann is the right choice of transition curve and superelevation section. By adjusting the vertical inclination of the subsequent parts of the transition curve, the construction of the track can be improved, increasing the cyclist's riding efficiency and thus enabling athletes to improve their performance. In order to modify the vertical geometry of the track accordingly, it is necessary to have experience in this type of design and an appropriate set of data, both based on measurements of the cyclist's lap time, the value of the centrifugal acceleration acting on the cyclist during ride on a horizontal curve, or insight into the measurement of

the power generated during the lap, but also taking into account the subjective feelings of the cyclist concerning the comfort of riding when passing from a straight section into a horizontal curve.

It is worth noting that when designing car and railway roads, the transverse slope of the road changes over a long distance, in a rather slow way, while on the cycling track the change takes place over a short distance by a value often exceeding 30°.

In the article [7], the authors analysed the construction of two cycling tracks: the Olympic track in Beijing (where four Olympic records were broken; constructed by Ralph Schürmann) and the one located in the Chinese Sports Institute in Nanjing. They considered the minimization of the rider's time during the 200-metre time trial to be the reference point for the calculation. They suggested using the mathematical model of the track in MATLAB to optimize the slope angles in the horizontal curve. The calculations of the authors show that after applying the proposed solutions, 0.021 s can be saved during the ride. Additionally, the scientists were critical of the existing objects: *Both Beijing cycling track and Nanjing cycling track are praised by athletes, but there still exist some problems (...) caused by inappropriate superelevation runoff models for these tracks.* It should be stressed, however, that there are also other competitions taking place on the track, not just the 200-metre time trial, which the authors considered in their work. The researchers found that *less vertical curvature values correspond to less riding time.* The UCI guidelines and the course of action for determining the slope of the track on a horizontal curve are presented above. By decreasing the slope value, the designer will also have to reduce the speed of minimum safety, which may lead to some limitations when carrying out some of the competitions on the track. It seems that the authors omitted this fact in their considerations. Moreover, they did not take into account the physical characteristics of the riders, which is questionable. When trying to break a record where the thousandths of a second are decisive, the component of the result corresponding to the human factor is very important, if not most important.

A proposal to solve the geometry of the cycling track in the form of a transition curve as a clothoid, and the superelevation section shaped in a straight line (linear increase in superelevation along the length of the transition curve) is presented in [12].

Fig. 7 shows a screenshot of a presentation by Hopkins Architects (responsible for the entire London velodrome construction) entitled "Track Record", which shows a comparison of the shape of the tracks designed by Ralph Schürmann and Ronald Webb. Schürmann's tracks are narrower and longer (the blue line in fig. 7), giving preference to sprinters who have more time to overtake their rival in the longer straight sections (after exiting the horizontal curve, where it is ineffective to overtake because there is a greater distance, the rider has a longer straight section to the finish line). Webb's track is more oval (the red line in fig. 7), which gives better conditions for breaking time records, because when comparing the speed of a rider in a straight section and a horizontal curve it can be observed that the rider achieves higher speed in the area of horizontal curves of the track than in straight sections.
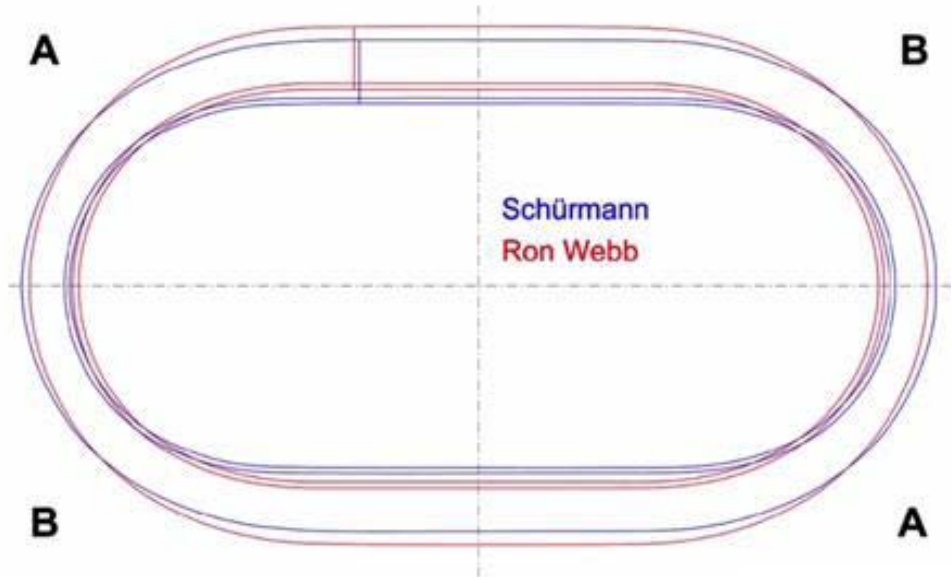
Fig. 7.   Comparison of the shape of cycling tracks according to Ralph Schürmann and Ronald Webb; source:
           screenshot of a presentation by Michael Taylor (Hopkins Architects) entitled Track Record, registered
           on 18.01.2013, link to the film: https://vimeo.com/59175243, accessed on 20.08.2015.

It is also worth noting the letters A and B in Fig. 7. They show the differences in track slope angles in these places. The part of the horizontal curve marked with the letter A is situated lower than the part indicated with the letter B. As it was written in [6], *the track in the London Velodrome does not have the usual reflection symmetry that can be found in buildings. If the track was built in half lengthwise, the two halves would not match. The track does have rotational symmetry. The slope of the track going into and out of the turns is not the same. This is simply because the cyclist always moves the same way around the track, and go shallower into the turn and steeper out of it.*

5. Summary

The designer has the ability to change the angles that form transition curves and can allow for a smooth transition from steep curves down into smaller angles on straight sections. However, any change of angle must still be governed by laws of physics. At every point and at every angle, the track must be capable of handling the rider's speed and friction. The intention is to shape the track in such a way that a cyclist who rides out of a horizontal curve and enters a straight section has no difficulty in maintaining his line of riding, without the need for additional steering control of the bicycle and can actually benefit greatly from the transition from a horizontal curve to a straight section.

When designing the geometry of the cycling track, the following points must be considered:

● type of transition curve,
● type of superelevation section on the length of the transition curve,

- finding the interaction between the transition curve and the superelevation section in relation to the bicycle as a single-wheeler (a difficult task in comparison with designing car or rail roads, where the vehicle rests on a minimum of four wheels, where the issue of vehicle deviation from the direction perpendicular to the driving surface can be omitted),
- variable position at the entrance and exit height of the horizontal curve of the cycling track.

It will be useful to collect data from the competitors themselves in order to select the above mentioned factors properly. Their feelings and suggestions while riding may significantly improve the solution. Riding in a horizontal curve with an inclination of about 45° requires considerable courage from the cyclist. During the ride an unbalanced centrifugal acceleration affects them. This is the subjective feeling of each competitor. Therefore, it can be concluded that there is no universal track where records in this sport will certainly be achieved.

Literature

[1] Fitzgerald S., Kelso R., Grimshaw P., Warr A.: „Measurement of the air velocity and turbulence in a simulated track cycling team pursuit race". *Journal of Wind Engineering and Industrial Aerodynamics*, Volume 190, July 2019, p. 322-330. https://doi.org/10.1016/j.jweia.2019.05.014

[2] Fitton B., Symons D.: „A mathematical model for simulating cycling: applied to track cycling". *Sports Engineering*, Volume 21, Issue 4, December 2018, p. 409-418. https://doi.org/10.1007/s12283-018-0283-0

[3] Lukes R., Hart J., Haake S.: „An analytical model for track cycling". *Proceedings of the Institution of Mechanical Engineers, Part P: Journal of Sports Engineering and Technology*, Volume 226, Issue 2, June 2012, p. 143-151. https://doi.org/10.1177/1754337111433242

[4] Douglas L.: „Olympics watch: The velodrome". *Engineering and Technology*, Volume 5, Issue 2, 2010, p. 20-22.

[5] Girard O., Brocherie F., Millet G.P.: „Effects of Altitude/Hypoxia on Single- and Multiple-Sprint Performance: A Comprehensive Review". *Sports Medicine*, Volume 47, Issue 10, 1 October 2017, p. 1931-1949. https://doi.org/10.1007/s40279-017-0733-z

[6] Thomas R.: „How the velodrome found its form". Available: www.plus.maths.org [Access: 20 Aug 2015]

[7] Cheng J., Du X., Shi J., Zhang Y., Li F.: „Optimization of superelevation runoff model for cycling tracks". *Journal of Central South University of Technology*, April 2011, Volume 18, Issue 2, p. 587-592. https://doi.org/10.1007/s11771-011-0735-1

[8] „UCI Regulations Part III: Track Races", version from 1.02.2015. Available: www.uci.ch [Access: 20 Aug 2015]

[9] „Przepisy sportowe PZKol Część III – Wyścigi torowe", version from 01.10.2013. Avaialbe: www.kspzkol.pl [Access: 20 Aug 2015]

[10] Wirszyłło R. i inni., *Urządzenia sportowe: planowanie, projektowanie, budowa, użytkowanie*. Arkady, Warszawa 1982.

[11] Hopkins Architects., „London 2012 Velodrome Design in pursuit of efficiency". *The Architects' Journal*, London, September 2011.

[12] Solarczyk M.T., *Olimpijski tor kolarski (welodrom) przykryty dachem wiszącym (z analizą cięgna nieodkształcalnego i odkształcalnego),* in English: Olympic cycling track (velodrome) covered by a suspension roof (with the analysis of non-deformable and deformable cable), master's thesis, Gdańsk University of Technology, supervisor Krystyna Nagrodzka–Godycka, september 2015.

Crossref
Similarity Check
Powered by iThenticate

Orginal Article

Contemporary symbols in the space of Baku

Elżbieta Kaczmarska

Faculty of Architecture and Fine Arts; Andrzej Frycz Modrzewski Krakow University;
Gustaw Herlinga-Grudziński St. 1, 30-705 Kraków, Poland;
kaczmarskaelzbieta@poczta.onet.pl (iD) *0000-0002-4271-8462*

Abstract: When performing even a cursory analysis of the visual image of contemporary Baku, the capital of Azerbaijan, one simply cannot ignore its ancient history, the political influence of nearby powers and the almost age-old dependence on Soviet Russia. The regaining of independence in 1991, associated with the policy of then-national leader Heydar Aliyev, stimulated the young country's ambition to open up to the world and organise an international cultural event. The preparation for the Eurovision Song Contest in 2012 initiated another construction boom in the history of Baku, fuelled with petrodollars, and became an occasion to present a new vision of the capital. In the years 2007–2012, numerous new cultural, artistic and sports buildings were constructed and which are now a hallmark and symbol of contemporary Baku. One such building, which creates a new, futuristic city space and is presented in the article, is the Heydar Aliyev Centre, a centre of art and museum designed by Zaha Hadid. The author notes the creative intent, external appearance and structure of the building, as well as new means of expression in creating place-based ambience. Also noted were the use of contemporary art in the creation of attractive utilitarian spaces. Other presented buildings display the ages-old symbols of the 'Land of Fire' in a new way and are embedded into the contemporary panorama of the city.

Keywords: history; symbols; form; Flame Towers; construction boom; urban space; public space; contemporaneity; futuristic vision; Baku; Azerbaijan

1. Introduction

Of the three capitals of Transcaucasia—Tbilisi, Erevan and Baku—it is Baku that has been developing the quickest in the twenty-first century. The city, located on the shore of the Caspian Sea, in the in the southern zone of the Absheron Peninsula, is the capital of Azerbaijan[1] [1][2].

---

[1]   Contemporary outlooks on Azerbaijan's historic sites and its modern image are not widely known. Two Polish-language publications can be listed, however. The first is a work by Tadeusz Święto-chowski—a Pole, orientalist and lecturer at American universities and at Germany's Heidelberg University, the author of numerous academic works on the history and contemporary problems of

This metropolis with a population of 2 million, which is a quarter of the country's population, is characterised by high ethnic diversity and an interesting structure of space [3] [4] [5]. Here, areas of traditional development and singular modern buildings or complexes are located on sites that are attractive in terms of the landscape and define the visual perception of the city.

The ancient part of the city currently occupies a small, walled area that is near the coast. This 'Inner City', separated from the remaining development and isolated by existing fortifications, has retained its past psychological atmosphere and irregular urban layout stemming from defensive strategies and climate conditions, in addition to numerous historical monuments.[2]

At present, new projects in the capital, that stand out through atypical and futuristic forms, have been sited in various areas of the seaside boulevard or in its immediate area, as well as in the city's north-eastern zone. The areas in question, occupying a large territory, are linked by comfortable vehicular circulation, including marshrutkas, the railway and a modern underground railway, and are also equipped with park areas. The latter enable the city's cross-ventilation—which is not easy when winds constantly change direction, which is also a feature of the peninsula's climate.

The development of Baku has been tied with natural resources, particularly oil and natural gas, for ages. In the twenty-first century, it makes use of the current economic and political situation to awe the world with the new image of the capital. Buildings with cosmic shapes and many new facilities associated with culture, art and sports were built at the start of the new century [6], [7]. The new symbols of Baku, which build the ambience of places and the physical image of the city, mark another period in the life of the city and the country since it regained independence in 1991 and after the fall of the Soviet Union.[3] They are also a monument to the Aliyev family which holds political and economic power in the country and which makes exaggerated references to the engineering traditions and skills of contemporary structural engineers and contractors. Among the gigantic monuments to power there is, among others, the Heydat Aliyev Centre, which houses a museum and is dedicated to the first president of Azerbaijan and the architect of its independence.

---

the Middle East and the Muslim nations of the former USSR, particularly Azerbaijan. The second Polish-language publication is Azerbejdżan, publ. Oficyna Wydawnicza „Rewasz", Pruszków 2014, commissioned by the Ministry of Culture and Tourism of the republic of Azerbaijan and on the initiative of His Excellency the Ambassador of the Republic of Azerbaijan in Poland Hasan Hasanov, PhD.

[2] They include: the quintessence of Baku's Old Town—the buildings along Asaf Zeynalli and the Maiden Tower, the surviving fortifications; the heart of the capital—the palace complex of the palace of the Shirvanshahs., the caravanserais and city baths; residences of the wealthy from the turn of the twentieth century. The genius loci of this location is also associated with a place conducive to remembrance and meditation sited near the Old Town—the Path of Martyrs, as well as a region to the south of Baku—Gobustan, with prehistoric carvings and mud volcanoes.

[3] Azerbaijan is a country of contrasts. The extraordinary wealth of the capital and the visible prosperity of a number of significant cities border on the clear poverty of smaller cities. The life of towns and scattered villages is as calm as it was centuries ago, with not much being built; the panorama of their landscape is dominated by the majestic and frightening Greater Caucasus and it is this proximity that is their wealth.

The current dynamic development of Baku and the construction of newer and newer spectacular buildings can be seen as associated with the threat of uneven expansion. While all of the country's energy and financial resources are pooled in the formal zone, the unprivileged majority remains forgotten. Socially and spatially marginalised, these people will be forced to move to districts further away, where they can potentially form areas of poverty endangered by rising crime rates and violence [6].
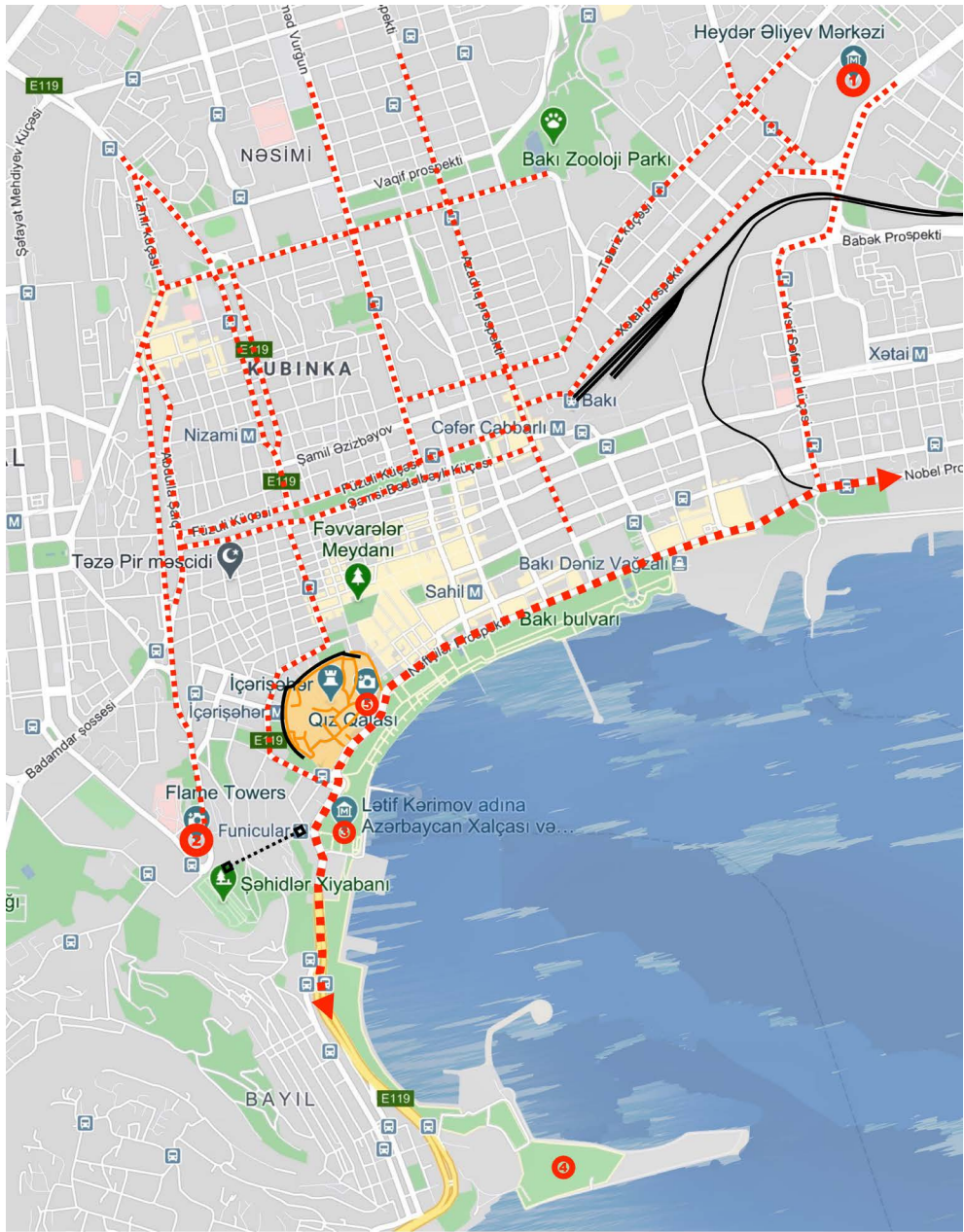
1. Heydar Aliyev Center, design by Zaha Hadid
2. Flame Towers, design by HOK
3. Azerbaijan National Carpet Museum, design by Franz Janz
4. Baku Cristal Hall, design by GMP Architekten
5. Maiden Tower

Fig. 1. Baku—structure of the city and selected elements that crystallise its spatial layout—original work based on Google Maps, 2020

2. The Heydar Aliyev Centre by Zaha Hadid

The building, hidden deep in the city's northern zone, is a legend, an aesthetic feast, one of the best works of 'ingenious Zaha'—the Heydar Aliyev Centre is Azerbaijan's main building to feature this use. The soft, dynamic forms of the new building clearly depart from the distinct administrative and residential buildings of the Soviet period found in this area of the city. Monumental, Socialist Realist style buildings are a panoramic background of its 'second plane' and clearly contrast in terms of function, scale and style.

The Heydar Aliyev Centre is an atypically shaped building. Its external reflection inspires awe, fascinates and intimidates, while also stimulating the imagination. It may bring to mind a poorly curled up carpet, a handkerchief thrown down from space or a lost, gigantic brooch. The fluid, undulating waves of its roof can bring to mind a stormy sea and the oil that gushes out from it and falls heavily downwards—the age-old wealth of the country. To pragmatists, this work can denote a reaction and rebellion against the rigid architecture of Soviet times, or perhaps it is a reference to the ornaments of Islamic calligraphy and elements of traditional Azeri architecture[4] [8].

---

[4] "The Center, designed to become the primary building for the nation's cultural programs, breaks from the rigid and often monumental Soviet architecture that is so prevalent in Baku, aspiring instead to express the sensibilities of Azeri culture and the optimism of a nation that looks to the future'. and 'Fluidity in architecture is not new to this region. […] Our intention was to relate to that historical understanding of architecture, not through the use of mimicry or a limiting adherence to the iconography of the past, but rather by developing a firmly contemporary interpretation, reflecting a more nuanced understanding" [8].

Fig. 2–3. Heydar Aliyev Center, design by Zaha Hadid. Photo by E. Kaczmarska, 2018

However, it appears that the building that has become the symbol of Baku's twenty-first-century architecture has two practical functions: to present its designer and her 'artistic thinking'; and in the museum section, to commemorate the first president of independent Azerbaijan, Heydar Aliyev, a national hero and a man offered almost divine praise, the father of the current president Ilham Aliyev. Zaha Hadid fulfilled both of these tasks. The design was completed after an international competition in the years 2007–2012, also in connection with the construction of many new buildings that accompanied the Eurovision Song Contest, which took place in 2012 in Baku.

The centre and museum form one mixed-use building that has eight levels (it has a height of 74 metres). It includes an auditorium with 1000 seats, a temporary exhibition area, a conference centre, spaces for workshops and a museum. The massing of the centre harmoniously blends with its interior, while also being in a relationship with the nearby square.

The centre and all of its functions, apart from the entrance, are laid out into a fluid form with a continuous surface. The centre's functional spaces, without any supports, are surrounded by a curvilinear skin made from glass fibre reinforced concrete (GFRC) and glass fibre reinforced polyester. This cladding (which can also suggest a tent and reference the nomadic traditions of the Azeri) is suspended by a load-bearing structure comprised of a complex system of concrete and steel elements. The 'satin' finish of the building's surface resulted from the application of semi-reflective glass that causes the building's appearance to change depending on the time of day and season of the year, and the interior and exterior enter into a harmonious relationship.

The interior of the building, coloured white, is filled with light and half-shadows. The rhythm of softly profiled stairs creates an undulating internal amphitheatre. White American oak was used as a finishing material, which provides good parameters under conditions of changing weather associated with temperature and humidity, which resulted in a uniform texture, an effect of lightness and luminosity, as well as excellent acoustic properties [9] [10].
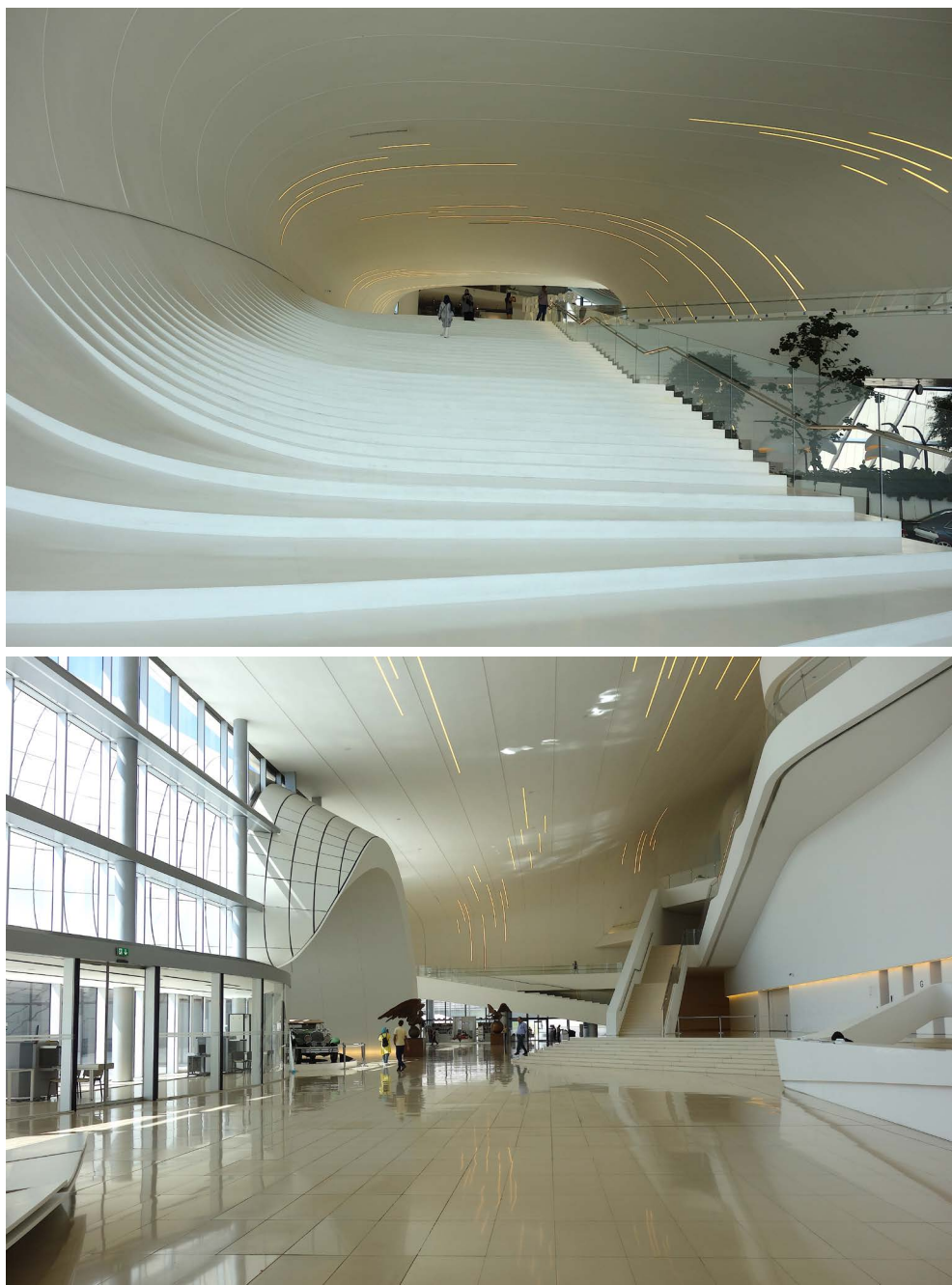
Fig. 4–5. Heydar Aliyev Center, design by Zaha Hadid; interior. Photo by E. Kaczmarska, 2018

The museum is located on a ten-hectare green lawn of varying height, maintaining the principle of the undulation of the place and the building. Located on a slightly elevated plateau, the building has interesting surroundings, to which unpretentious yet varied sculptural motifs have been introduced. Families of gigantic red and blue snails march across the grass, serving as a source of shade. A green rabbit of similar size sits as if slightly to the side. Their saturated colours are probably a distant reflection of the Azerbaijani flag, but their practical use is different. They provide protection from the sun and wind and are a pleasant spot to rest at. This space, accessible from the side of the driveway, is perceived as pleasant. The facade of a likewise new sports hall, designed in a mellow style, forms a direct, northern screen for this space. The entirety of the centre's space is a sophisticated work of art and design; it escapes traditional analyses and evaluations. It is difficult to speak of windows, roofs or staircases here, or other supplementations to this form for that matter; it is a complete work.

Fig. 6.   Heydar Aliyev Center, design by Zaha Hadid; mock-up. Photo by E. Kaczmarska, 2018

Fig. 7–9. Heydar Aliyev Center, design by Zaha Hadid; site detail. Photo by E. Kaczmarska, 2018

3. The Flame Towers by HOK

The Flame Towers—a complex of contemporary office towers, have likewise become an important symbol of Baku. They are excellent representatives of the strategy that the government of Azerbaijan has adopted for Baku. The city, by using its petrodollars, wants to quickly create a global tourist destination similar to the UAE's Dubai. Using spectacular architecture that meets various expectations (in aesthetic and functional aspects), this plan is consistently being implemented[5] [11].

Azerbaijan has been known as the Land of Fire. The flame in the name of the complex is a reference to the tradition of pillars of fire that have been emerging from the ground since ancient times across the entire area of the Absheron Peninsula, primarily around its coastal

---

[5]   The construction of the Flame Towers—an unquestionable symbol, and the construction of the Heydar Aliyev Centre—a building that is more refined in its appearance and function and attracts a different type of recipient, the organisation of international mass events like the Eurovision Song Contest (the construction of Cristall Hall), Formula 1 races, etc. All these efforts carry over to the visibility of the country in the media and increased tourist interest. Following Dubai's model includes the currently halted Khazar project featuring the construction of artificial islands around 25 km to the south-west from Baku. It is currently difficult to assess whether the intended effect can be fully obtained, particularly as the determinants of the expansion of Dubai and Baku are different; however, the current aesthetic outcome within the urbanised space of Azerbaijan's capital is undeniable [11].

area. However, we should also note the Ateshgah fire temple and Yanar Dag, the 'burning mountain' near the country's capital, where natural gas has been leaking for thousands of years. These sites were holy to Zoroastrian fire worshippers.

In the area of the contemporary city, the futuristic towers are a modern equivalent to the thirty-metres-tall Maiden Tower (seventh–twelfth century AD)—the ancient symbol of İçərişəhər, the Inner City. This tower—and around fifteen others that have survived in Azerbaijan—was a defensive structure in the past. It is a valuable monument, the most famous vertical element of the historic centre. In 2000, it was inscribed onto the UNESCO World Heritage Sites List along with other monuments of the Old Town.

Tower-building traditions are also linked with drilling towers, which were erected in association with oil and natural gas mining towards the end of the nineteenth century. The country's economic boom contributed to the change in the city's image. Numerous palaces, villas and elegant townhouses were built, new avenues were delineated along with a seaside promenade and an accompanying park. Baku transformed into a modern city with a grid of streets, broad walkways and formal squares. The compact development spread amphitheatrically across the undulating coast of the Bay of Biscay. The mining of natural resources was a foundation for many fortunes. [6] During this period, the entire Absheron Peninsula and the immediate vicinity of Baku became dotted with drilling towers and pumpjacks. Surviving postcards are an interesting document of the landscape of these resource-mining areas. Small escarpments in various locations across the peninsulas are still burning, while small volcanic cones pour out hot mud saturated with the smell of oil.

---

[6]   Businessmen from the oil sector from all over the world (e.g. the Nobel brothers, Rothschild) gained their riches here; some competed with each other by wide-ranging charity and patronage of culture and the arts. Of note is Hacı Zeynalabdin Tağıyev and his efforts to ensure the comprehensive development of Baku and the city's community. These included efforts and financial contributions to building the city's waterworks, making the capital's streets greener and better illuminated. Outstanding architects from the period were commissioned to design important public buildings. These architects were mostly Poles: Józef Płoszko, Eugeniusz Skibinski, Kazimierz Skórewicz, Józef Gosławski and Konstanty Borisoglebski. Most of their works were in the Secession style, enriched with Moorish, Romanesque and Gothic elements [2].
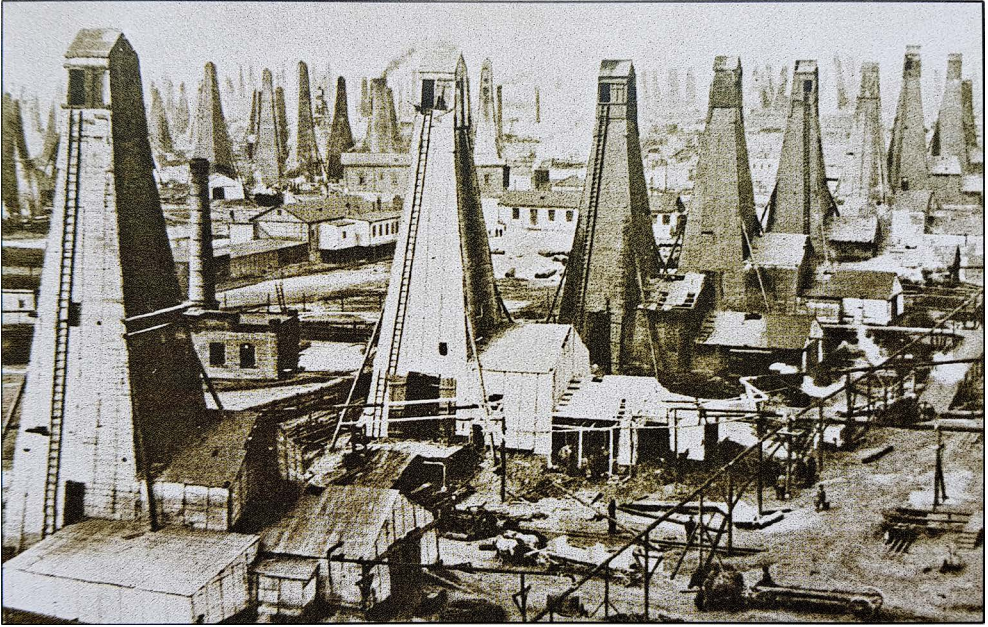
Fig. 10.   Towards the end of the nineteenth century, the entire Absheron Peninsula and the immediate surroundings of Baku became dotted with drilling towers and pumpjacks [from:] Old Baku. Oil Production, Project of Khanlar Mamedov, 2011

Fig. 11.   The present-day appearance of the general area of Baku has not changed much since the nineteenth century. Photo by E. Kaczmarska, 2011

The towers in question are three, similar buildings of varying height (190 metres, 160 metres and 140 metres) and atypical, slightly bent silhouettes modelled after flames and clad in a 'shining skin'. They were sited near Baku's Old Town, to its west, in the direct vicinity of the Path of Martyrs. The tallest building of the complex, the thirty-nine-storey southern tower, houses apartments; the thirty-six-storey northern tower is a hotel, while the western one has office spaces. They were designed by HOK and, after five years of construction, were opened in 2013 [12]. They are monumental, vertical giants, visible from every part of the city—they form its new, contemporary panorama while also referencing tradition and history. Perhaps this is why these symbols were copied in another complex of buildings at Neftchiler Avenue, as evidenced by the structures of new colossal buildings being erected along the avenue[7] [13]. These buildings are overbearing in terms of scale, although they do have a discrete charm, grace and originality.

[7] In 1997, the Baku promenade was placed by Heydar Aliyev on a list of strategic places for the city's development and gained a new status and a new name (Primorsky Park). The costly revitalisation of state property began in 2007, and has been publically funded and managed by the Council of Ministers. The municipal administration does not have much say in these matters. Previously unintended divisions into a high-class west and a low-class east began to appear across the promenade. The eastern side is slowly being characterised as 'unprepared for urban life' [13].

Fig. 12–13. Flame Towers dominating the skyline of Baku in a view from the interior of urban tissue and in the perspective of the horizon, design by HOK. Photo by E. Kaczmarska

The application of LED lights on the surfaces of the towers enabled an extraordinarily attractive spectacle that is presented to residents and tourists every night after sunset. It references the concept of towers that symbolise flames. When seen from the Caspian boulevard or a ship on 'oil lake', it is an array of point lights that dance on the building's facades and rhythmically pulsate in the intensive colours of Azerbaijan's flag, with a figurative, educational message. The reflections of this spectacle on the calm waters of the Caspian Sea only intensify the aesthetic experiences of this event. The display was acknowledged as the best illumination in the world.

Fig. 14.   The light spectacle on the facades of the Flame Towers. Photo by E. Kaczmarska

4. Conclusions

The places presented in the paper are important symbols of modern Azerbaijan and its capital, Baku. The fact that this country—located at the crossing of Eurasia's most important routes and the most ethnically diverse state in the entire Caucasus—has clear political and economic goals, and an ambition to become a dominant force within the region. It is a great synthesis of various cultures and places that connect the East with the West. The capital of Azerbaijan—Baku—makes effective use of this, combining magic, the mysticism of fire and the charming atmosphere of the orient with the pragmatism and engineering knowledge of the West.

References

[1]   Świętochowski T., *Azerbejdżan i Rosja; Kolonializm, Islam i Narodowość w podzielonym kraju*, Instytut Nauk Politycznych PAN, Warszawa 1998

[2]   *Azerbejdżan. Panorama turystyczna. Przewodnik.* Oficyna Wydawnicza Rewasz, Pruszków 2014.

[3]   Baku Research Institute, 2020. Available: https://bakuresearchinstitute.org [Accessed: 30 Apr 2020]

[4]   Melvyn G. et al., "Azerbaijan", in Encyclopaedia Britannica, Encyclopædia Britannica, inc., 2019. Available: https://www.britannica.com/place/Azerbaijan [Accessed: 30 Apr 2020]

[5]   The Editors of Encyclopaedia Britannica, "Baku", in Encyclopaedia Britannica, Encyclopædia Britannica, inc., 2019. Available: https://www.britannica.com/place/Baku [Accessed: 30.04.2020]

[6]   Guliyev F., *Urban Planning in Baku: Who is Involved and How It Works By*, 2018 [in:] *Urbanization and Urban Public Policy in Baku*, Caucasus Analytical Digest, No 101, 2018

[7]   Azerbaijan State Statistical Committee. Available: http://www.stat.gov.az/source/construction/?lang=en> [Accessed: 30 Apr 2020]

[8]   Zaha Hadid Architects, *Heydar Aliyev Centre.* Available: https://www.zaha-hadid.com/architecture/heydar-aliyev-centre/ [Accessed: 30 Apr 2020]

[9]   Bianchini R., *Heydar Aliyev Center – Baku.*, 2019. Available: https://www.inexhibit.com/mymuseum/heydar-aliyev-center-baku-azerbaijan-zaha-hadid/ [Accessed: 19 Dec 2018]

[10]   Muratorplus.pl, *Centrum Hejdara Alijewa w Baku*, 2016. Available: https://www.muratorplus.pl/inwestycje/inwestycje-publiczne/centrum-hejdara-alijewa-w-baku-aa-yREp-sF5L-4MkQ.html [Accessed: 19 Dec 2018]

[11]   Valiyev A., "Baku's Quest to Become a Major City: Did the Dubai Model Work?", in *Urbanization and Urban Public Policy in Baku*, Caucasus Analytical Digest, no 101, 2018.

[12]   HOK, *Baku Flame Towers*. Available: https://www.hok.com/projects/view/baku-flame-towers/ [Accessed: 30 Apr 2020]

[13]   Darieva T., *Reconfiguring a Public Place. Baku Promenade between Europe and Asia*, 2011, based on Darieva T., *A Remarkable Gift in a Postcolonial City: The Past and Present of Baku Promenade,* in *Urban Spaces after Socialism: Ethnographies of Public Places in Eurasian Cities* (ed.) Tsypylma Darieva, Wolfgang Kaschuba, and Melanie Krebs, Frankfurt: Campus Verlag, 2011.